The Action of a Causal Set

by

Dionigi Maria Teofilo Benincasa

Submitted to the Department of Physics at Imperial College London in partial fulfillment of the requirements for the degree of

Doctor of Philosophy in Physics
of Imperial College London

March 2013

Declaration

I declare that this work is entirely my own, except where otherwise stated. Most of Chapter 3 will appear in a joint paper with Fay Dowker [1]. Most of Chapter 5 appears in [2]. Most of Chapter 6 will appear in a joint paper with Fay Dowker and David Rideout [3]. All simulations, except those of Chapter 5, were done using the CausalSets toolkit in the Cactus framework (www.cactuscode.org) developed by David Rideout.

Dionigi M. T. Benincasa May 2013

Acknowledgements

I want to thank my supervisor Fay Dowker, for being what I can only describe as the best supervisor I could have ever hoped for. Her guidance throughout my PhD has been invaluable, and her patience with me greatly appreciated.

I want to thank Rafael Sorkin for the many hours spent explaining things to me. His supreme intellect, boundless knowledge and constant creativity have been a continuous source of inspiration.

I want to thank David Rideout for teaching me almost everything I know about programming, and always being helpful with simulations.

I want to thank my friends Michel, Andre, Stefano and Jurgis for sharing the PhD experience with me, and always being interested in discussing my work with me.

I want to thank my dear love Giovanna, for sticking with me every step of the way, and providing constant love and support over the last 7 years.

I want to thank my aunt Silvia, whose generous support allowed me to continue my studies at a crucial stage of my life. I will be forever grateful to her.

Finally I want to thank my family, especially my mother and father, for being the foundations on top of which I've been able to build my life. Without their constant love and support I would not be where I am now.

Abstract

A causal set is a model for a discrete spacetime in which the "atoms of spacetime" carry a relation of ancestry. This order relation is mathematically given by a partial order, and is is taken to underly the macroscopic causal notions of before and after. The work presented in this thesis proposes a definition for the action of a causal set analogous to the continuum Einstein-Hilbert action.

The path taken towards the definition of this action is somewhat indirect. We first construct a retarded wave operator on causal sets well-approximated by 4-dimensional spacetimes and prove, under certain assumptions, that this operator gives the usual continuum d'Alembertian and the scalar curvature of the approximating spacetime in the continuum limit. We use this result to define both the scalar curvature and the action of a causal set. This definition can be shown to work in any dimension, so that an explicit form of the action exists in all dimensions. We conjecture that, under certain conditions, the continuum limit of the action is given by the Einstein-Hilbert action up to boundary terms, whose explicit form we also conjecture. We provide evidence for this conjecture through analytic and numerical calculations of the expected action of various spacetime regions.

The 2-dimensional action is shown to possess topological properties by calculating its expectation value for various regions of 2-dimensional spacetimes with different topologies. We find that the topological character of the $2d$ action breaks down for causally convex regions of the trousers spacetime that contain the singularity, and for non-causally convex rectangles.

Finally, we propose a microscopic account of the entropy of causal horizons based on the action. It is a form of "spacetime mutual information" arising from the partition of spacetime by the horizon. Evidence for the proposal is provided by analytic results and numerical simulations in 2-dimensional examples. Further evidence is provided by numerical results for the Rindler and cosmic deSitter horizons in both 3 and 4-dimensions, and for a non-equilibrium horizon in a collapsing shell spacetime in 4-dimensions.

Contents

List of Figures

Chapter 1

Introduction

1.1 Quantum Gravity

The last 80 years have seen many attempts at solving the problem of quantum gravity; that is, trying to construct a framework within which gravity can be consistently described quantum mechanically. Some attempts have been more successful than others, in the sense that they have provided useful insights into what such a theory might look like, but so far none are fully understood theoretically, let alone confirmed experimentally. The various approaches differ widely – it suffices to look at the two most popular approaches, string theory and loop quantum gravity, to see how different they can be[1]. This can be traced back to two important aspects of the situation fundamental physics finds itself in: an almost total lack of experimental evidence to guide us in any particular direction, together with the lack of general consensus regarding the fundamental principles which will underly *the* theory of quantum gravity (QG). The latter point is perfectly highlighted by Hawking's famous black hole information paradox [4], and the subsequent flurry of work which followed since [5, 6], which shows a clear inconsistency between the basic principles of quantum mechanics, general relativity and locality, when these are put together in trying to understand the evaporation of black holes [7]. These studies, together with other unresolved puzzles in fundamental physics, show us that physics is at a crossroads – only some of the principles we believe to be fundamental can survive the transition to a

[1] It is worth pointing out that sting theory is an attempt at something much more grand than "simply" unifying gravity with quantum mechanics; it tries to unify all the forces of nature.

theory of quantum gravity – and it is our job as physicists to explore the various possibilities. Causal set theory is one such route, and will be the subject of the rest of this thesis.

In the rest of this Chapter we will explore some of the ideas underlying causal set (causet) theory. In Chapter 2 we define causal sets more precisely and introduce the mathematical tools required for the rest of the thesis. Chapter 3 is concerned with the construction of a wave operator on causal sets and is largely based on both published and unpublished work [8, 1]. In Chapter 4 we use the causet wave operator to define an action for causal sets and explore its properties both numerically and analytically. Chapter 5 is devoted to the study of the (2 dimensional) causet action of causal sets well-approximated by 2 dimensional Lorentzian spacetimes, and a possible relation to the Lorentzian version of the Gauss-Bonnet theorem is investigated. Again this work is based on published work [2]. In Chapter 6 a conjecture for a novel interpretation of the entropy of any causal horizon, which makes use of the causal set action, is given. Numerical evidence is provided for this conjecture and consequences of the results are explored. Chapter 7 wraps up the thesis by providing an overview of the work covered, discussing also current and future work.

1.2 Causal Sets as a Basis for Quantum Gravity

Twentieth century physics has given us the two most successful theories of physics ever, Quantum Mechanics and General Relativity. In GR, spacetime is elevated from the absolute, fixed, background role it played in pre-general relativistic physics, to the same status as the matter which it supports[2], thus becoming a physical, dynamical structure in itself. Its physical nature is usually represented by a metric field, whose dynamical evolution and interaction with matter is determined by the Einstein equations. The spacetime points themselves do not possess any individuality per se, but rather act as carriers for the metric and matter fields. This does not however imply that the underlying spacetime manifold is formless, since its points in fact carry first a foremost topology and differentiable structure. These structures though, unlike the fields they support, remain absolute. The kinematical structure

[2]Matter here is taken to mean anything that is not spacetime itself, e.g. a massive particle, the electromagnetic field etc.

of GR thus comprises a 4 dimensional manifold $\mathcal{M}$, and a Lorentzian metric g on $\mathcal{M}$. We will see in the next chapter that this dual structure can be replaced by something arguably more primitive, causal structure (denoted $<$) together with volume information, V.

Now any approach to Quantum Gravity must begin its journey by defining the kinematics of the theory. In other words it must define what it is it wants to "quantise" (having done this, it must then say what it means by "quantising"). The infinities of existing theories, namely the divergences of Quantum Field Theory, the singularities of GR, the infinite entropy of black holes in the absence of a cutoff and the non-renormalisability of gravity, suggest that the spacetime continuum of GR is not the correct kinematical structure to quantise (however this quantisation may proceed). Indeed, all of the above infinities indicate that the spacetime continuum should be replaced by something fundamentally discrete. This discrete substratum must possess the property that at sufficiently large scales it reduces to the spacetime continuum of GR, approximately. When spacetime is expressed as the pair $(\mathcal{M}, g)$, it is hard to see what such discrete structure might be. However, when expressed as the pair $(<, V)$ things look more promising. The causal set approach to QG is based on the hypothesis that the discrete substratum, underlying the spacetime continuum, is a locally finite partial order, where the order relation, $\prec$, is taken to underly the macroscopic causal structure $<$, and the number of elements N corresponds to the volume V.

Having defined the kinematical structure, we must now specify what we mean by quantisation. There are two main approaches to quantisation, the canonical, "state vector/observable" quantisation based on the Hamiltonian, and the Sum-Over-Histories approach based on the Lagrangian. From the early days of quantum mechanics it was argued by Dirac that an approach to quantum theory based on the Lagrangian would probably be more fundamental than one based on the Hamiltonian, since the former is relativistically invariant whereas the latter is "essentially nonrelativistic". It should therefore come as no surprise that the causal set approach, which is rooted in spacetime causal structure, and is therefore essentially relativistic, fits naturally in the SOH framework. As it is usually taught in undergraduate courses, the SOH approach (more commonly known as the Path Integral approach) is seen as an equivalent alternative to the canonical approach (which in most cases it is), but whose interpretation still relies on the mathematical

machinery of the canonical Hamiltonian approach. The point of view we will take, however, is that the SOH should be viewed as a free standing formulation of quantum mechanics, whose interpretation can be made precise independently of the machinery used in canonical quantum theory. In particular, we view the SOH as a generalised stochastic dynamics, characterised by a non-classical (quantum) measure which allows for interference between pairs of histories.

It is not the scope of this thesis to give precise meaning to the SOH [3], or how to use the SOH to define a quantum dynamics for causal sets. The only thing we will mention is that in the free standing SOH formalism the history itself plays the central role. This history can be whatever we want and in particular, it can be a causal set. So it should be intuitive, if not clear, why quantum causal set dynamics will likely be based on a SOH, which write we as

$$Z = \sum_{\mathcal{C}} e^{iS[\mathcal{C}]},$$

where the sum is over the space of causal sets $\mathcal{C}$, and $S[\mathcal{C}]$ is the action of a causal set.

[3]The interested reader can look at [12] for an introduction to the particular interpretation of the SOH that we have in mind. Or [11] for a good review of the SOH in general.

Chapter 2

Causal Sets

As mentioned in the previous chapter, causal set theory is an approach to quantum gravity in which the fundamental structure of spacetime is postulated to be discrete, and where the only information carried by the sets' elements is causal order, which mathematically defines a partial order. This idea was originally proposed independently by Myrheim [14], t'Hooft [15] and Bombelli *et al.* [16], and has been championed by Sorkin ever since. The causal set approach rests on theorems by D. Malament [17], Levichev [18] and Hawking et al. [19] which state that for distinguishing spacetimes one can recover topological, differentiable and metric structure, up to a conformal factor, from causal structure alone [1]. Therefore in the continuum, causal order and volume information together are enough to recover the full geometry of the spacetime, schematically we could write

"Order + Volume = Geometry".

As was first pointed out by Riemann [20], in a "discrete manifold" volume information is simply given by counting the number of points. Thus, if the order relation of a causal set provides the causal structure and the *number* of elements encodes the volume, then a causal set is capable of giving back the full geometry on scales much larger than the discreteness scale. This is

[1] The precise statement in Malament's theorem is that if there is a bijective map between two past and future distinguishing spacetimes that preserves their causal structure then the map is a conformal isomorphism.

neatly encapsulated in Rafael Sorkin's slogan

"Order + Number = Geometry".

For a more complete review of causal sets see [21, 22, 23, 24].

In the rest of this chapter we define the necessary mathematics needed in the rest of this thesis.

2.1 Definition

A causal set is a locally finite partial order, i.e. it is a pair $(\mathcal{C}, \preceq)$ where $\mathcal{C}$ is a set and $\preceq$ is a partial order relation on $\mathcal{C}$ which is

1. Reflexive $x \preceq x$
2. Acyclic $x \preceq y \preceq x \Rightarrow x = y$
3. Transitive $x \preceq y \preceq z \Rightarrow x \preceq z$, $\forall x, y, z \in \mathcal{C}$.

Local finiteness is the condition that the cardinality of any order interval is finite, i.e. $|I(x, y)| < \infty$, where $I(x, y) = \{z \in \mathcal{C} \,|\, y \preceq z \preceq x\}$. We will write $x \prec y$ when $x \preceq y$ and $x \neq y$. We call $x \prec y$ a link if $x \prec y$ and $n(x, y) := I(x, y) - 2 = 0$. Links are the irreducible relations in a causet.

2.2 Sprinklings

A basic question about a causal set is, under what circumstances can we claim that a spacetime $(\mathcal{M}, g)$ is a good approximation to an underlying causal set $\mathcal{C}$? To answer to this question we introduce the notion of a sprinkling. A sprinkling is a way of generating a causet from a d-dimensional Lorentzian manifold $(\mathcal{M}, g)$. It is a Poisson process of selecting points in $\mathcal{M}$ with density ρ so that the expected number of points sprinkled in a region of space-time volume V is ρV. This process generates a causet whose elements are the sprinkled points and whose order is that induced by the manifolds causal order restricted to the sprinkled points. We say that a causet C is well approximated by a manifold $(\mathcal{M}, g)$ if it could have been generated, with relatively high probability, by sprinkling into $(\mathcal{M}, g)$. Note that this process is *kinematical*, i.e. it is not how causal sets will be generated dynamically. An essential property of the sprinkling process is that it is Lorentz invariant.

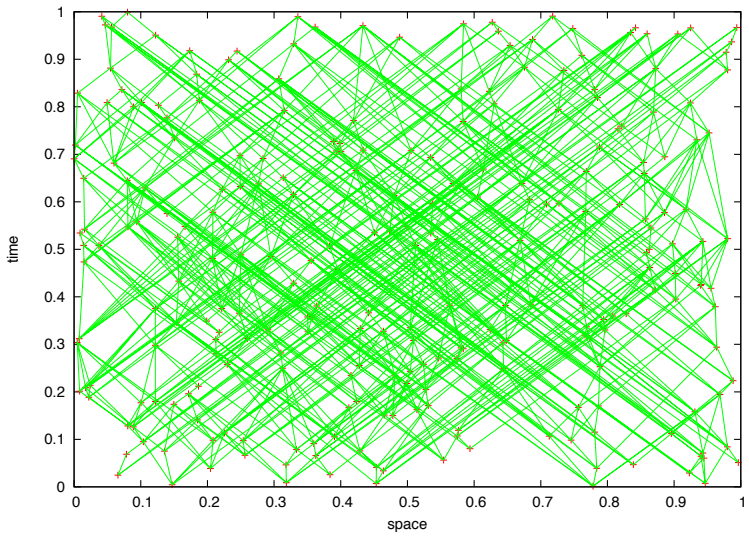

Figure 2.1: A sprinkling of a region of 2D Minkowski spacetime spacetime with links. Note how each point has a large number of nearest neighbours, and how these lie close to the boundary of its casual future or past.

This ensures that the causal sets produced this way are Lorentz invariant [25].

The interplay between discreteness and Lorentz invariance results in a radical (but causal) kind of nonlocality. This can be seen as follows: since the causal set elements, or "atoms of spacetime", that are nearest neighbours to a given atom will be of order one Planck unit of proper time away from it, the locus of such points in the approximating continuum Minkowski spacetime is a hyperboloid of infinite spatial volume, on which Lorentz transformations act transitively. The nearest neighbours therefore will (loosely) comprise this hyperboloid and so there will be an infinite number of them. Where curvature limits Lorentz symmetry, it may render the number of nearest neighbours finite but it will still be huge so long as the radius of curvature is large compared to the Planck length. This effect can be seen clearly in figures 2.1 and 2.2, which show sprinklings into finite regions of $\mathbb{M}^2$ and $2d$ de Sitter respectively, with links.

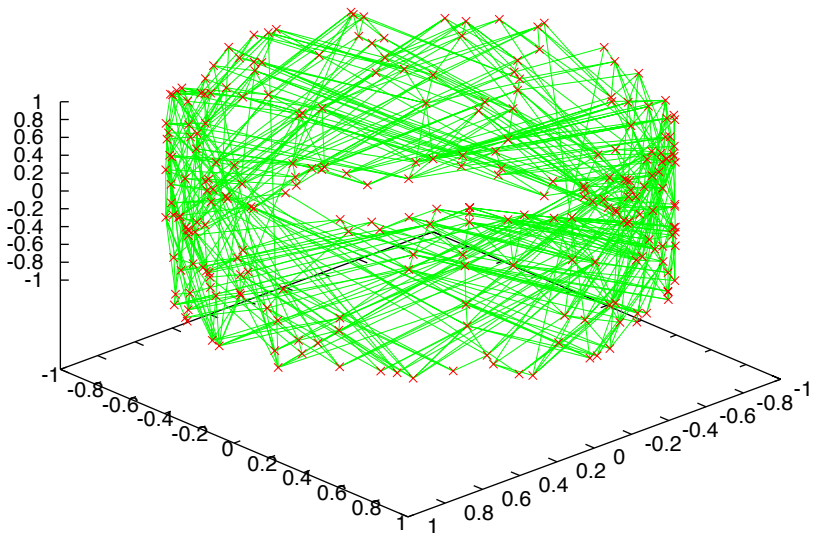

Figure 2.2: A sprinkling of a region of 2D de Sitter spacetime with links. Note how each point has a large number of nearest neighbours, and how these lie close to the boundary of its casual future or past.

Chapter 3

Causal Set d'Alembertians

3.1 Lorentz Invariance, Discreteness and Non-locality

We showed in the previous chapter that the discreteness and Lorentz invariance of causal sets together result in a radical kind of nonlocality. This nonlocality, were it incorrigible, would block causal sets from being useful phenomenologically and threaten to derail the causal set programme altogether. There is growing evidence however that the nonlocality of Lorentz invariant discrete structures can be tamed. For example there is a quasi-local scalar wave operator, $B^{(2)}$, for fields on causal sets well-approximated by 2 dimensional Minkowski spacetime [26, 21]. This operator tends to the exact (2-dimensional) continuum flat scalar d'Alembertian in the continuum limit. In this chapter we extend this result to 4 dimensions, with the introduction of an analogous operator $B^{(4)}$. We will also prove, under certain conditions, that when $B^{(4)}$ is applied to scalar fields on causal sets which are approximated by 4-dimensional Lorentzian spacetimes, its mean tends in the continuum limit to the curved space operator, $\Box - \frac{1}{2}R$, where $\Box$ is the curved spacetime scalar d'Alembertian and R is the Ricci scalar curvature.

3.2 The 4-dimensional Causet d'Alembertian

We begin by defining some important quantities which will be used throughout the rest of this thesis. Given a point $x \in \mathcal{C}$ we define the set of all its past nearest neighbours to be

$$L_1(x) := \{y \in \mathcal{C} \mid y \prec x,\ n(x,y) = 0\}, \tag{3.1}$$

where $n(x,y) := |I(x,y)| - 2$. We refer to this set of elements as *past layer* 1. We can generalise this by defining the sets of next nearest neighbours, L_2, next next nearest neighbours, L_3, and so on. In general the i-th past layer is defined as

$$L_i(x) := \{y \in \mathcal{C} \mid y \prec x \text{ and } n(x,y) = i-1\}. \tag{3.2}$$

Now consider the following discrete retarded operator B, on a causet $\mathcal{C}$, [8]. If $\phi : \mathcal{C} \to \mathbb{R}$ is a scalar field, then

$$\begin{aligned} B\phi(x) := \frac{4}{\sqrt{6}l^2}\big[&-\phi(x) \\ &+ \Big(\sum_{y\in L_1(x)} -9 \sum_{y\in L_2(x)} +16 \sum_{y\in L_3(x)} -8 \sum_{y\in L_4(x)}\Big)\phi(y)\big], \end{aligned} \tag{3.3}$$

where l is a length. B is defined on scalar fields on any causal set but is particularly relevant for causal sets that are well-approximated by a 4-dimensional Lorentzian manifold, $(\mathcal{M}, g)$.

Let ϕ be a real test field of compact support on $\mathcal{M}$ and $x \in \mathcal{M}$. If we sprinkle $\mathcal{M}$ at density ρ, include x in the resulting causet $\mathcal{C}$, then, as mentioned in section 2.2, $L_1(x) \subset \mathcal{C}$ will be a very large set whose elements lie in the causal past of x, $J^-(x)$, and hug the boundary of $J^-(x)$, their locus being roughly that of the surface of points which lies one Planck time away from x. The elements of $L_2(x)$ will also be distributed down the inside of the boundary of $J^-(x)$, just inside layer 1, and so on. The value of $B\phi(x)$ on $\mathcal{C}$ looks like a highly nonlocal quantity, involving the value of ϕ at enormous numbers of points outside any fixed neighbourhood of x.

The sprinkling process at density ρ produces, for each point x of $\mathcal{M}$, a random variable whose value is $B\phi(x)$ on the realisation $\mathcal{C}$ of the process. The expectation value of this random variable is given by the spacetime integral

$$\begin{aligned} \bar{B}\phi(x) := \mathbb{E}(B\phi(x)) = \frac{4\sqrt{\rho}}{\sqrt{6}}\big[&-\phi(x) \\ &+ \rho \int_{y\in J^-(x)} d^4y\, \sqrt{-g}\, \phi(y)\, e^{-\xi}(1 - 9\xi + 8\xi^2 - \frac{4}{3}\xi^3)\big], \end{aligned} \tag{3.4}$$

where $\xi := \rho V(y)$, $V(y)$ is the volume of the causal interval between x and y. To prove this imagine discretising the sprinkled spacetime into small cells of

volume ΔV, labelled by I, and let m_I be the number of elements sprinkled between x and the I-th cell. Define a random variable χ_I by

$$\chi_I = \begin{cases} 1 & \text{if cell } I \text{ is filled} \\ 0 & \text{otherwise.} \end{cases} \tag{3.5}$$

then $\mathbb{E}(\chi_I) = \rho\Delta V + \text{h.o.t.}$. The mean of the sum over the first layer, L_1, is

$$\langle \sum_I \sum_{y \in L_1} \chi_I \phi(y) \rangle = \sum_I \langle \chi_I \rangle \times \mathbb{P}(m_I = 0)\phi(y) = \sum_I \rho\Delta V \, e^{-\rho V_I} \phi(y), \tag{3.6}$$

where we used angled brackets to denote expectation values, V_I is the volume of the causal interval between x and the I-th cell, and the first equality holds because the two random variables are independent. Taking the limit in which the cells become infinitesimally small, $\Delta V \to dV$ we get

$$\int_{y \in J^-(x)} \rho dV e^{-\rho V(x,y)} \phi(y). \tag{3.7}$$

And similarly for the sums over the other layers.

We can see that the integrand in (3.4) is small wherever ξ is large, *i.e.* wherever the spacetime volume of the causal interval between x and y is larger than a few Planck volumes. But, ξ is small for the part of the integration range which is exactly that region close to the boundary of $J^-(x)$. In the following sections we will prove that, for large enough ρ, $\bar{B}\phi(x)$ is effectively local and is dominated by contributions from a neighbourhood of x: the contributions from far down the boundary of $J^-(x)$ cancel out. In particular we will prove

$$\lim_{\rho \to \infty} \bar{B}\phi(x) = \Box\phi(x) - \frac{1}{2} R(x)\phi(x) \tag{3.8}$$

under certain assumptions about the support of ϕ in $(\mathcal{M}^{(4)}, g)$.

3.3 Proof: Sprinklings of Minkowski Spacetime

Before proving the curved spacetime result (3.8), it is instructive to consider the simpler case of a sprinkling in $\mathbb{M}^4$ for which we will show that $\lim_{\rho\to\infty} \bar{B}\phi(x) = \Box\phi(x)$. This will provide the basic framework on which

the curved spacetime proof rests.

Choose x as the origin of cartesian coordinates $\{y^\mu\}$ and in that frame define the usual spatial polar coordinates: $r = \sqrt{\sum_{i=1}^3 (y^i)^2}$, θ and φ. Null radial coordinates are defined by $u = \frac{1}{\sqrt{2}}(y^0 - r)$ and $v = \frac{1}{\sqrt{2}}(y^0 + r)$. For convenience in what follows, so that we don't have negative coordinates to deal with, we use time reversed coordinates, $y^0 \to -y^0$ so that $u \to -v$ and $v \to -u$. The volume, $V(y)$, of the causal interval between $\{y^\mu\}$ and the origin is $V(y) = \frac{\pi}{6} u^2 v^2$.

Let us take the region of integration $\mathcal{R}$ to be the portion of the causal past of the origin for which $u^2 + v^2 \leq L^2$, where L is large enough that the support of ϕ is well within $\mathcal{R}$. $\mathcal{R}$ can be split into 3 parts:

$$W_1 := \{y \in \mathcal{R} \,|\, 0 \leq u \leq v \leq a\} \tag{3.9}$$

$$W_2 := \{y \in \mathcal{R} \,|\, a \leq v \leq L,\ 0 \leq u \leq \frac{a^2}{v}\} \tag{3.10}$$

$$W_3 := \mathcal{R} \setminus (W_1 \cup W_2)\,, \tag{3.11}$$

where $a > 0$ is chosen small enough that the expansions of ϕ used in the following calculation are valid, and is independent of ρ. W_1 is a neighbourhood of the origin, W_2 is a neighbourhood of the past lightcone and bounded away from the origin and W_3 is a subset of the interior of the causal past that is bounded away from the lightcone.

Consider first the integral in (3.4) with the range of integration restricted to W_3

$$\int_{W_3} d^4y\ \phi(y) e^{-\rho V(y)} \times (1 - 9\rho V(y) + 8(\rho V(y))^2 - \frac{4}{3}(\rho V(y))^3)\,. \tag{3.12}$$

$V(y)$ is bounded away from zero in W_3, indeed $V(y) \geq V_{\min} = \frac{\pi}{6} a^4$ so

$$\begin{aligned} &\left| \int_{W_3} d^4y\ \phi(y)\, e^{-\rho V(y)} (1 - 9\rho V(y) + 8(\rho V(y))^2 - \frac{4}{3}(\rho V(y))^3) \right| \\ \leq\, & e^{-\rho V_{\min}} \int_{W_3} \left| \phi(y)(1 - 9\rho V(y) + 8(\rho V(y))^2 - \frac{4}{3}(\rho V(y))^3) \right| \end{aligned} \tag{3.13}$$

which tends to zero faster than any power of ρ^{-1} as $\rho \to \infty$.

Consider now the integral over W_2. Note first that

$$e^{-\xi}(1 - 9\xi + 8\xi^2 - \frac{4}{3}\xi^3) = \hat{\mathcal{O}}e^{-\xi} \tag{3.14}$$

where

$$\hat{\mathcal{O}} := \frac{4}{3}(H + \frac{1}{2})(H + 1)(H + \frac{3}{2}) \tag{3.15}$$

$$= 1 + 9H_1 + 8H_2 + \frac{4}{3}H_3 \tag{3.16}$$

and

$$H_n := \rho^n \frac{\partial^n}{\partial \rho^n} \quad \text{and} \quad H \equiv H_1 \,. \tag{3.17}$$

$\hat{\mathcal{O}}$ annihilates $\rho^{-\frac{1}{2}}$, ρ^{-1} and $\rho^{-\frac{3}{2}}$. The integral we are evaluating can be rewritten as $J_2 = \hat{\mathcal{O}} I_2$, where

$$I_2 = \int_a^L dv \int_0^{\frac{a^2}{v}} du \int d\Omega_2 \, \frac{1}{2}(v-u)^2 \phi(y) e^{-\rho V_0(y)}. \tag{3.18}$$

We will show that J_2 tends to zero faster than $\rho^{-\frac{3}{2}}$ and so makes no contribution to the limit. Let $g(u,v) := \int d\Omega_2 \, \frac{1}{2}(v-u)^2 \phi(y)$, then

$$I_2 = \int_a^L dv \int_0^{\frac{a^2}{v}} du \, g(u,v) e^{-\rho \frac{\pi}{6} u^2 v^2}, \tag{3.19}$$

where we used the fact that $\tau^2 = 2uv$. Integrating by parts in u and absorbing $\pi/6$ in the definition of ρ gives

$$\begin{aligned}
&\int_a^L dv \int_0^{\frac{a^2}{v}} du \, g(u,v) e^{-\rho u^2 v^2} \\
&= \int_a^L dv \left[\frac{\sqrt{\pi}\,\mathrm{erf}(a^2\sqrt{\rho})}{2\sqrt{\rho}v} g(\frac{a^2}{v}, v) - \int_0^{\frac{a^2}{v}} du \frac{\sqrt{\pi}\,\mathrm{erf}(uv\sqrt{\rho})}{2\sqrt{\rho}v} g_{,u}(u,v) \right] \\
&= \rho^{-\frac{1}{2}} \int_a^L \frac{dv}{2v} \sqrt{\pi} g(\frac{a^2}{v}, v) - \rho^{-\frac{1}{2}} \int_a^L \frac{dv}{2v} \sqrt{\pi}\,\mathrm{erfc}(a^2\sqrt{\rho}) g(\frac{a^2}{v}, v) \\
&\quad - \rho^{-\frac{1}{2}} \int_a^L \frac{dv}{2v} \int_0^{\frac{a^2}{v}} du \sqrt{\pi}\,\mathrm{erf}(uv\sqrt{\rho}) g_{,u}(u,v)
\end{aligned} \tag{3.20}$$

The first term of (3.20) vanishes on application of $\hat{\mathcal{O}}$. Since $v \geq a$, the second

term tends to zero exponentially in the limit $\rho \to \infty$, as do all derivatives of the second term w.r.t. ρ. Thus $\hat{\mathcal{O}}$ acting on the second term gives something that tends to zero exponentially fast in the limit. For the third term we use the following property of $\hat{\mathcal{O}}$

$$\hat{\mathcal{O}}\left(\frac{\mathrm{erf}(\sqrt{\rho}uv)}{\sqrt{\rho}}\right) = \frac{2}{\sqrt{\pi}}uv\hat{\mathcal{P}}e^{-\rho u^2v^2}, \tag{3.21}$$

where $\hat{\mathcal{P}} = \frac{2}{3}(H+1)(H+\frac{3}{2})$ ($\hat{\mathcal{P}}$ annihilates ρ^{-1} and $\rho^{-\frac{3}{2}}$), so we get

$$-\hat{\mathcal{P}}\int_a^L dv \int_0^{\frac{a^2}{v}} du\, u\, g_{,u}(u,v)e^{-\rho u^2v^2}\,. \tag{3.22}$$

We repeat the steps of integrating by parts and discarding terms that vanish in the limit. We have to do it twice more before we obtain an integral we can bound. So,

$$\begin{aligned}
&\int_a^L dv \int_0^{\frac{a^2}{v}} du\, u\, g_{,u}(u,v)e^{-\rho u^2v^2} \\
&= -\rho^{-1}\int_a^L \frac{dv}{2v^2}\, g_{,u}(0,v) + \rho^{-1}\int_a^L \frac{dv}{2v^2}\, e^{-\rho a^2v^2}\, g_{,u}(\frac{a^2}{v},v) \\
&\quad - \rho^{-1}\int_a^L \frac{dv}{2v^2}\int_0^{\frac{a^2}{v}} du\, e^{-\rho u^2v^2} g_{,uu}(u,v)\,.
\end{aligned} \tag{3.23}$$

The first term is killed by $\hat{\mathcal{P}}$ and the second term (and its ρ derivatives) tends to zero exponentially fast as $\rho \to \infty$. The final term gives, on integration by parts,

$$\begin{aligned}
&-\rho^{-\frac{3}{2}}\int_a^L \frac{dv}{4v^3}\sqrt{\pi}\left(g_{,uu}(\frac{a^2}{v},v) - g_{,uu}(0,v)\right) \\
&+\rho^{-\frac{3}{2}}\int_a^L \frac{dv}{4v^3}\sqrt{\pi}\,\mathrm{erfc}(a^2\sqrt{\rho})g_{,uu}(\frac{a^2}{v},v) \\
&+\rho^{-\frac{3}{2}}\int_a^L \frac{dv}{4v^3}\int_0^{\frac{a^2}{v}} du\,\sqrt{\pi}\,\mathrm{erf}(uv\sqrt{\rho})g_{,uuu}(u,v).
\end{aligned} \tag{3.24}$$

The first term is killed by $\hat{\mathcal{P}}$ and the second and its derivatives are expo-

nentially small. The third and final term on application of $\hat{\mathcal{P}}$ is

$$\begin{aligned}&\hat{\mathcal{P}}\rho^{-\frac{3}{2}}\int_a^L \frac{dv}{4v^3}\int_0^{\frac{a^2}{v}} du\sqrt{\pi}\,\mathrm{erf}(uv\sqrt{\rho})g_{,uuu}(u,v)\\&=-\frac{1}{6}\int_a^L dv\int_0^{\frac{a^2}{v}} du\,u^3e^{-\rho u^2v^2}g_{,uuu}(u,v).\end{aligned}\tag{3.25}$$

We can now bound this term

$$\left|\int_a^L dv\int_0^{\frac{a^2}{v}} du\,u^3e^{-\rho u^2v^2}g_{,uuu}(u,v)\right|\leq \|g_{,uuu}\|_2\int_a^L dv\int_0^{\frac{a^2}{v}} du\,u^3e^{-\rho u^2v^2}\tag{3.26}$$

where $\|g_{,uuu}\|_2$ is the uniform norm of $g_{,uuu}$ over the integration range. The remaining integral can be done

$$\int_a^L dv\int_0^{\frac{a^2}{v}} du\,u^3e^{-\rho u^2v^2}=\left(\frac{1}{6a^3}-\frac{1}{6L^3}\right)\rho^{-2}\tag{3.27}$$

up to exponentially decaying terms as $\rho\to\infty$.

Now consider the contribution coming from the near region, I_1. Since the integral is over a small neighbourhood of the origin we can expand the field as

$$\phi(y)=\phi(0)+y^\mu\phi_{,\mu}(0)+\frac{1}{2}y^{,\mu}y^\nu\phi_{,\mu\nu}(0)+y^\mu y^\nu y^\alpha\psi_{\mu\nu\alpha}(y),\tag{3.28}$$

where $\psi_{\mu\nu\alpha}(y)$ is some smooth function of the y^μ. Plugging this into I_1 and performing a few simple integrations gives

$$\hat{\mathcal{O}}\int_0^a dv\int_0^v du\int d\Omega_2\frac{(v-u)^2}{2}\phi(0)e^{-\rho\frac{\pi}{6}u^2v^2}=\frac{1}{\rho}(1-e^{-\frac{\pi}{6}\rho a^4})\phi(0),\tag{3.29}$$

$$\begin{aligned}&\hat{\mathcal{O}}\int_0^a dv\int_0^v du\int d\Omega_2\frac{(v-u)^2}{2}y^\mu\phi_{,\mu}(0)e^{-\rho\frac{\pi}{6}u^2v^2}\\&=\left(\frac{6\sqrt{2}}{a^3\pi\rho^2}(1-e^{-\frac{\pi}{6}\rho a^4})-\frac{\sqrt{2}a}{\rho}e^{-\frac{\pi}{6}\rho a^4}\right)\phi_{,t}(0)\end{aligned}\tag{3.30}$$

for the first two terms of (3.28). After multiplying by $\rho^{3/2}$, (3.29) cancels with the delta function term in (3.38) (up to exponentially small terms)

while (3.30) goes to zero in the limit $\rho \to \infty$. The third term in (3.28) is that of most interest to us, it gives

$$\begin{aligned}&\rho^{\frac{3}{2}}\hat{\mathcal{O}}\int_0^a dv\int_0^v du\int d\Omega_2\frac{1}{2}(v-u)^2 y^\mu y^\nu \phi_{,\mu\nu}(0)e^{-\rho\frac{\pi}{6}u^2v^2}\\&=\Box\phi(0)-\frac{4\sqrt{6}}{a^2\pi\sqrt{\rho}}\phi_{,ii}(0)+\frac{9}{a^4\pi\rho}\left(\phi_{,ii}(0)+3\phi_{,tt}(0)\right)\end{aligned}\tag{3.31}$$

up to exponentially small terms. Finally we need to show that the integral

$$\hat{\mathcal{O}}\int_0^a dv\int_0^v du\int d\Omega_2\frac{(v-u)^2}{2}y^\mu y^\nu y^\alpha \psi_{,\mu\nu\alpha}(y)e^{-\rho\frac{\pi}{6}u^2v^2}\tag{3.32}$$

does not contribute in the limit. Integrating over the angles one finds that the above is given by a sum of integrals of the form

$$\hat{\mathcal{O}}\int_0^a dv\int_0^v du\, u^m v^n\,\psi(u,v)\,e^{-\rho\frac{\pi}{6}u^2v^2},\quad m+n=5\tag{3.33}$$

where $\psi(u,v)$ is some unknown function which involves at least three derivatives of ϕ. These integrals are shown to go to zero in the limit in appendix A. We can see that (3.31) contains the only term which survives in the limit $\rho\to\infty$, the d'Alembertian $\Box\phi$, which proves the result.

3.3.1 Corrections

We can estimate the size of the corrections to the limiting value of the causet d'Alembertian, B, at finite ρ. If spacetime truly is fundamentally discrete then such corrections can play an important phenomenological role.

Using (A.13) we find that, to first order, the corrections go like

$$||\phi''''||_1\rho^{-\frac{1}{2}}\log(\rho a^4),\tag{3.34}$$

where $||\phi''''||_1$ is the uniform norm of the fourth derivative of ϕ in W_1. So $B\phi$ will be a good approximation to $\Box\phi$ when the characteristic length scale λ over which ϕ varies satisfies $\lambda^2 \gg l^2\log(\frac{a}{l})$. This inequality expresses the simple fact that the causal set cannot support waves whose wavelength is smaller than the discreteness scale itself. There are other corrections coming from W_2, (3.26)-(3.27), which lead to the following extra conditions for B

to be a good approximation to $\Box$ at finite density

$$\frac{l^2}{a^3}||\tilde{\phi}_{,u}||_2 \ll \Box\phi, \quad \frac{l^2}{a^2}||\tilde{\phi}_{,uu}||_2 \ll \Box\phi, \quad \frac{l^4}{a^3}||\tilde{\phi}_{,uuu}||_2 \ll \Box\phi \tag{3.35}$$

where $\tilde{\phi} = \int d\Omega\, \phi$.

3.4 Proof: Sprinklings of Curved Spacetimes

Having proved the result for flat spacetimes we now prove it for sprinklings into curved spacetimes. We assume that the field ϕ is of compact support, and that $J^-(x) \cap \mathrm{supp}(\phi)$ is contained in a normal neighbourhood of the origin (further details about the assumptions will be given at the relevant stages of the proof). These assumptions will allow us to expand the metric and the volume of causal intervals around their flat limits, and hence to closely mimic the flat spacetime proof of the previous section in the sense that we will do the integrals by splitting the region of integration into three parts and show that only the contribution coming from a small neighbourhood of the origin is non-zero in the limit.

Consider first the integral in (3.4) with the range of integration restricted to the complement of any neighbourhood, $\mathcal{U}$ of $\partial J^-(x)$:

$$\int_{J^-(x)\setminus\mathcal{U}} d^4y\, \sqrt{-g}\, \phi(y) e^{-\rho V(y)} \times (1 - 9\rho V(y) + 8(\rho V(y))^2 - \frac{4}{3}(\rho V(y))^3)\,. \tag{3.36}$$

$V(y)$ is bounded away from zero over $J^-(x)\setminus\mathcal{U}$. Since, otherwise there'd be a point p in the interior of $J^-(x)$ which is timelike related to x but such that the volume of the causal interval between p and x is zero, a contradiction. So

$$\begin{aligned}&\left|\int_{J^-(x)\setminus\mathcal{U}} d^4y\, \sqrt{-g}\, \phi(y)\, e^{-\rho V(y)}(1 - 9\rho V(y) + 8(\rho V(y))^2 - \frac{4}{3}(\rho V(y))^3)\right| \\ &\leq\ e^{-\rho V_{\min}} \int_{J^-(x)\setminus\mathcal{U}} \sqrt{-g}\left|\phi(y)(1 - 9\rho V(y) + 8(\rho V(y))^2 - \frac{4}{3}(\rho V(y))^3)\right|\end{aligned} \tag{3.37}$$

which tends to zero faster than any power of ρ^{-1} as $\rho \to \infty$. Therefore, to

prove the result, we need only show

$$\lim_{\rho\to\infty}\frac{4\sqrt{\rho}}{\sqrt{6}}\left[-\phi(x)+\rho\int_{y\in\mathcal{U}\cap J^-(x)}d^4y\,\sqrt{-g}\,\phi(y)\,e^{-\xi}(1-9\xi+8\xi^2-\frac{4}{3}\xi^3)\right]$$
$$=\Box\phi(x)-\frac{1}{2}R(x)\phi(x), \tag{3.38}$$

for any single neighbourhood, $\mathcal{U}$, of $\partial J^-(x)$, which we may take as small as we like.

Consider "partitioning" this neighbourhood into a normal neighbourhood $\mathcal{N}$ of x and a neighbourhood of the light cone bounded away from the origin, $\mathcal{M}$, such that their union contains $\partial J^-(x)\cap\mathrm{Supp}(\phi)$. Define null Riemann normal coordinates in $\mathcal{N}$: $t:=y^0$, $r^2:=\sum_{i=1,2,3}(y^i)^2$, null coordinates $u=\frac{1}{\sqrt{2}}(t-r)$ and $v=\frac{1}{\sqrt{2}}(t+r)$, and the usual polar angular coordinates, θ and ϕ, together with global Fermi normal coordinates (w,z,θ,φ) defined in the next section, in $\mathcal{M}$. Again we use time reversed coordinates, $t\to-t$ so that $u\to-v$, $v\to-u$, $w\to-z$ and $z\to-w$. Consider the subsets W_1 and W_2 of $\mathcal{N}$ and $\mathcal{M}$ respectively:

$$W_1:=\{y\in\mathcal{U}\,|\,0\le u\le v\le a\}, \tag{3.39}$$
$$W_2:=\{y\in\mathcal{U}\,|\,a'\le w\le L,\ 0\le z\le A(w,\theta,\varphi)\}, \tag{3.40}$$

where where $L>0$ is large enough so that $W_1\cup W_2$ contains $\partial J^-(x)\cap\mathrm{Supp}(\phi)$, $a>0$ is chosen small enough so that the derivatives taken in the following calculations are defined and so that the correction to the first term in the expansion of $V(y)$ in proper time is small, and $A=A(w,\theta,\varphi)$ is also "small" in a sense which will be explained at the appropriate step in the proof. a' is chosen small enough such that regions W_1 and W_2 overlap (see figure (3.1)) in a subregion, $W_1\cap W_2\subset W_1$, which is bounded away from the origin. It follows from the "near region" proof in section 3.4.2 that any contribution coming from a subregion of W_1 which is bounded away from the origin is zero in the limit, so that this overlap does not contribute in the limit. Again let $J_i=\hat{\mathcal{O}}I_i$ where

$$I_i=\int_{W_i}d^4y\,\sqrt{-g}\,\phi(y)e^{-\xi} \tag{3.41}$$

$i=1,2$.

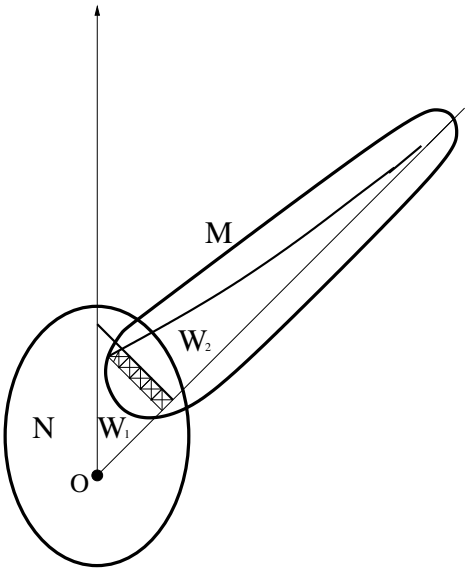

Figure 3.1: A sketch of the neighbourhoods $\mathcal{N}$ and $\mathcal{M}$, and the regions of integration $W_1 \subset \mathcal{N}$ and $W_2 \subset \mathcal{M}$.

3.4.1 Down the light cone

We begin by proving that the the contribution coming from W_2, namely J_2, goes to zero in the limit. Choose a normal neighbourhood of the origin together with a Riemann normal coordinate (RNC) system centred at the origin, and fix a set of null vectors, $N(\theta, \varphi)$, parametrized by θ, φ according to the RNC. On each null geodesic $\gamma(\theta, \varphi)$ defined by parallely transporting $N(\theta, \varphi)$ along itself we define affine coordinate w. The final coordinate is given by affine distance z along a null geodesic λ from "base point" p on $\gamma(\theta, \varphi)$ with coordinates $(w, 0, \theta, \phi)$, whose tangent vector, when parallely transported to the origin of the coordinates is $N(\pi - \theta, \pi + \varphi)$. We assume there is a neighbourhood of the lightcone in which coords (w, z, θ, ϕ) exist and such that in a neighbourhood of any null geodesic $\gamma(\theta, \varphi)$, Fermi Null coordinates (x^+, x^-, x^1, x^2) [27] defined using the two null vectors at the origin, $N(\theta, \varphi)$ to define x^+ and $N(\pi - \theta, \pi + \varphi)$ to define x^-, coincide to the extent that the point (w, z, θ, φ) is the point $(x^+ = w, x^- = z, x^a = 0)$.

We want to bound $\rho^{\frac{3}{2}}\hat{\mathcal{O}}I_2$ where

$$I_2 = \int_a^L dw \int d\Omega_2 \int_0^{\frac{a^2}{\sqrt{h(w,\theta,\varphi)}}} dz \sqrt{-g(y)} \frac{1}{2}(w-z)^2 \phi(y) e^{-\rho V(y)}, \qquad (3.42)$$

$\int d\Omega_2 = \int_0^\pi d\theta \int_0^{2\pi} d\varphi \sin\theta$ and $h(w,\theta,\varphi)$ is some unknown function which we define shortly. It is shown in appendix B that in the limit $z \to 0$

$$V(y) = z^2 h(w,\theta,\varphi) + z^3 g(w,z,\theta,\varphi). \tag{3.43}$$

We will assume that z is always chosen to be sufficiently small so that the causal interval between y and the origin is contained in the normal neighbourhood in which global FNCs hold. Using (3.43) we can write the exponential term in (3.42) as

$$e^{-\rho V(y)} = e^{-\rho z^2 h}\left(1 - \rho z^3 g + \frac{1}{2}\rho^2 z^6 g^2 + \sum_{k=3}^{\infty} \frac{(-\rho)^k}{k!} z^{3k} g^k\right). \tag{3.44}$$

Then $I_2 = I_{21} + I_{22} + I_{23} + I_{24}$, where

$$I_{21} = \int_a^L dw \int d\Omega_2 \int_0^{\frac{a^2}{\sqrt{h}}} dz f_1(w,z,\theta,\varphi) e^{-\rho z^2 h(w,\theta,\varphi)}, \tag{3.45}$$

$$I_{22} = -\rho \int_a^L dw \int d\Omega_2 \int_0^{\frac{a^2}{\sqrt{h}}} dz\, z^3 f_2(w,z,\theta,\varphi) e^{-\rho z^2 h(z,\theta,\varphi)}, \tag{3.46}$$

$$I_{23} = +\frac{1}{2}\rho^2 \int_a^L dw \int d\Omega_2 \int_0^{\frac{a^2}{\sqrt{h}}} dz\, z^6 f_3(w,z,\theta,\varphi) e^{-\rho z^2 h(w,\theta,\varphi)}, \tag{3.47}$$

$$\begin{aligned} I_{24} = -\frac{1}{2}\rho^3 \int_a^L dz \int d\Omega_2 \int_0^{\frac{a^2}{\sqrt{h}}} dw \sqrt{-g(y)}\phi(y)(w-z)^2 e^{-\rho z^2 h(w,\theta,\varphi)} \\ \times g(w,z,\theta,\varphi)^3 z^9 \sum_{k=0}^{\infty} \frac{(-\rho)^k}{(k+3)!}(z^3 g(w,z,\theta,\varphi))^k, \end{aligned} \tag{3.48}$$

and where

$$f_i(w,z,\theta,\varphi) = \frac{1}{2}\sqrt{-g(y)}(w-z)^2\phi(y)\, g(w,z,\theta,\varphi)^{i-1}, \quad i = 1,2,3. \tag{3.49}$$

Note that the region of integration for all the integrals is bounded because ϕ is of compact support, and the sum in the integrand of I_{24} is uniformly convergent. It is shown in appendix A.2 that $\hat{\mathcal{O}} I_{21} = O(\rho^{-2})$, $\hat{\mathcal{O}} I_{22} = O(\rho^{-2})$ and $\hat{\mathcal{O}} I_{23} = O(\rho^{-2})$ as $\rho \to \infty$. The only term left to bound is $\hat{\mathcal{O}} I_{24}$ and we can bound each term in $(1 + 9H_1 + 8H_2 + \frac{4}{3}H_3) I_{24}$ separately.

Let $\bar{g}(w,\theta,\varphi) := \|g(w,z,\theta,\varphi)\|_z$ where $\|\cdot\|_z$ denotes uniform norm over

the range of z for some fixed (w, θ, φ), then

$$\left| \sum_{k=0}^{\infty} \frac{(-\rho)^k}{(k+3)!} (z^3 g(w, z, \theta, \varphi))^k \right| \leq \frac{1}{6} e^{\rho z^3 \bar{g}} \tag{3.50}$$

$\forall y \in W_2$. We now need to choose a small enough value of a (independent of ρ) such that $z^3 \bar{g} < \frac{z^2 h}{2}$ in W_2. Choosing $a^2 < h^{3/2}/(2\bar{g})$ ensures the above is satisfied – note that $\bar{g}$ depends on a but it decreases monotonically with decreasing a and so the condition can be satisfied – then

$$|I_{24}| \leq \frac{\rho^3}{2} \int_a^L dw \int d\Omega_2 \int_0^{\frac{a^2}{\sqrt{h}}} dz \, (w-z)^2 \left| \sqrt{-g(y)} \phi(y) \right| \bar{g}^3 z^9 \tag{3.51}$$

$$\leq \#c\rho^3 \int_a^L dw \int d\Omega_2 \int_0^{\frac{a^2}{\sqrt{h}}} dz \, z^9 e^{-\frac{\rho}{2} z^2 h} \tag{3.52}$$

where $c = \bar{g}^3 \left\| (w-z)^2 \int d\Omega_2 \sqrt{-g(y)} |\phi(y)| \right\|_2$ and "#" denotes a constant numerical factor independent of the parameters. The integral

$$\int_0^{\frac{a^2}{\sqrt{h}}} dz \, z^9 e^{-\frac{\rho}{2} z^2 h} = \# \frac{1}{\rho^5 h(w, \theta, \varphi)^5}, \tag{3.53}$$

ignoring exponentially decaying terms so $I_{24} = O(\rho^{-2})$. The other terms in $\hat{\mathcal{O}} I_{24}$ are also $O(\rho^{-2})$. The calculations are similar to that shown above and are relegated to appendix A.3.

3.4.2 The near region

Having shown that the contributions to the mean from down the light cone vanish in the continuum limit, we can conclude that the result must be local, since we can choose a to be arbitrarily small. The value of $\lim_{\rho \to \infty} \bar{B}\phi(x)$ must therefore only depend on quantities local at x. The only terms of the correct dimensions are $\Box\phi(x)$ and $R(x)\phi(x)$ and if it is finite, the answer will be a linear combination of the two.

So we want to show that

$$\lim_{\rho \to \infty} \left(\rho^{\frac{3}{2}} \hat{\mathcal{O}} I_1 - \rho^{\frac{1}{2}} \phi(x) \right) = \frac{\sqrt{6}}{4} \left(\Box\phi(x) - \frac{1}{2} R(x) \phi(x) \right), \tag{3.54}$$

where

$$I_1 = \int_0^a dv \int_0^v du \int d\Omega_2 \frac{(v-u)^2}{2} \sqrt{-g(y)}\phi(y) e^{-\rho V(y)}. \tag{3.55}$$

In W_1, we have expansions in normal coordinates:

$$\sqrt{-g} = 1 - \frac{1}{6} y^\mu y^\nu R_{\mu\nu}(0) + y^\mu y^\nu y^\rho T_{\mu\nu\rho}(y). \tag{3.56}$$

$$\begin{aligned}\phi(y) = \phi(0) + y^\mu \phi_{,\mu}(0) + \frac{1}{2} y^\mu y^\nu \phi_{,\mu\nu}(0) \\ + y^\mu y^\nu y^\alpha \psi_{\mu\nu\alpha}(y)\end{aligned} \tag{3.57}$$

$$\begin{aligned}V(y) = \frac{\pi}{24}\tau^4 - \frac{\pi}{4320}\tau^6 R(0) + \frac{\pi}{720}\tau^4 y^\mu y^\nu R_{\mu\nu}(0) \\ + y^{\mu_1} \dots y^{\mu_7} S_{\mu_1 \dots \mu_7}(y) = V_0(y) + \delta V(y)\end{aligned} \tag{3.58}$$

where $V_0(y) = \frac{\pi}{24}\tau^4$ and $\delta V(y)$ is the rest, $T_{\mu\nu\rho}(y)$, $\psi_{\mu\nu\alpha}(y)$ and $S_{\mu_1\dots\mu_7}(y)$ are smooth functions of y, and we used the Myrheim-Gibbons-Soloduhkin formula for the volume of small causal intervals in curved spacetimes [14, 28]. Equation (7) of [28] uses the scalar curvature and Ricci tensor evaluated at the midpoint of the causal diamond. In our case however, these are evaluated at the future tip[1]. It can be shown that to the order we're interested in, this does not affect the volume expansion.

Using (3.44) and (3.56)-(3.58) one can expand the integrand in (3.55) and collect the terms in 4 groups:

$$A(y) = \phi + \frac{1}{2} y^\mu y^\nu \phi_{,\mu\nu} - \frac{1}{6}\phi\, y^\mu y^\nu R_{\mu\nu} + \frac{\rho\pi\tau^4}{4320}\phi(\tau^2 R - 6 y^\mu y^\nu R_{\mu\nu}), \tag{3.59}$$

$$\begin{aligned}B(y) = &\left(1 - \frac{1}{6} y^\mu y^\nu R_{\mu\nu}\right) y^\alpha \phi_{,\alpha} - \frac{1}{12} y^\mu y^\nu y^\alpha y^\beta R_{\mu\nu}\phi_{,\alpha\beta} \\ &- \frac{1}{6}\rho y^\mu y^\nu R_{\mu\nu}\phi \left(\frac{\pi}{4320}\tau^6 R - \frac{\pi}{720}\tau^4 y^\alpha y^\beta R_{\alpha\beta}\right) \\ &+ \frac{1}{2}\rho(y^\mu y^\nu \phi_{,\mu\nu} + 2 y^\mu \phi_{,\mu})(1 - \frac{1}{6} y^\alpha y^\beta R_{\alpha\beta}) \\ &\times \left(\frac{\pi}{4320}\tau^6 R - \frac{\pi}{720}\tau^4 y^\gamma y^\delta R_{\gamma\delta}\right)\end{aligned} \tag{3.60}$$

[1] In fact it's the past tip since we have reversed the direction of time

$$
\begin{aligned}
C(y) = &\left[\sqrt{-g}\, y^\mu y^\nu y^\alpha \psi_{\mu\nu\alpha}(y) + y^\mu y^\nu y^\rho T_{\mu\nu\rho}(y) \left(\phi + y^\beta \phi_{,\beta} + \frac{1}{2} y^\beta y^\gamma \phi_{,\beta\gamma}\right)\right] \\
&\times \left(1 - \rho\delta V + \frac{1}{2}\rho^2 \delta V(y)^2\right) \\
&- \rho\, y^{\mu_1} \dots y^{\mu_7} S_{\mu_1 \dots \mu_7}(y) \left(\phi + y^\mu \phi_{,\mu} + \frac{1}{2} y^\mu y^\nu \phi_{,\mu\nu}\right) \\
&\times \left(1 - \frac{1}{6} y^\rho y^\sigma R_{\rho\sigma}\right), \\
D(y) = &\sqrt{-g(y)}\phi(y) \sum_{k=3}^{\infty} \frac{(-\rho)^k}{k!} (\delta V)^k,
\end{aligned}
\tag{3.61}
$$

such that

$$
\sqrt{-g}\phi(y) e^{-\rho V} = \left(A(y) + B(y) + C(y) + D(y)\right) e^{-\rho V_0}, \tag{3.62}
$$

and

$$
I_A := \frac{1}{2} \int_0^a dv \int_0^v du \int d\Omega_2 (v-u)^2 A(y) e^{-\rho V_0}, \tag{3.63}
$$

and similarly for I_B, I_C and I_D. I_A and I_B are doable integrals involving no unknown functions. We will see that $\hat{\mathcal{O}} I_A$ gives the nonzero contributions in the limit and $\hat{\mathcal{O}} I_B$, $\hat{\mathcal{O}} I_C$ and $\hat{\mathcal{O}} I_D$ vanish in the limit.

Consider I_A first. Integrating over the angular coordinates gives

$$
\begin{aligned}
I_A = \int_0^a dv \int_0^v du \frac{(v-u)^2}{2} \Bigg(&4\pi\phi + \frac{1}{2} 4\pi (t^2 \phi_{,00} + \frac{1}{3} r^2 \phi_{,ii}) \\
&- \frac{1}{6}\phi\, 4\pi (t^2 R_{00} + \frac{1}{3} r^2 R_{ii}) + \frac{32\pi^2 \rho}{4320} u^3 v^3 \phi R \\
&- \frac{96\pi^2 \rho}{4320} u^2 v^2 \phi (t^2 R_{00} + \frac{1}{3} r^2 R_{ii}) \Bigg) e^{-\rho V_0}.
\end{aligned}
\tag{3.64}
$$

We use the symmetry of the integrand under the exchange of u and v to double the integration range to $u \in [0, a]$ and $v \in [0, a]$ and divide the resulting integral by two, then all the integrals are of the form

$$
I_{n,m} := \int_0^a dv \int_0^a du\, v^n u^m e^{-\frac{\pi}{6}\rho u^2 v^2}, \tag{3.65}
$$

up to some constant factors. For $n \neq m$ we have

$$I_{n,m} = \frac{1}{2(m-n)\rho'^{\frac{1}{2}}}\left[\frac{a^{m-n}}{\rho'^{\frac{n}{2}}}\left(\Gamma(\frac{n+1}{2}) - \Gamma(\frac{n+1}{2}, \rho' a^4)\right)\right.$$
$$\left. - \frac{a^{n-m}}{\rho'^{\frac{m}{2}}}\left(\Gamma(\frac{m+1}{2}) - \Gamma(\frac{m+1}{2}, \rho' a^4)\right)\right] \tag{3.66}$$

where $\rho' := \frac{\rho\pi}{6}$. Here $\Gamma(z) = \int_0^\infty t^{z-1}e^{-t}dt$ is the Euler gamma function and $\Gamma(b,z) = \int_z^\infty t^{b-1}e^{-t}dt$ is the incomplete gamma function. For $n = m$,

$$I_{n,n} = \frac{a^{2(1+n)}}{(1+n)^2}\,{}_2F_2\left(\frac{1+n}{2}, \frac{1+n}{2}; \frac{3+n}{2}, \frac{3+n}{2}; -a^4\rho'\right) \tag{3.67}$$

where ${}_pF_q(a_1, \ldots, a_p; b_1, \ldots, b_q; z)$ is the generalised hypergeometric function. In the limit $\rho \to \infty$ the leading order term is [29]

$$I_{n,n} = \frac{\log(\rho' a^4)}{4\rho'^{\frac{n+1}{2}}}\Gamma(\frac{1+n}{2}). \tag{3.68}$$

The incomplete gamma functions in (3.66) are exponentially decaying in the limit, and do not contribute. So any term proportional to $I_{n,m}$ with $n \neq m$ will behave like a negative half integer power $\rho^{-\frac{p}{2}}$, $p \in \mathbb{N}$. Acting with $\hat{\mathcal{O}}$ on such a power annihilates such terms with $p = 1, 2$, or 3 leaving the first correction $O(\rho^{-2})$, which does not contribute in the limit. Therefore the only terms which contribute are those proportional to $I_{n,n}$. In I_A, only terms proportional to $I_{n,n}$ with $n = 1$, 2 and 4 appear, it is then a simple exercise to show that

$$\lim_{\rho\to\infty}\frac{4}{\sqrt{6}}\left(-\sqrt{\rho}\phi(0) + \rho^{3/2}\hat{\mathcal{O}}I_A\right) = (\Box - \frac{1}{2}R(0))\phi(0). \tag{3.69}$$

Consider I_B next. Again it is a linear combination of integrals $I_{n,m}$ of which only those for which $n = m$ are not exponentially suppressed, and from (3.67) we see that $I_{n,n} = O(\rho^{-\frac{n+1}{2}}\log\rho)$ in the limit. It is straightforward then to show that

$$\rho^{3/2}\hat{\mathcal{O}}I_B = O(\frac{\log\rho}{\sqrt{\rho}}) \tag{3.70}$$

as $\rho \to \infty$.

We now deal with $C(y)$. Terms in C can be grouped as follows

$$y^n\Omega(y), \qquad 3 \leq n \leq 6 \tag{3.71}$$

$$\rho\, y^n\Omega(y), \qquad 7 \leq n \leq 12 \tag{3.72}$$

$$\rho^2 y^n\Omega(y), \qquad 15 \leq n \leq 18, \tag{3.73}$$

where $y \in \{u, v\}$, $\Omega(y)$ represents one (or product) of the unknown functions $\psi_{\mu\nu\alpha}(y)$, $T(y)$, $S_{\mu_1\ldots\mu_7}(y)$ and we have omitted constant factors. Integrating over the angles leaves us with the following integrals

$$I_{m,n} := \int_0^a dv \int_0^v du\, u^m v^n \Omega(u,v) e^{-\rho u^2 v^2}, \quad 5 \leq m+n \leq 8, \tag{3.74}$$

$$I'_{m,n} := \rho \int_0^a dv \int_0^v du\, u^m v^n \Omega(u,v) e^{-\rho u^2 v^2}, \quad 9 \leq m+n \leq 14, \tag{3.75}$$

$$I''_{m,n} := \rho^2 \int_0^a dv \int_0^v du\, u^m v^n \Omega(u,v) e^{-\rho u^2 v^2}, \quad 17 \leq m+n \leq 20, \tag{3.76}$$

where we have absorbed a constant factor into ρ. Note that (3.75) and (3.76) can be rewritten as $H_1 I_{n-2,m-2}$, $n-2, m-2 \geq 0$ and $H_2 I_{n-4,m-4}$, $n-4, m-4 \geq 0$ respectively and since $[H_i, \hat{\mathcal{O}}] = 0$, $i = 1, 2$, we only need $\hat{\mathcal{O}} I_{m,n} = O(\rho^{-2})$ for $n + m \geq 5$. We relegate the proof of this result to appendix A.1. It follows that $\lim_{\rho\to\infty} \rho^{3/2} \hat{\mathcal{O}} I_C = 0$.

Finally we deal with I_D,

$$I_D = \int_0^a dv \int_0^v du \int d\Omega_2 f(y) \sum_{k=3}^{\infty} \frac{(-\rho)^k}{k!} (\delta V)^k e^{-\rho V_0} \tag{3.77}$$

where $f(y) = \sqrt{-g(y)}\phi(y)\frac{1}{2}(v-u)^2$. Using $\eta_{\mu\nu} y^\mu y^\nu = -\tau^2$ we can rewrite δV as

$$\delta V(y) = \tau^6 \left(-\frac{\pi}{4320} R(0) + \frac{\pi}{720} R_{\hat{0}\hat{0}}(y) + y^{\mu_7} S_{\hat{0}\ldots\hat{0}\mu_7}(y) \right) =: \tau^6 \bar{S}(y), \tag{3.78}$$

where $R_{\hat{0}\hat{0}}$ is the time-time component of the Ricci tensor, and similarly for $S_{\hat{0}\ldots\hat{0}\mu_7}$, evaluated in an orthonormal frame at the origin whose zero leg is aligned with the tangent vector of the geodesic connecting the origin and y.

So

$$I_D = -\int_0^a dv \int_0^v du \int d\Omega_2 f(y)\rho^3\tau^{18}\bar{S}(y)^3 \sum_{k=0}^{\infty} \frac{(-\rho)^k}{(k+3)!}(\tau^6\bar{S}(y))^k e^{-\rho V_0}. \tag{3.79}$$

As for the similar term in the previous section we can show that each term in $\hat{\mathcal{O}}I_D$ is $O(\rho^{-2}\log\rho)$ starting with I_D itself.

Let $S' := \|\overline{S}(y)\|_1$, where $\|\cdot\|_1$ denotes uniform norm over W_1, the current range of integration. Then

$$\left|\sum_{k=0}^{\infty} \frac{(-\rho)^k}{(k+3)!}\tau^{6k}\overline{S}(y)^k\right| \leq \frac{1}{6}e^{\rho\tau^6 S'} \tag{3.80}$$

$\forall y \in W_1$. Choosing the neighbourhood size parameter $a^2 < \frac{\pi}{96S'}$ leads to

$$|I_D| \leq \#c'\rho^3 \int_0^a dv \int_0^v du\, u^9 v^9 e^{-\frac{\pi}{12}\rho u^2 v^2} \approx \#c'\rho^{-2}\log(\rho a^4) \tag{3.81}$$

where $c' = S'^3\|(v-u)^2 \int d\Omega_2\sqrt{-g}\,|\phi|\,\|_1$. Similar calculations to the one shown in appendix A.3 show that $H_1 I_D$, $H_2 I_D$ and $H_3 I_D$ are also $O(\rho^{-2})$ with coefficient c', up to numerical factors.

3.4.3 Corrections

The curved spacetime result proved in the previous section is only valid in the limit of infinite sprinkling density, and does not shed any light on when the mean of $B\phi$ is a good approximation to $(\Box - \frac{1}{2}R)\phi$ at finite density. This is because in order to estimate the corrections one needs an explicit form for the volume of causal intervals which hug the past light cone of x,[2] which are not known. We can remedy this by further restricting the region of integration to be contained in a neighbourhood of the origin for which the curvature components are small, i.e. $R_{\mu\nu\alpha\beta}x^\sigma x^\rho \ll 1$ for all components. This is effectively restricting the region of integration to be the near region of the previous section, for which we have an explicit form for the corrections to the volume of causal intervals. One of the leading order corrections comes

[2]These intervals have small volume but stretch over vast regions of the spacetime and therefore probe the global spacetime curvature.

form the term $y^\mu y^\nu y^\alpha y^\beta R_{\mu\nu}\phi_{,\alpha\beta}$ in I_B and goes like

$$l^2 \log(a/l) R_{\hat{\mu}\hat{\nu}}\phi_{,\hat{\alpha}\hat{\beta}}. \tag{3.82}$$

where $\hat{\mu}$, $\hat{\nu}$, etc. represent some specific choice of μ, ν etc. Similarly to the flat spacetime result we find that in this restricted case, $B\phi$ is a good approximation to $(\Box - \frac{1}{2}R)\phi$ at finite density ρ if $\lambda^2 \gg l^2 \log(a/l)$ *and* $r^2 \gg l^2 \log(a/l)$, where r is the radius of curvature.

3.5 Fluctuations

So far we have only been concerned with the mean of the causet operator B, (3.3), but what about fluctuations? If the physical IR cutoff L is fixed and the discreteness scale l sent to zero, *i.e.*, the number of causet elements N grows, simulations show the fluctuations around the mean grow rather than die away and $B\phi(x)$ will not be approximately equal to the continuum $\Box\phi(x)$. This would mean that, for example, if one intends to use B to classically propagate a scalar field on a causal set, then the discrete propagation couldn't approximate the continuum one, since, for large enough density, the value of $B\phi$ at every step would be far from 0. It's possible that by averaging over many Planck lengths, the fluctuations would be tamed. But even if this were the case, which remains to be shown, the fluctuations would be bound to affect even the coarse grained field, if large enough. For the rest of this section we will assume that large fluctuations are unwanted.

To dampen the fluctuations we follow [26] and introduce an intermediate length scale $l_k \geq l$ and smear out the expressions above over this new scale, with the expectation that when $l_k >> l$ the inherent averaging will suppress the fluctuations via the law of large numbers. Thus we seek a discrete operator, B_k, whose mean is given by (3.83) but with l replaced by l_k:

$$\bar{B}_k\phi(x) = \frac{4}{\sqrt{6}l_k^2}\Big[-\phi(x) + \frac{1}{l_k^4}\int_{y\in J^-(x)} d^4y\, \phi(y)\, e^{-\xi}(1 - 9\xi + 8\xi^2 - \frac{4}{3}\xi^3)\Big], \tag{3.83}$$

where now $\xi := l_k^{-4}V(x,y)$. Working back, one can show that the discrete

operator, B_k, with this mean is

$$B_k\phi(x) = \frac{4}{\sqrt{6}l_k^2}\Big[-\phi(x) + \epsilon \sum_{y \prec x} f(n(x,y),\epsilon)\phi(y)\Big], \tag{3.84}$$

where $\epsilon = (l/l_k)^4$ and

$$f(n,\epsilon) = (1-\epsilon)^n \left[1 - \frac{9\epsilon n}{1-\epsilon} + \frac{8\epsilon^2 n!}{(n-2)!(1-\epsilon)^2} - \frac{4\epsilon^3 n!}{3(n-3)!(1-\epsilon)^3}\right]. \tag{3.85}$$

We prove that the mean of (3.84) is (3.83) by using the same technique used in proving (3.4), i.e. by discretising the sprinkled spacetime into cells of volume ΔV. The average of the second term in (3.84) is given by

$$\langle \sum_I \chi_I f(m_I,\epsilon)\rangle = \sum_I \langle\chi_I\rangle\langle f(m_I,\epsilon)\rangle = \sum_I \rho\Delta V \langle f(m_I,\epsilon)\rangle. \tag{3.86}$$

To find the continuum expectation value we take the limit as the spacetime cells become infinitesimally small, i.e. $\Delta V \to dV$. The first term of (3.85) gives

$$\begin{aligned}\langle (1-\epsilon)^{m_I}\rangle &= \sum_{m=0}^{\infty} (1-\epsilon)^m \times \mathrm{Prob}(m_I = m) \\ &= \sum_{m=0}^{\infty} (1-\epsilon)^m \frac{(\rho V_I)^m e^{-\rho V_I}}{m!} \\ &= e^{-\rho V_I} e^{\rho V_I (1-\epsilon)} = e^{-V_I/l_k^4}\end{aligned} \tag{3.87}$$

where we defined $k := \epsilon\rho = 1/l_k^4$. So

$$\epsilon \sum_I \langle \chi_I (1-\epsilon)^n\rangle \phi_I = \sum_I \frac{1}{l_k^4}\Delta V_I \, e^{-V_I/l_k^4} \to \frac{1}{l_k^4}\int d^4y \; e^{-V(x,y)/l_k^4}\phi(y) \tag{3.88}$$

where the arrow denotes taking the limit $\Delta V \to dV$. The average of the other three terms in (3.85) can be similarly calculated.

Note that B_k reduces to B when $\epsilon = 1$. B_k effectively samples ϕ over elements in 4 broad bands with a characteristic depth l_k, the bands' contributions being weighted with the same set of alternating sign coefficients as

d	n_d	α_d	β_d	$C_1^{(d)}$	$C_2^{(d)}$	$C_3^{(d)}$	$C_4^{(d)}$
2	3	-2	4	1	-2	1	0
3	3	$-\frac{1}{\Gamma\left(\frac{5}{3}\right)}\left(\frac{\pi}{3\sqrt{2}}\right)^{\frac{2}{3}}$	$\frac{1}{\Gamma\left(\frac{5}{3}\right)}\left(\frac{\pi}{3\sqrt{2}}\right)^{\frac{2}{3}}$	1	$-\frac{27}{8}$	$\frac{9}{4}$	0
4	4	$-\frac{4}{\sqrt{6}}$	$\frac{4}{\sqrt{6}}$	1	-9	16	-8

Table 3.1: bf

in B. Since (3.83) is just (3.4) with l replaced by l_k, the mean of $B_k\phi(x)$ is close to $\Box\phi(x)$ when the characteristic scale over which ϕ varies is large compared to l_k. Now, however, numerical simulations show that the fluctuations are tamed. Points were sprinkled into a fixed causal interval in $\mathbb{M}^4$ between the origin and $t = 1$ on the t axis, at varying density $\rho = \frac{N}{V}$, where volume $V = \frac{\pi}{24}$. For each N, 100 sprinklings were done and for each sprinkling, $B_k\phi$ was calculated at the topmost point of the interval for $\phi = 1$ and $l_k = 0.16$. For $N = 5000$, the mean was $\mu = 9,35$ and the standard deviation $s.d = 134.8$. For $N = 10000$, $\mu = -4.00$ and $s.d. = 102.6$ and for $N = 20000$, $\mu = 1.12$ and $s.d. = 58.8$. These results indicate that the fluctuations do die away, as anticipated, as N increases and are consistent with the dependence $N^{-1/2}$.

3.6 Causet d'Alembertians in Other Dimensions

So far our discussion has been restricted to the $4d$ d'Alembertian. However there exist d'Alembertians, $B^{(d)}$, in all other dimensions d [30]. Since we will be needing them in later chapters we give here the explicit form of the d'Alembertians in 2, 3 and 4 dimensions.

Let $\mathcal{C}$ be a causal set which is well approximated by a d-dimensional spacetime $(\mathcal{M}, g)$ and let $\phi : \mathcal{C} \to \mathbb{R}$ be a real scalar field defined on $\mathcal{C}$. Then the d-dimensional causet d'Alembertian is

$$B^{(d)}\phi(x) = \frac{1}{l^2}\left(\alpha_d\phi(x) + \beta_d \sum_{i=1}^{n_d} C_i^{(d)} \sum_{y\in L_i} \phi(y)\right), \tag{3.89}$$

where the various coefficients are given in table (3.1).

It is shown in [30] that if the spacetime region into which one is sprinkling is small enough such that Riemann normal coordinates hold everywhere[3] then

$$\lim_{\rho\to\infty} \bar{B}_k^{(d)}\phi(x) = \Box^{(d)}\phi(x) - \frac{1}{2}R(x)\phi(x). \tag{3.90}$$

So far this result has been proven starting from weaker assumptions only in $4d$, c.f. Chapter 3). For other dimensions the proof analogous to the $4d$ one remains to be done.

For completeness we also give the non-local expressions one gets by smearing the above expressions over $l_k \geq l$. Let $\epsilon_d = (l/l_k)^d$, then

$$B_k^{(d)}\phi(x) = \frac{1}{l_k^2}\left(\alpha_d\phi(x) + \beta_d\epsilon_d \sum_{y\prec x} f_d(n(x,y),\epsilon_d)\right) \tag{3.91}$$

where α_d and β_d are again given in table (3.1) and

$$f_d(n,\epsilon_d) := (1-\epsilon_d)^d \sum_{i=1}^{n_d} C_i^{(d)} \begin{pmatrix} n \\ i-1 \end{pmatrix} \left(\frac{\epsilon_d}{1-\epsilon_d}\right)^{i-1}. \tag{3.92}$$

The mean of (3.91) is the same as the mean of (3.89) with l replaced by l_k.

[3] Equivalently if the field ϕ is taken to have support only in a spacetime region in which RNCs hold.

Chapter 4

The Action of a Causal Set

4.1 From d'Alembertian to Action

In the previous chapter we saw how, in spite of the radical non-locality, it is possible to define a quasi-local wave operator on causal sets and hence recover approximately local dynamics. In particular we constructed an operator B whose mean, when applied to scalar fields living on sprinklings of curved spacetimes, gives both the continuum d'Alembertian *and* the scalar curvature of the approximating manifold, in the continuum limit (3.8).

We use (3.3) to define the scalar curvature of a causal set, $\mathcal{C}$, at $x \in \mathcal{C}$ by

$$\begin{aligned}\mathcal{R}(x) &:= B(-1)|_x \\ &= \frac{4}{\sqrt{6}l^2}\left[\sum_{y\preceq x}\delta_{xy} - \sum_{y\in L_1(x)} +9\sum_{y\in L_2(x)} -16\sum_{y\in L_3(x)} +8\sum_{y\in L_4(x)}\right]. \quad (4.1)\end{aligned}$$

This is a weighted alternating sum of the number of elements in the causet which share the most basic relations with the point x: x itself, links, 3-chains etc. We call this the scalar curvature because the mean, in the continuum limit, gives the scalar curvature of the approximating spacetime

$$\lim_{l\to 0}\bar{B}(-1)|_x = \frac{1}{2}R(x), \quad (4.2)$$

up to a factor of 2.

Recall that the proof for the continuum limit of $\bar{B}\phi$ of the previous chapter, c.f. equation (3.8), only holds for ϕ of compact support. In definition

(4.1) however we have set ϕ to be a constant, so strictly, our result does not hold. One way around this is to act with B on some field ϕ which is constant in some spacetime region of compact support, $\mathcal{N}$, and zero everywhere else [1]. For our result to be valid we would then have to require that $\mathcal{N}$ be small enough such that the assumptions made in proving the continuum limit of $\bar{B}\phi$ are valid. Nonetheless, we will stick to the above definition, keeping in mind that equation (4.2) will only be true for sprinklings of spacetime regions $\mathcal{N}$ for which our assumptions hold.

We now use the causet scalar curvature $\mathcal{R}$ to define the action $S[\mathcal{C}]$ of a (finite) casual set $\mathcal{C}$ by summing $\mathcal{R}$ over $\mathcal{C}$. In 4D,

$$\frac{S^{(4)}[\mathcal{C}]}{\hbar} := \frac{l^4}{l_p^2}\sum_{x\in\mathcal{C}}\mathcal{R}(x) = \frac{4}{\sqrt{6}}\frac{l^2}{l_p^2}(N - N_1 + 9N_2 - 16N_3 + 8N_4) \tag{4.3}$$

where the normalisation has been chosen so that the continuum limit of the mean gives the Einstein-Hilbert action with the usual normalisation up to possible boundary terms, N is the number of elements in $\mathcal{C}$, N_i is the number of $(i+1)$ element inclusive order intervals in $\mathcal{C}$, and $l_p = \sqrt{8\pi G\hbar}$ is the rationalised Planck length

We can in fact define a *one-parameter* family of actions, $S_k^{(4)}[\mathcal{C}]$, by summing the non-local scalar curvature, $\mathcal{R}_k^{(4)} := B_k^{(4)}(-1)$, over the causal set $\mathcal{C}$, times $\hbar l^2$ to get the units right, times a number of order one, which in 4D is the ratio of l^2 to l_p^2. So

$$\frac{S_k^{(4)}[\mathcal{C}]}{\hbar} := \frac{l^4}{l_p^2}\sum_{x\in\mathcal{C}}\mathcal{R}_k(x) = \frac{l^2}{l_p^2}\frac{4}{\sqrt{6}}\left(\sqrt{\epsilon_4}N - \epsilon_4^{3/2}\sum_{x\in\mathcal{C}}\sum_{y\prec x} f_4(n(x,y),\epsilon)\right). \tag{4.4}$$

When the nonlocality length l_k equals the discreteness length l, $B_k = B$ and the action, $S[\mathcal{C}]$ takes the particularly simple form (4.3): an alternating sum of the number of small order intervals in $\mathcal{C}$.

Just as for the scalar curvature (4.1), we expect that the continuum limit of the causet action will yield the Einstein-Hilbert action only for sufficiently small spacetime regions $\mathcal{N}$, for which our original assumptions hold. We discuss what might happen for $\mathcal{N}$ larger than this at the end of this chapter.

Note that because B is the most non-nonlocal of the operators in the

[1] This would also introduce boundary contributions.

family, the action $S[\mathcal{C}]$ is a sum of contributions each of which is not close to the value of the Ricci scalar at the corresponding point of the continuum approximation, c.f. section 3.5. However, one might expect that if the curvature is slowly varying on some intermediate scale, which we might as well call l_k, the averaging involved in the summation might perform the same role of suppressing the fluctuations as the smearing out of the operator itself so that the whole action $S[\mathcal{C}]$ is a good approximation to the continuum action when l_k is the appropriate size. Whether this is the case is yet to be determined and will be studied in future work.

4.1.1 The Causet Action in Other Dimensions

Causet actions exist in all dimensions [30]. Again these are defined as

$$\frac{S_k^{(d)}[\mathcal{C}]}{\hbar} := \frac{l^d}{l_p^{d-2}} \sum_{x \in \mathcal{C}} \mathcal{R}_k^{(d)} \tag{4.5}$$

where

$$\mathcal{R}_k^{(d)} := B_k^{(d)}(-1). \tag{4.6}$$

In the previous section we saw the $4d$ action. Here we give the expressions for the 2 and 3 dimensional actions.

In $2d$

$$\begin{aligned} \frac{S_k^{(2)}[\mathcal{C}]}{\hbar} :&= l^2 \sum_{x \in \mathcal{C}} \mathcal{R}_k^{(2)}(x) \\ &= 2\left(\epsilon_2 N - 2\epsilon_2^2 \sum_{x \in \mathcal{C}} \sum_{y \prec x} f_2(n(x,y), \epsilon_2)\right), \end{aligned} \tag{4.7}$$

and in $3d$

$$\begin{aligned} \frac{S_k^{(3)}[\mathcal{C}]}{\hbar} &:= \frac{l^3}{l_p} \sum_{x \in \mathcal{C}} \mathcal{R}_k^{(3)}(x) \\ &= \frac{l}{l_p} \frac{1}{\Gamma\left(\frac{5}{3}\right)} \left(\frac{\pi}{3\sqrt{2}}\right)^{\frac{2}{3}} \left(\epsilon_3^{2/3} N - \epsilon_3^{5/3} \sum_{x \in \mathcal{C}} \sum_{y \prec x} f_3(n(x,y), \epsilon_3)\right). \end{aligned} \tag{4.8}$$

As for 4 dimensions, when we set $l_k = l$, i.e. $\epsilon_d = 1$, the above expressions

reduce to an alternating sum of small order intervals

$$\frac{S^{(2)}[\mathcal{C}]}{\hbar} = 2(N - 2N_1 + 4N_2 - 2N_3), \tag{4.9}$$

$$\frac{S^{(3)}[\mathcal{C}]}{\hbar} = \frac{1}{\Gamma\left(\frac{5}{3}\right)}\left(\frac{\pi}{3\sqrt{2}}\right)^{\frac{2}{3}}\frac{l}{l_p}(N - N_1 + \frac{27}{8}N_2 - \frac{9}{4}N_3). \tag{4.10}$$

In general we write

$$S_k^{(d)}[\mathcal{C}] = \left(\frac{l}{l_p}\right)^{d-2}\zeta_d[\epsilon_d, \mathcal{C}], \tag{4.11}$$

where

$$\zeta_2[\epsilon_2, \mathcal{C}] := 2\left(\epsilon_2 N - 2\epsilon_2^2 \sum_{x\in\mathcal{C}}\sum_{y\prec x} f_2(n(x,y),\epsilon_2)\right), \tag{4.12}$$

$$\zeta_3[\epsilon_3, \mathcal{C}] := \frac{1}{\Gamma\left(\frac{5}{3}\right)}\left(\frac{\pi}{3\sqrt{2}}\right)^{\frac{2}{3}}\left(\epsilon_3^{2/3} N - \epsilon_3^{5/3}\sum_{x\in\mathcal{C}}\sum_{y\prec x} f_3(n(x,y),\epsilon_3)\right), \tag{4.13}$$

$$\zeta_4[\epsilon_4, \mathcal{C}] := \frac{4}{\sqrt{6}}\left(\sqrt{\epsilon_4} N - \epsilon_4^{3/2}\sum_{x\in\mathcal{C}}\sum_{y\prec x} f_4(n(x,y),\epsilon)\right), \tag{4.14}$$

and we set $\hbar = 1$ throughout the rest of this chapter.

4.1.2 Bi-local Nature of the Action

The causet action S is *bi*-local[2] (we drop the dimension superscript since these arguments apply in all dimensions). Among other things, this means that it's not additive. To see this consider a partition of a causet $\mathcal{C} = X \cup Y$ where $X \cap Y = \emptyset$, shown in figure (4.1). Then $S[\mathcal{C}] \neq S[X] + S[Y]$, since there exist links, 3-chains, diamonds, etc., whose past most element is in X and future most in Y, which are therefore not contained in X or Y. Taking this into account one finds that for the general partition defined above

$$S[\mathcal{C}] = S[X, X] + S[Y, Y] + S[X, Y] + S[Y, X], \tag{4.15}$$

where the notation $S[I, J]$ means that the future most point of the order interval $i \in I$, and the past most point $j \in J$. Note that the third and

[2]If the action were truly local it would be a sum of contributions from each causet element only, and would therefore be proportional to N.

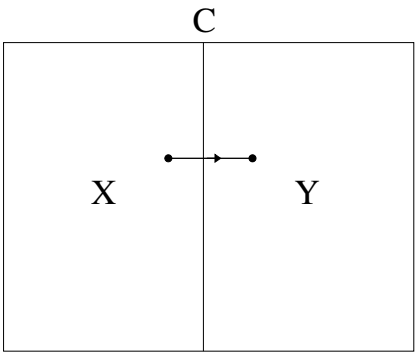

Figure 4.1: A schematic picture of the partition of a causet C where the full box represents the whole causet C. A typical element of $S[Y, X]$ is shown. The link $x \prec\!\!* y$ is not contained in either X or Y but is contained in C.

fourth terms are quintessentially non-local: they are made up of the non-local terms in the action only. Note also that the terms $S[X, X]$ and $S[Y, Y]$ are not independent of Y and X respectively. To see what we mean by this consider the following example: sprinkle into a square in $\mathbb{M}^2$ and partition the square evenly in two by a timelike curve, say $x = 0$. Figure (4.2) shows this setup with the elements of X represented by blue crosses and those of Y by red plusses. The 4 element order interval shown has both the future and past most elements in X, however one of the elements causally between these two lies in Y. This interval is an element of $\mathcal{C}$, so it must also appear on the right hand side of (4.15), which means that we must include it in $S[X, X]$ (both its future and past most elements are in X so it cannot be part of the other terms). Therefore $S[X, X]$, $X \subset \mathcal{C}$, is *not* the same as the action of a sprinkling into the $x < 0$ region only, i.e. when X is the whole causal set. The fact that X is a subset of a larger causet $\mathcal{C}$ matters. We distinguish the two cases by writing in $S[X, X]$ (as we've been doing already) when the set X is a proper subset of a causet $\mathcal{C}$, and $S[X]$ when $X = \mathcal{C}$ is the full causal set. So whenever we write $S[X, X]$ we are are assuming that some kind of partition of the full causet has been performed, and one should therefore keep in mind that some elements of the order intervals contained in $S[X, X]$ might lie in some set Y, with $X \cap Y = \emptyset$.

Finally note that for geometric partitions like the one above, the ambiguity only arises if the partitioning surface has spacelike normal. This is due to the fact that the relations in the causet are *causal* relations, so

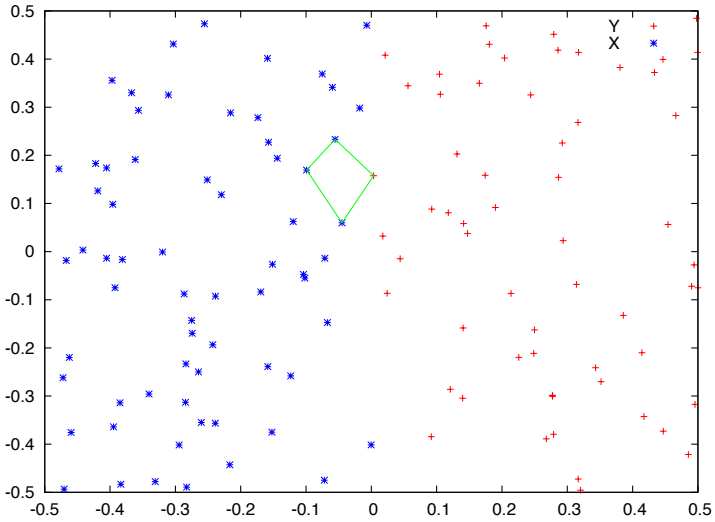

Figure 4.2: A 4-element (inclusive) order interval, member of the subcauset $\mathcal{C}_{x<0} \subset \mathcal{C}$, is shown. Note how one of the elements in this order interval (the right most) is actually in $\mathcal{C}_{x>0} \subset \mathcal{C}$.

if the partitioning surface is spacelike or null then a relation between two elements crossing the surface cannot precede a relation that "crosses-back" across the same surface. It also follows that if $\mathcal{C}$ is a sprinkling of a spacetime $(\mathcal{M}, g)$, and X is the subcauset of $\mathcal{C}$ corresponding to a causally convex neighbourhood $\mathcal{N}$ of $\mathcal{M}$, then $S[X, X] = S[X]$.

4.2 The Continuum Limit: A Conjecture

In this section we propose a conjecture for the continuum limit of the action $S^{(d)}$.

Let $\mathcal{C}$ be a sprinkling of a d-dimensional spacetime $(\mathcal{M}, g)$. Let $\mathcal{C}_{\mathcal{N}}$ be a subset of $\mathcal{C}$, $\mathcal{C}_{\mathcal{N}} \subseteq \mathcal{C}$, corresponding to a normal neighbourhood $\mathcal{N} \subseteq \mathcal{M}$ with volume $V(\mathcal{N}) \gg l^d$. Then the mean of the causet action $S^{(d)}[\mathcal{C}_{\mathcal{N}}]$ over sprinklings, in the limit $l \to 0$ is

$$\lim_{l\to 0}\langle S[\mathcal{C}]\rangle = \frac{1}{2l_p^{d-2}}\int_{\mathcal{N}} d^dx\sqrt{-g(x)}R(x) + \frac{a_d}{l_p^{d-2}l}\int_{\Xi} d^{d-1}x\sqrt{-h(x)} + \frac{b_d}{l_p^{d-2}}A\left(N_f \cap N_p\right) \tag{4.16}$$

where Ξ is the portion of the boundary of the closure of $\mathcal{N}$ with non-timelike normal, h is the induced metric on Ξ, a_d and b_d are dimension dependent coefficients, and $A(N_f \cap N_p)$ is the codimension 2 volume of the intersection of the $(d-1)$-surfaces N_f and N_p defined as

$$N_f = \{x \in \bar{\mathcal{N}} \mid \text{for every future directed non-spacelike curve,} \\ \gamma : [0,\infty) \to \mathcal{M} \text{ such that } \gamma(0) = x,\ \gamma(t) \cap \mathcal{N} = \emptyset\ \forall t > 0\} \quad (4.17)$$

where $\bar{\mathcal{N}}$ is the closure of $\mathcal{N}$, and N_p is similarly defined with γ a past-directed curve. Note that when the subregion $\mathcal{N}$ is not globally hyperbolic the second term in (4.16) will dominate (diverge) in the limit $l \to 0$. If $\mathcal{N}$ is globally hyperbolic then[3]

$$\lim_{l\to 0}\langle S[\mathcal{C}]\rangle = \frac{1}{2l_p^{d-2}}\int_{\mathcal{M}} d^dx\sqrt{-g(x)}R(x) + \frac{b_d}{l_p^{d-2}}A\left(N_f \cap N_p\right). \quad (4.18)$$

As an example consider a sprinkling, $\mathcal{C}$, into $\mathbb{M}^d$ and the subset $\mathcal{C}_\mathcal{I} \subset \mathcal{C}$ corresponding to the causal interval $\mathcal{I} := [p,q] \subset \mathbb{M}^d$. Since the subregion $\mathcal{I}$ is globally hyperbolic we can use equation (4.18), and since the spacetime is flat the bulk term vanishes. Now $N_p = \partial(J^+(q) \cap \bar{\mathcal{N}})$ and $N_f = \partial(J^-(q) \cap \bar{\mathcal{N}})$, so their intersection is a codimension 2 surface which, when p and q are purely timelike separated, is a $(d-2)$-sphere of radius $\tau(p,q)/2$, τ being the proper time between p and q.

4.3 The Action of Spacetime Regions

In this section we study the mean of the causet action for various spacetime regions. All our numerical results are obtained by averaging $S_k^{(d)}[\mathcal{C}]$ over 10 sprinklings, with $l_k = 3l$ and $l_k = 2l$ in $3d$ and $4d$ respectively, as a function of sprinkling density ρ, where we use the non-local version of the action with $l_k > l$ to reduce the size of the fluctuations. [4]

[3] Note that for $\mathcal{N}$ globally hyperbolic,the causet $\mathcal{C}_\mathcal{N}$ obtained by the restriction of $\mathcal{C}$ to the subregion $\mathcal{N}$ is equivalent to a sprinkling (at the same density) of the subregion $\mathcal{N}$ alone.

[4] The fluctuations will not go to zero as $l \to 0$ since we have fixed $\epsilon_d = (l/l_k)^d$, not l_k [26], c.f. section 3.5.

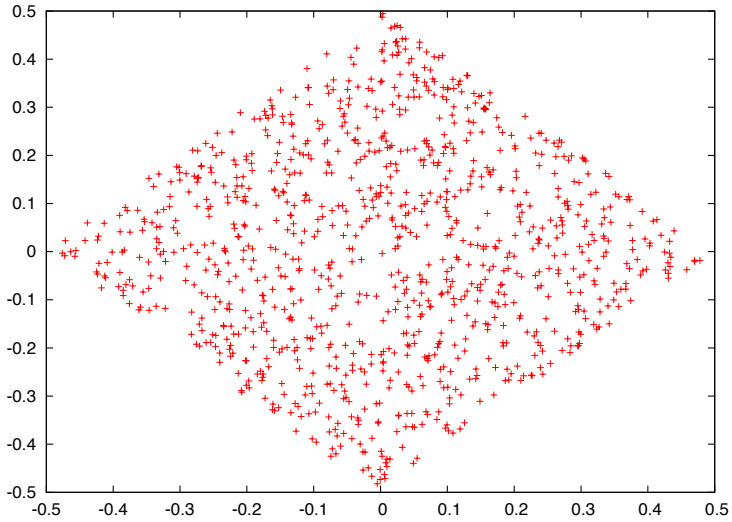

Figure 4.3: A sprinkling of a causal interval in $\mathbb{M}^2$.

4.3.1 The Action of a Causal Interval in Minkowski

Consider sprinklings of causally convex regions (CCR) in flat spacetimes. The simplest CCR is the causal interval/diamond between two spacetime points p and q, defined by

$$I(p,q) = J^+(q) \cap J^-(p). \tag{4.19}$$

4.3.1.1 2 Dimensions

Let $\mathcal{C}$ be a causet that is a sprinkling of an interval $\mathcal{I} := [p,q] \subset \mathbb{M}^2$ at density ρ between points p and q with cartesian coordinates $(0.5, 0)$ and $(-0.5, 0)$ respectively, see figure 4.3. The mean of the 2D action $\langle S^{(2)}[\mathcal{C}]\rangle$ is given by

$$\langle S[\mathcal{C}]\rangle = 2\rho V - 4\rho^2 \int_{\mathcal{M}} d^2x \int_{\mathcal{M}\cap J^-(x)} d^2y (1 - 2\rho V(x,y) + \frac{1}{2}\rho^2 V(x,y)^2) e^{-\rho V(x,y)} \tag{4.20}$$

In Chapter 5 we compute this integral explicitly, it gives

$$\langle S[\mathcal{C}]\rangle = 2(1 - e^{-\rho V}) \to 2 \text{ as } \rho \to \infty \tag{4.21}$$

where V is the volume of $\mathcal{I}$. Since the spacetime is flat and $A(N_f \cap N_p) = A(S^0) = 2$, so this result is consistent with our conjecture, and fixes $b_d = 1$. That the action of a $2d$ spacetime region is a constant is reminiscent of the Gauss-Bonnet theorem. We will investigate the topological character of the $2d$ action, and its relation to the Gauss-Bonnet theorem in Chapter 5

4.3.1.2 3 and 4 dimensions

Next consider sprinklings into higher dimensional intervals $\mathcal{I} = [p, q] \subset \mathbb{M}^d$, $d = 3$ and $d = 4$. The mean of the higher dimensional actions is given by integral expressions similar to (4.20). These integrals are much harder to compute analytically because of the complicated geometry of $[x, y]$, $x, y \in \mathcal{I}$, so we compute the expected action numerically instead. Following our conjecture (4.16), we expect the only contribution to the expected action in the limit to be

$$\langle S_k^{(d)}[\mathcal{I}]\rangle = b_d \frac{A\left(J^+(q) \cap J^-(p)\right)}{l_p^{d-2}}, \tag{4.22}$$

where $A\left(J^+(q) \cap J^-(p)\right)$ is the area of the codimension 2 surface defined by the intersection of the causal future of q with the causal past of p [5]. Using (4.11) and $l = (V/N)^{1/d}$ we can rewrite (4.22) as

$$\frac{V^{1/3}}{A_3}\langle \zeta_3[\epsilon_3, \mathcal{C}]\rangle = b_3 N^{1/3} \tag{4.23}$$

$$\frac{\sqrt{V}}{A_4}\langle \zeta_4[\epsilon_4, \mathcal{C}]\rangle = b_4\sqrt{N}, \tag{4.24}$$

in $3d$ and $4d$ respectively, where $A_d = A\left(J^+(q) \cap J^-(p)\right)$, $d = 3, 4$.

Results are shown in figures 4.5 and 4.4. The straight lines are two-parameter, power-law fits $f(b_d, k_d, N) = b_d N^{k_d}$, where

$$b_3 = 0.44 \pm 0.024, \quad k_3 = 0.43 \pm 0.01, \tag{4.25}$$

$$b_4 = 0.46 \pm 0.055, \quad k_4 = 0.56 \pm 0.01. \tag{4.26}$$

Both k_3 and k_4 are inconsistent with the conjectured value, $k_d = (d-2)/2$. However we believe that this inconsistency is due to not having reached the asymptotic regime yet, as we will argue later in the chapter. Evidence for this will be provided in Chapters 5 and 6.

[5] Note that in this case $J^+(q) \cap J^-(p) = N_f \cap N_p$.

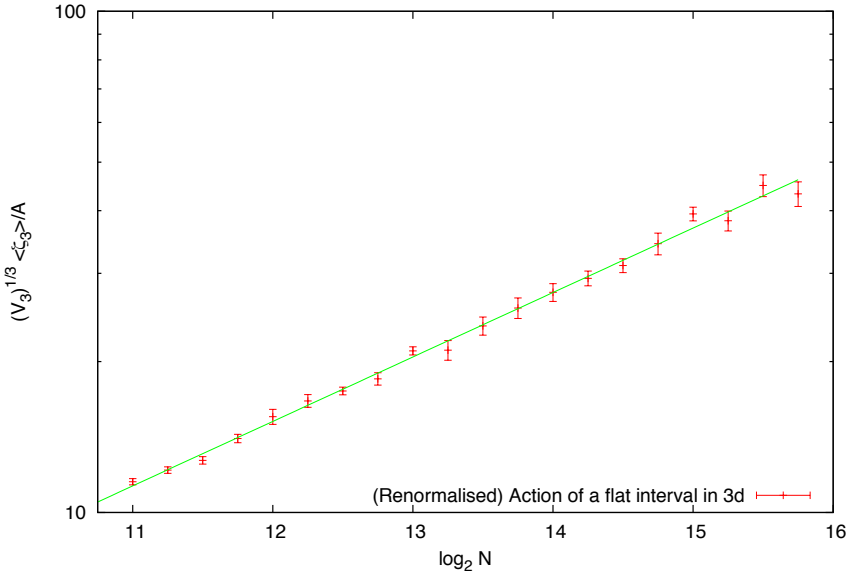

Figure 4.4: log-log plot of simulation data for the action of a causal interval in $\mathbb{M}^3$ with $\tau(p,q) = 1$, $l_k = 3l$, varying density ρ with a power law fit. Data averaged over 10 runs. Fit function $f(b_d, k_d, N) = b_d N^{k_d}$.

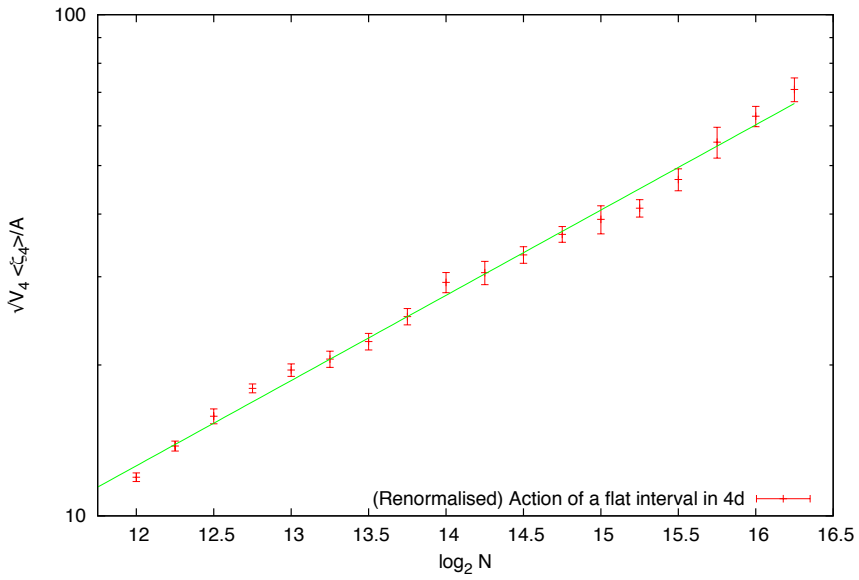

Figure 4.5: log-log plot of simulation data for the action of a causal interval in $\mathbb{M}^4$ with $\tau(p,q) = 1$, $l_k = 2l$, varying density ρ with a power law fit. Data averaged over 10 runs. Fit function $f(b_d, k_d, N) = b_d N^{k_d}$.

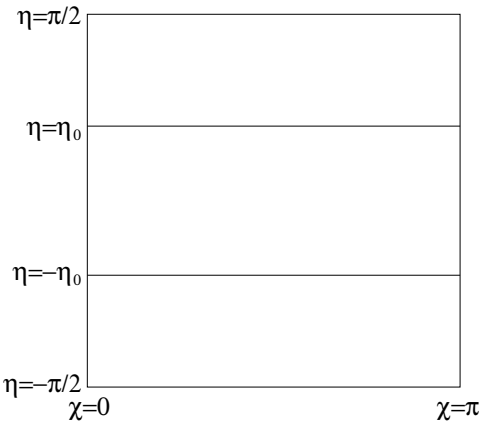

Figure 4.6: Penrose diagram for de Sitter spacetime. Each line of constant η represents a 3-sphere whose north pole is at $\chi = 0$ and south pole at $\chi = \pi$. The lines $\eta = \pm\pi/2$ represent future and past null infinity.

4.3.2 The Action of Causally Convex Regions in de Sitter

We sprinkle into a portion of d-dimensional global de Sitter (dS) spacetime defined by $-\eta_0 \leq \eta \leq \eta_0$, $0 \leq \theta_1, \ldots, \theta_{d-2} < \pi$, $0 \leq \theta_{d-1} < 2\pi$, where $(\eta, \theta_1, \ldots, \theta_{d-1})$ are global conformal coordinates in which the line element takes the form

$$ds^2 = \lambda^2 \sec^2(\eta)(-d\eta^2 + d\Omega_{d-1}^2), \tag{4.27}$$

$d\Omega_{d-1}^2$ is the metric on the $(d-1)$-sphere and λ is the radius of curvature. The volume of the sprinkled region in $3d$ and $4d$ is given by (we set $\lambda = 1$)

$$V_3(\eta_0) = 4\pi \left(\tan\eta_0 \sec\eta_0 + \ln\left(\frac{\sin(\eta_0/2) + \cos(\eta_0/2)}{\cos\eta_0/2) - \sin(\eta_0/2)} \right) \right), \tag{4.28}$$

$$V_4(\eta_0) = \frac{4\pi^2}{3} \tan\eta_0 \sec^2\eta_0 (\cos 2\eta_0 + 2), \tag{4.29}$$

respectively[6].

Figure 4.6 shows the Penrose diagram for global dS together with the portion we sprinkle into. Since the region is globally hyperbolic, and $N_f \cap N_p = \emptyset$, we expect

$$\langle \frac{S_k^{(d)}[\mathcal{C}]}{\hbar} \rangle = \frac{R}{2l_p^{d-2}} V_d(\eta_0), \tag{4.30}$$

[6]Note that the volume is a function of η_0 only because we've chosen the sprinkling region to be symmetric about $\eta = 0$.

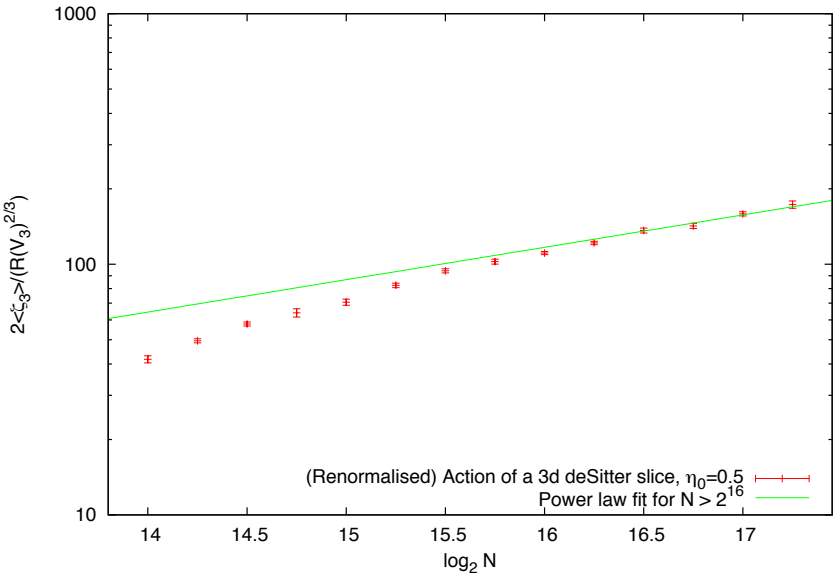

Figure 4.7: log-log plot of simulation data for the action of a slice of global dS^3 with $\eta_0 = 0.5$, $l_k = 3l$, varying density ρ with a power law fit. Data averaged over 10 runs. Fit function $h(k_d, N) = N^{k_d}$.

where $R = \frac{d(d-1)}{\lambda^2} = \frac{2d}{d-2}\Lambda$, and $\Lambda = \frac{(d-2)(d-1)}{2\lambda^2}$ is the usual cosmological constant. Using (4.11) we find

$$\frac{2}{RV_3^{2/3}}\langle\zeta_3[\epsilon_3, \mathcal{C}]\rangle = N^{1/3}, \tag{4.31}$$

$$\frac{2}{R\sqrt{V_4}}\langle\zeta_4[\epsilon_4, \mathcal{C}]\rangle = \sqrt{N}, \tag{4.32}$$

in $3d$ and $4d$ respectively.

Figures 4.7 and 4.8 show log-log plots of the renormalised expected action against N. A one-parameter, power law fit with $h(k_d, N) = N^{k_d}$ gives

$$k_3 = 0.429 \pm 0.001 \tag{4.33}$$

$$k_4 = 0.480 \pm 0.001. \tag{4.34}$$

Again both of these values are inconsistent with the conjectured value, $k_d = (d-2)/2$. We believe that this is due to not having reached the asymptotic regime.

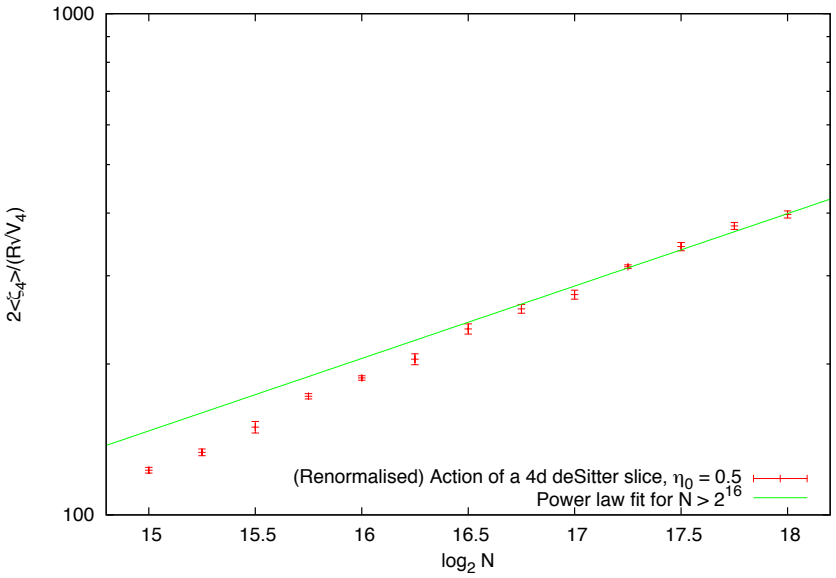

Figure 4.8: log-log plot of simulation data for the action of a slice of global dS^4 with $\eta_0 = 0.5$, $l_k = 2l$, varying density ρ with a power law fit. Data averaged over 10 runs. Fit function $h(k_d, N) = N^{k_d}$.

4.3.3 The Action of Non-Globally Hyperbolic Regions

We sprinkle into a portion of a d-dimensional "ball spacetime": $\mathcal{M} = I \times B^{d-1}$, where B^{d-1} is the $(d-1)$-ball and $I = [a, b]$, see figure 4.9. The spacetime is flat and has a timelike boundary so using (4.16) and (4.11) we find

$$\frac{(\pi r^2 \Delta t)^{2/3}}{2\pi r \Delta t} \langle \zeta_3[\epsilon_3, \mathcal{C}] \rangle = a_3 N^{\frac{2}{3}} \tag{4.35}$$

$$\frac{(4\pi r^3 \Delta t/3)^{3/4}}{4\pi r^2 \Delta t} \langle \zeta_4[\epsilon_4, \mathcal{C}] \rangle = a_4 N^{\frac{3}{4}} \tag{4.36}$$

for $d = 3$ and 4 respectively, where we have written the volume of the sprinkled regions and that of their respective codimension-1 boundaries explicitly.

Figures 4.10 and 4.11 show plots of (4.35) and (4.36) as a function of N. The straight lines are a two-parameter power law fit $f(a_d, k_d, N) = a_d N^{k_d}$

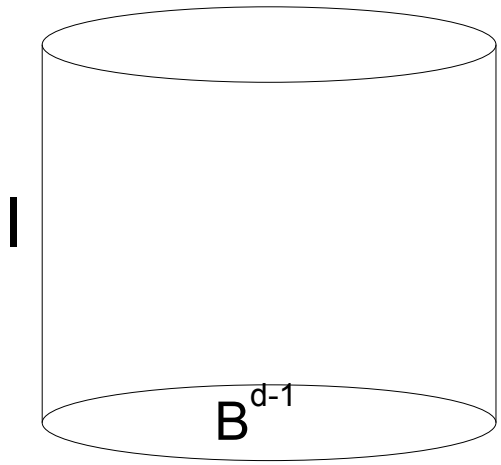

Figure 4.9: A sketch of the $3d$ ball spacetime where each constant time slice (time running vertically) represents a $(d-1)$-ball of radius r.

with

$$\begin{aligned} a_3 &= 0.025 \pm 0.003, \quad k_3 = 0.69 \pm 0.01 \\ a_4 &= 0.053 \pm 0.013, \quad k_4 = 0.74 \pm 0.02. \end{aligned} \tag{4.37}$$

Both of these values for k_d are consistent with our conjecture.

4.4 Cancellations

It is instructive to appreciate the effectiveness of the cancellations taking place in the computation of the action. Let us take the action of a flat interval in $4d$ as an example, and let us consider the most local action (i.e. $l_k = l$) for simplicity, $S[\mathcal{C}] = \beta_4 (l/l_p)^2 (N - N_1 + 9N_2 - 16N_3 + 8N_4)$. The first term in the action (trivially) grows like $O(N)$, so even if the higher order intervals only ever grew as fast as $O(N)$, we would still need these to cancel out to be able to have sub-$O(N)$ growth. But the higher order intervals grow even faster than $O(N)$ with increasing density. To see how fast consider the number of past-links connected to any given point x in the sprinkling. These links will roughly lie on a hyperboloid hugging the past light cone of x, and

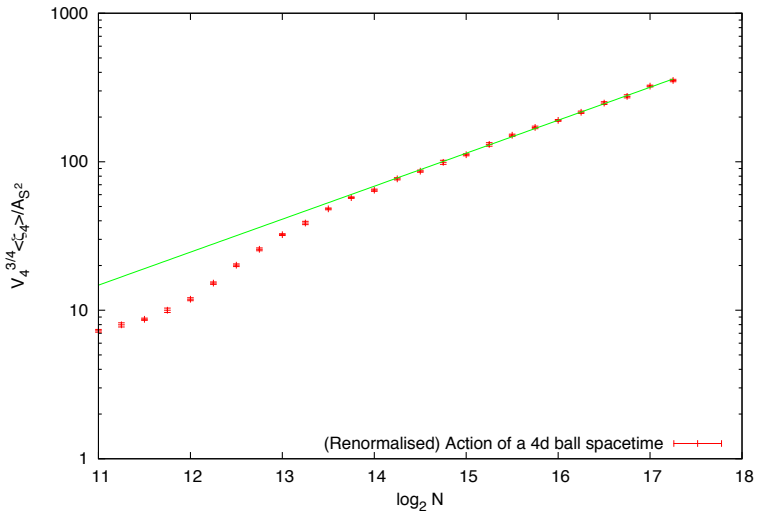

Figure 4.10: log-log plot of simulation data for a portion of a ball spacetime, $I \times B^2$, where $I \in [-0.5, 0.5]$ and $r = 1.5$, $l_k = 3l$, varying density ρ with a power law fit. Data averaged over 10 runs. Fit function $f(b_d, k_d, N) = b_d N^{k_d}$.

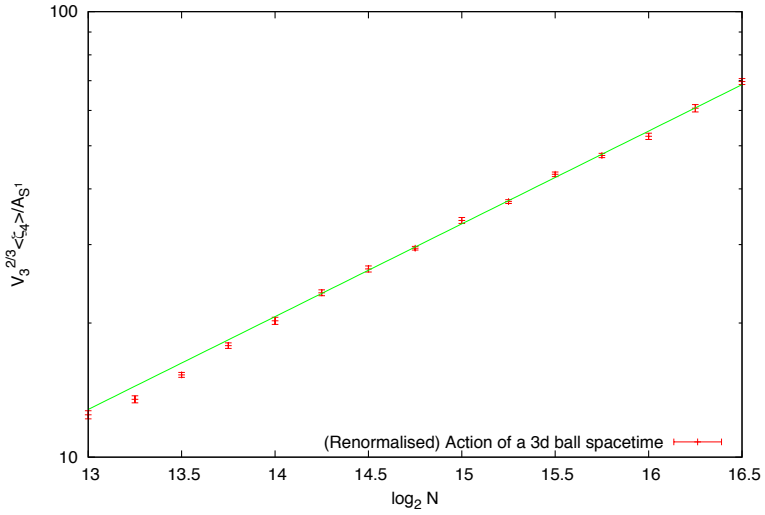

Figure 4.11: log-log plot of simulation data for a portion of a ball spacetime, $I \times B^3$, where $I \in [-0.5, 0.5]$ and $r = 1.5$, $l_k = 2l$, varying density ρ with a power law fit. Data averaged over 10 runs. Fit function $f(b_d, k_d, N) = b_d N^{k_d}$.

so, to leading order, will grow like the volume of hyperboloid $\sim O(\sqrt{N})$. Multiplying by N we find that the number of links grows like $O(N^{3/2})$. It is easy to see that higher order intervals will also have this leading order behaviour, so the cancellations are not only happening at order N, but also at order $N^{3/2}$! This should put into perspective how remarkable the above result are, even with the current inconsistencies, since they all scale with sub-$O(N)$ behaviour, and in most cases the actual scaling is very close to the conjectured one.

4.5 Discussion

Much of the evidence we have provided in the previous sections is inconsistent with the conjectured continuum limit of the causet action (4.16). In particular we found that the expected action of a globally hyperbolic subregion of deSitter is inconsistent with the Einstein-Hilbert bulk term, and the expected action of an interval in $\mathbb{M}^d$, $d = 3, 4$, is inconsistent with the codimension 2 boundary term. However, in $2d$ the analytic results are consistent with the conjectured codimension 2 boundary term (albeit being degenerate in $2d$), and also the expected action of a non-globally hyperbolic spacetime is consistent with the volume of the codimension 1 timelike boundary of the spacetime.

The status of the conjecture at this point can therefore be summarised as follows. Evidence for the bulk term being the EH action in the continuum limit is tentative at best. Evidence for the diverging boundary term proportional to the codimension 1 volume of the timelike boundary is positive. Evidence for the codimension 2 volume of the intersection of the "future boundary" with the "past boundary" is conflicting.

Out of these three terms the bulk term is arguably the most important one, since the whole reason behind this definition of the action was that it would reproduce the EH action in the continuum limit. It is therefore unfortunate that this is the term for which we have the least evidence, and that the evidence we do have is inconsistent with the conjecture. We do however have good reasons to believe that these negative results are due to not having reached the asymptotic regime, c.f. Chapter 6, and leave it for future work to establish the veracity of this claim. Regarding the boundary terms, evidence given in chapters 5 and 6 will settle the conflicting nature

of the results given here in favour of our conjecture.

Provided the above expectations are realised, and the conjecture is verified, an important question left to answer is what is the continuum limit of the action of a globally hyperbolic spacetime which is not a normal neighbourhood? In other words, is the continuum limit of the expected action of a globally hyperbolic spacetime the EH action up to boundary terms? To answer this question we would either need to prove a result for the causet d'Alembertian B acting on fields ϕ whose support is not contained in a normal neighbourhood, or directly calculate the action for such spacetimes and see what it gives. Both of these options possess their own difficulties, and so far neither have been explored in much detail.

A final comment regarding fluctuations. It was shown in Chapter 3 that for fixed $l_k > l$, fluctuations in the d'Alembertian go to zero in the limit $l \to 0$. Furthermore we claimed that if $l_k \gg l$ and the characteristic length scale of the field ϕ, $\lambda > l_k$, then, for a given sprinkling, $B_k\phi \approx (\Box - R/2)\phi$. Although it has yet to be shown explicitly, simulations suggest that the same will be true about the action of a spacetime region $\mathcal{N}$, i.e. fix $l_k \gg l$ and let the radius of curvature r of $\mathcal{N}$ be everywhere large compared to l_k, $r \gg l_k$, then for any sprinkling $\mathcal{C}$ of $\mathcal{N}$, the action $S_k[\mathcal{C}]$ will be close to the mean.

Chapter 5

Lorentzian Gauss-Bonnet Theorem and the 2D Action

We saw in the previous chapter that the action of a sprinkling of causal interval in 2 dimensional Minkowski spacetime is a constant. This raises the question whether the $2d$ action is in some sense topological and if so, if there is a relation to the Lorentzian Gauss-Bonnet theorem [31, 32, 33]. In this chapter we explore this question.

Recall that the $2d$ action, S, of a finite causal set $\mathcal{C}$ is [8]

$$S[\mathcal{C}] = N - 2N_1 + 4N_2 - 2N_3 \tag{5.1}$$

where N is the cardinality of $\mathcal{C}$, and N_m is the number of inclusive order intervals in $\mathcal{C}$ of cardinality $m+1$. N_1 therefore is the number of links in $\mathcal{C}$, N_2 is the number of order intervals that are 3-chains (3 element chains), N_3 is the number of order intervals that are 4-chains plus the number that are "diamonds" (with two mutually unrelated elements between the top and bottom elements), and we have used a different normalisation from previous chapters. Note that N_3 is not the number of subcausets that are 3-chains but the number of *order intervals* that are 3-chains. The form of S as an alternating sum of (weighted) numbers of things is intriguingly reminiscent of certain topological indices.

One can think of the action (5.1) as an integer valued random variable, the *Discrete Action* $\mathbf{S}_{\mathcal{M},\rho}$, for each finite volume spacetime $\mathcal{M}$ and density ρ via the sprinkling process: $\mathbf{S}_{\mathcal{M},\rho}$ takes the value $S[\mathcal{C}]$ with probability

$\mathbb{P}_{\mathcal{M},\rho}(\mathcal{C})$. We also define the random variable $\mathbf{S}_{\mathcal{M},N}$ which takes the value $S[\mathcal{C}]$ with the probability that causet $\mathcal{C}$ arises in the process of selecting exactly N elements uniformly at random – according to the spacetime volume measure – from $\mathcal{M}$. We then have

$$\langle \mathbf{S}_{\mathcal{M},\rho} \rangle = \sum_{N=0}^{\infty} \frac{(\rho V)^N}{N!} e^{-\rho V} \langle \mathbf{S}_{\mathcal{M},N} \rangle \tag{5.2}$$

where $\langle \cdot \rangle$ denotes the expected value, V is the spacetime volume of $\mathcal{M}$, and $\frac{(\rho V)^N}{N!} e^{-\rho V}$ is the probability that N elements are selected in the Poisson process of sprinkling into $\mathcal{M}$ at density ρ.

The Poisson distribution gives for the mean,

$$\langle \mathbf{S}_{\mathcal{M},\rho} \rangle = \rho V - 2\rho^2 \int_{\mathcal{M}} d^d y \sqrt{-g(y)} \int_{\mathcal{M} \cap J^+(y)} d^d x \sqrt{-g(x)} \left(1 - 2\rho V_{xy} + \frac{1}{2} (\rho V_{xy})^2 \right) e^{-\rho V_{xy}} \tag{5.3}$$

where V_{xy} is the volume of the spacetime causal interval, $[x, y] := J^+(y) \cap J^-(x)$, between x and y and d is the dimension of $\mathcal{M}$. This can be understood thus: $\rho \, d^d x \sqrt{-g(x)}$ is the probability that an element is sprinkled in an elemental volume at x and similarly for y; $e^{-\rho V_{xy}}$, $\rho V_{xy} e^{-\rho V_{xy}}$ or $\frac{1}{2}(\rho V_{xy})^2 e^{-\rho V_{xy}}$ is the probability that there is no element, one element or two elements, respectively, sprinkled in $[x, y]$.

Note that the double integration may be done in either order:

$$\langle \mathbf{S}_{\mathcal{M},\rho} \rangle = \rho V - 2\rho^2 \int_{\mathcal{M}} d^d x \sqrt{-g(x)} \int_{\mathcal{M} \cap J^-(x)} d^d y \sqrt{-g(y)} \left(1 - 2\rho V_{xy} + \frac{1}{2} (\rho V_{xy})^2 \right) e^{-\rho V_{xy}} . \tag{5.4}$$

Indeed, the causet action (5.1) is invariant under reversal of the order relation on $\mathcal{C}$, and so the Discrete Action (DA) for any spacetime $(\mathcal{M}, g)$ is equal to the DA of its time-orientation-reverse.

Since L is thus related to the Ricci scalar when the causal set is a $2d$ sprinkling and S is a sum of $L(\cdot)$ over the causal set, this implies that when $\mathcal{M}$ is 2-dimensional and as $\rho \to \infty$, $\langle \mathbf{S}_{\mathcal{M},\rho} \rangle$ will tend to something that contains a term $\frac{1}{4} \int_{\mathcal{M}} d^2 x \sqrt{-g} R$ plus terms arising from boundary effects. We now investigate this and in particular the nature of the boundary

terms. In doing so we will be exploring whether the $2d$ Discrete Action is topological in character. The standard gravitational action for $2d$ Euclidean gravity, with its Einstein-Hilbert term and the ($2d$ analogue of the) Gibbons-Hawking boundary term, is known to be a topological invariant, due to the Gauss-Bonnet theorem. The Gauss-Bonnet Theorem has been extended to Lorentzian manifolds [34, 35], so for ordinary (Lorentzian) $2d$ gravity, the action with an appropriate boundary term is also topological and a question arises: to what extent is the $2d$ causal set action topological?

5.1 Intervals in $\mathbb{M}^2$

Consider a causal interval in $2d$ Minkowski spacetime, $\mathcal{I} := [p, q] \subset \mathbb{M}^2$. For definiteness consider the interval to have fixed volume (area), V.

Following a conjecture of R. Sorkin, G. Brightwell proved that the mean $\langle \mathbf{S}_{\mathcal{I},N} \rangle = 1$, for any $N \neq 0$ [36]. This implies that the mean of $\mathbf{S}_{\mathcal{I},\rho}$ is

$$\begin{aligned} \langle \mathbf{S}_{\mathcal{I},\rho} \rangle &= \sum_{N=1}^{\infty} \frac{(\rho V)^N}{N!} e^{-\rho V} \\ &= 1 - e^{-\rho V} \end{aligned} \tag{5.5}$$

where $\frac{(\rho V)^N}{N!} e^{-\rho V}$ is the probability, in the Poisson process, that N elements are sprinkled into $\mathcal{I}$.

We use (5.3) to prove this result in a different way:

$$\langle \mathbf{S}_{\mathcal{I}} \rangle = \rho V - 2\rho^2 \int_{\mathcal{I}} d^2y \int_{\mathcal{I} \cap J^+(y)} d^2x \;\; p(\rho V_{xy}) \tag{5.6}$$

where $p(\xi) = (1 - 2\xi + \frac{1}{2}\xi^2) \exp(-\xi)$ and we have suppressed the subscript ρ on the random variable $\mathbf{S}_{\mathcal{I},\rho}$.

We use coordinates in which p and q lie on the time axis and q is at the origin. We consider null coordinates $u_x = \frac{1}{\sqrt{2}}(x^0 - x^1)$, $v_x = \frac{1}{\sqrt{2}}(x^0 + x^1)$ and similarly for u_y, v_y. Then the interval is defined by $u, v \in [0, a]$ for $a = \sqrt{V}$.

$$\langle \mathbf{S}_{\mathcal{I}} \rangle = \rho V - 2 \int_0^a du_x \int_0^a dv_x \int_0^{u_x} du_y \int_0^{v_x} dv_y \, \rho^2 \, p(\rho \, \Delta u \, \Delta v) \tag{5.7}$$

where $\Delta u = u_x - u_y,\ \Delta v = v_x - v_y$.

$$\begin{aligned}\langle \mathbf{S}_{\mathcal{I}} \rangle &= \rho V - 2 \int_0^a du_x \int_0^a dv_x \int_0^{u_x} d\Delta u \int_0^{v_x} d\Delta v\, \rho^2\, p(\rho\, \Delta u\, \Delta v) \\ &= \rho V - 2 \int_0^a du_x \int_0^a dv_x \left[[\text{integrand 1}]_{\Delta v=0}^{\Delta v=v_x} \right]_{\Delta u=0}^{\Delta u=u_x}\end{aligned}$$

where

$$\begin{aligned}&\text{integrand 1} = -\frac{\rho}{2}\,(1 - \rho\, \Delta u\, \Delta v)\, \exp(-\rho\, \Delta u\, \Delta v) \\ &[g(\xi)]_{\xi=\beta}^{\xi=\alpha} = g(\alpha) - g(\beta).\end{aligned}$$

Hence

$$\langle \mathbf{S}_{\mathcal{I}} \rangle = 1 - \exp(-\rho\, a^2) = 1 - \exp(-\rho V)\,. \tag{5.8}$$

As $\rho \to \infty$, $\langle \mathbf{S}_{\mathcal{I}} \rangle \to 1$ and we write $\langle \mathbf{S}_{\mathcal{I}} \rangle \approx 1$ to denote this.

Consider now splitting up the interval $\mathcal{I}$ into four smaller intervals $\mathcal{I}_i$, $i = 1, \ldots 4$, as shown in Fig. 5.1a. When computing the expected value of $\mathbf{S}_{\mathcal{I}}$ one can split the integral up into the means of the actions of the four subintervals plus the "bilocal" contributions when x and y lie in two different subintervals. More concretely, given any subcausets, A and B of a causal set $\mathcal{C}$, we have

$$S[\mathcal{C}; A, B] = N(A, B) - 2N_1(A, B) + 4N_2(A, B) - 2N_3(A, B) \tag{5.9}$$

where $N(A, B)$ is the number of elements in $A \cap B$ and $N_m(A, B)$ is the number of inclusive order intervals in $\mathcal{C}$ of cardinality $m+1$ with top element in A and bottom element in B. Now let X and Y be submanifolds of spacetime $\mathcal{M}$. We define the random variable, $\mathbf{S}_{\mathcal{M};X,Y}$, the *Discrete Bilocal Action*, via the sprinkling process: sprinkle into $\mathcal{M}$ at density ρ [1] to obtain causet $\mathcal{C}$ with subcauset $A(B)$ being that sprinkled into $X(Y)$. For that realisation, $\mathbf{S}_{\mathcal{M};X,Y}$ takes the value $S[\mathcal{C}; A, B]$. Note that $\mathbf{S}_{\mathcal{M};X,X} = \mathbf{S}_X$ if X is a *causally convex* subset of $\mathcal{M}$.[2]

Now, consider $\mathcal{I}$ and its subintervals. If we adopt $\mathbf{S}_{ij}$ as simplified nota-

[1] To simplify notation, we don't make the dependence on the density explicit.

[2] A causally convex region, X, of $\mathcal{M}$ is one such that $x, y \in X$ implies that the causal interval in $\mathcal{M}$ between x and y is a subset of X.

tion for the bilocal action $\mathbf{S}_{\mathcal{I};\mathcal{I}_i,\mathcal{I}_j}$, then we have

$$\langle \mathbf{S}_{\mathcal{I}} \rangle = \sum_{i=1}^{4} \langle \mathbf{S}_{\mathcal{I}_i} \rangle + \sum_{\substack{i,j=1 \\ j<i}}^{4} \langle \mathbf{S}_{ij} \rangle \,. \tag{5.10}$$

The bilocal summands can be computed using the integral in Eq. (5.7) and

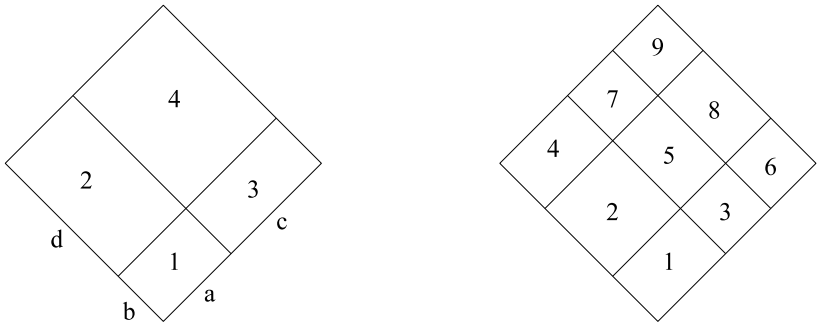

(a) a and c (b and d) are the v-coordinate (u-coordinate) lengths of the sides of the subintervals

(b)

Figure 5.1: Splitting up a causal interval in $2d$ Minkowski to compute the action

adjusting the boundaries. This yields

$$\begin{aligned}
\langle \mathbf{S}_{21} \rangle &= -2 \int_0^a dv_x \int_b^{b+d} du_x \int_0^{v_x} dv_y \int_0^b du_y \, \rho^2 \, p(\rho \, \Delta u \, \Delta v) \\
&= -2 \int_0^a dv_x \int_b^{b+d} du_x \left[[\text{integrand } 1]_{\Delta u = u_x - b}^{\Delta u = u_x} \right]_{\Delta v = 0}^{\Delta v = v_x} \\
&= -1 + \exp(-a\, b\, \rho) + \exp(-a\, d\, \rho) - \exp(-a\, (b+d)\, \rho) \qquad (5.11) \\
&\approx -1
\end{aligned}$$

and

$$\begin{aligned}
\langle \mathbf{S}_{41} \rangle &= -2 \int_a^{a+c} dv_x \int_b^{b+d} du_x \int_0^a dv_y \int_0^b du_y \, \rho^2 \, p(\rho \, \Delta u \, \Delta v) \\
&= -2 \int_a^{a+c} dv_x \int_b^{b+d} du_x \left[[\text{integrand 1}]^{\Delta u = u_x}_{\Delta u = u_x - b} \right]^{\Delta v = v_x}_{\Delta v = v_x - a} \\
&= 1 - \exp(-(a+c)\,(b+d)\,\rho) \\
&\quad + \exp(-a\,(b+d)\,\rho) + \exp(-c\,(b+d)\,\rho)) \\
&\quad + \exp(-(a+c)\,b\,\rho) + \exp(-(a+c)\,d\,\rho) \\
&\quad - \exp(-a\,b\,\rho) - \exp(-a\,d\,\rho) - \exp(-c\,b\,\rho) - \exp(-c\,d\,\rho) \qquad (5.12) \\
&\approx 1 \, .
\end{aligned}$$

The three other bilocal contributions $\langle \mathbf{S}_{ij} \rangle$ can be obtained from $\langle \mathbf{S}_{21} \rangle$ by changing the parameters appropriately. Putting together all parts of Eq. (5.10) one exactly recovers Eq. (5.5).

Now, one can continue this game and split up the interval even further as in Fig. 5.1b. To compute the mean of the action one must again calculate

$$\langle \mathbf{S}_{\mathcal{I}} \rangle = \sum_{i=1}^{9} \langle \mathbf{S}_{\mathcal{I}_i} \rangle + \sum_{\substack{i,j=1 \\ j<i}}^{9} \langle \mathbf{S}_{ij} \rangle \, . \qquad (5.13)$$

We already know the contributions $\langle \mathbf{S}_{I_i} \rangle \approx 1$ and the bilocal contributions from two intervals that either share an edge or lie above and below a shared vertex (*e.g.* $\langle \mathbf{S}_{21} \rangle$ and $\langle \mathbf{S}_{51} \rangle$ in Fig. 5.1b). It remains to compute the bilocal contributions from pairs of intervals such as (4,1),(7,1) and (9,1) in Fig. 5.1b. It turns out they consist only of exponential terms that are small when intervening intervals are large on the discreteness scale. In the limit of large density, we are left with a contribution of 1 for every subinterval, -1 for every edge and 1 for every vertex. One could write

$$\langle \mathbf{S} \rangle \approx F - E + V \qquad (5.14)$$

where F denotes the number of faces *i.e.* intervals, E the number of edges and V the number of vertices. $F - E + V$ is the formula for the Euler character of a polyhedron and motivates the question: Is the expected action (to some extent) a topological invariant? It is obvious that the formula can

be applied to arbitrary causally convex regions of $\mathbb{M}^2$ that can be tiled by causal intervals as long as each interval is large enough for the corrections to be negligible. It is not hard to verify that any such region will have a mean Discrete Action $\langle \mathbf{S} \rangle \approx 1$. So for example the region shown in Fig. 5.2a will give $\langle \mathbf{S} \rangle \approx 1$ but the region in Fig. 5.2b will not.

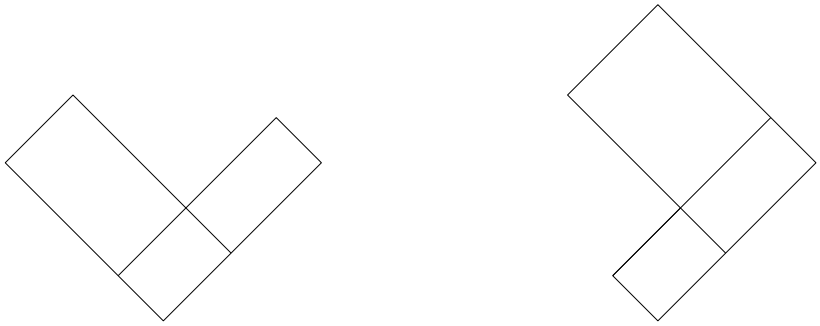

(a) causally convex (b) not causally convex

Figure 5.2: Different regions constructed from causal intervals in $\mathbb{M}^2$

5.2 Causally convex regions in $\mathbb{M}^2$

The boundary of a causally convex region of $\mathbb{M}^2$ can be spacelike in parts, but never timelike. If the region's boundary comprises straight line segments, such as the hexagon shown in Fig. 5.3b, then it can be divided up by null lines into a collection of intervals and causally convex triangles such as Fig. 5.3a. Then the formula (5.14) will apply if the mean of the Discrete Action for a causally convex triangle tends to 1 in the infinite density limit.

First note that by Poincaré invariance we can choose coordinates so that the spacelike edge of the triangle is at $t =$constant, and the apex lies at the origin.

Using null coordinates, as before, we have

$$\langle \mathbf{S}_{\triangle} \rangle = \rho V - 2\rho^2 \int_0^L dv_x \int_0^{v_x} du_x \int_0^{v_x} dv_y \int_0^{u_x} du_y \, p(\rho \Delta u \Delta v) \qquad (5.15)$$

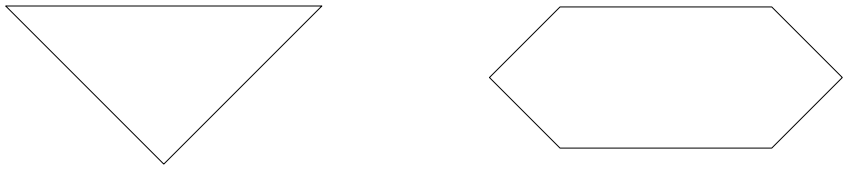

(a) causally convex triangle (b) causally convex hexagon

Figure 5.3: Causally convex regions with boundaries formed from null and spacelike line segments

where $L = \sqrt{2V}$ and V is the area of the triangle. This gives

$$\langle \mathbf{S}_{\triangle} \rangle = 1 + \frac{1}{\rho V} + O\left((\rho V)^{-2}\right) \approx 1\,. \tag{5.16}$$

We see that the mean DA of the triangle does indeed tend to 1 as $\rho \to \infty$, though the corrections are not exponentially small.

Now, consider a general causally convex region with a boundary whose spacelike portion is curved. So long as the discreteness scale is small enough – small compared to the radius of curvature of the boundary – we can tile the region with intervals and with causally convex approximate triangles along the spacelike boundary, all of which are large enough compared to the discreteness scale for the Formula (5.14) to hold approximately. We conclude that the mean of the DA for any causally convex region of $\mathbb{M}^2$ will tend to 1 in the limit of infinite density.

Is causal convexity necessary for the mean of the DA to be approximately 1? When a region, $R \subset \mathbb{M}^2$, is not causally convex, there will exist pairs of points $x, y \in R$ such that the causal interval in R between x and y is smaller than the causal interval between them in $\mathbb{M}^2$ (the "diamond"). Since it is the volume of the causal interval in R which appears in the expression for the mean of the DA, one might expect this to disrupt the result and indeed it does. As we shall see now this is consistent with the conjecture (4.16).

Consider the Discrete Action, $\mathbf{S}_{\square}$ of a rectangle with edges parallel to the t and x axes. Analytic computation of the expectation value $\langle \mathbf{S}_{\square} \rangle$ is hard

exactly because of the lack of causal convexity: the integral (5.3) breaks up into several subintegrals depending on the positions of x and y relative to the boundary. Therefore we use simulations to estimate the value. A sprinkling into a rectangle has three independent parameters that fully characterise the problem. One choice is the spatial width w, the height along the time-axis h and the sprinkling density ρ.[3] The expectation value $\langle \mathbf{S}_{\Box,w,h,\rho} \rangle$ must be invariant under rescaling

$$\begin{aligned} w &\rightarrow \lambda \cdot w \\ h &\rightarrow \lambda \cdot h \\ \rho &\rightarrow \lambda^{-2} \cdot \rho. \end{aligned} \tag{5.17}$$

Fig. 5.4 shows simulation data for two different setups with power-law fits. Fig. 5.4a shows $\langle \mathbf{S} \rangle$ for constant w and h and varying ρ, Fig. 5.4b for constant w and ρ and for varying h. Given the small relative error bars the power-law fits look quite convincing and we will assume that $\langle \mathbf{S}_{\Box} \rangle$ can, at least in the regime covered by the simulations, be written in the form

$$\langle \mathbf{S}_{\Box} \rangle = \text{const} \cdot h^{\alpha} w^{\beta} \rho^{\gamma}. \tag{5.18}$$

The scale invariance (5.17) demands $\alpha + \beta - 2\gamma = 0$. From simulation 1 (Fig. 5.4a) one is tempted to deduce $\gamma = 1/2$ and from simulation 2 (Fig. 5.4b) that $\alpha = 1$. It follows $\beta = 0$.

The fact that for constant ρ the width does not affect the value of the action whereas $\langle \mathbf{S}_{\Box} \rangle \propto h$ suggests that in general $\langle \mathbf{S}_{\Box} \rangle$ contains boundary terms from timelike boundaries only, which again is consistent with conjecture (4.16).

5.3 The flat cylinder

In order to apply formula Eq. (5.14) to a causal interval, $\mathcal{I}_c$, of height T on a cylinder with circumference L with $L \leq T \leq 2L$ one might come up with a tiling into subintervals, $\mathcal{I}_i$, $i = 1, \ldots 8$, as shown in Fig. 5.5. Taking into account the topological identification, we have $F = 8, E = 12, V = 4$ thus

[3] Width w, height h and expected number of sprinkled elements N would be another choice.

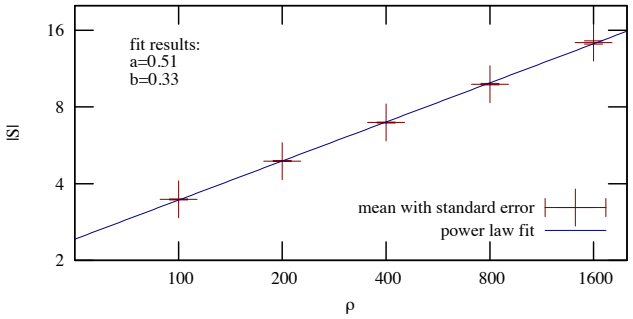

(a) Simulation data for the action of a rectangle in $\mathbb{M}^2$ for $w = h = 1$, varying density ρ with a power-law fit. Data averaged over 10^6 to 10^7 runs. Fit function: $\rho^a \cdot b$.

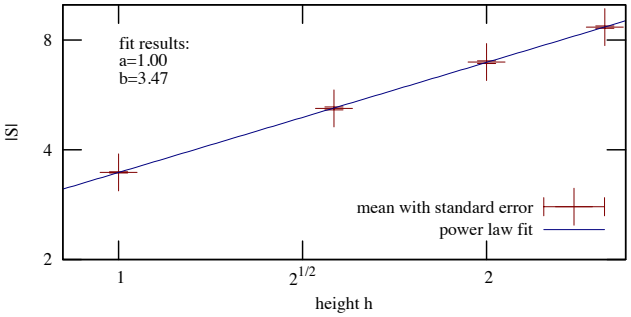

(b) Simulation data for the action of a rectangle in $\mathbb{M}^2$ for $w = 1, \rho = 100$, varying height h with a power-law fit. Data averaged over 10^6 to 10^7 runs. Fit function: $h^a \cdot b$.

Figure 5.4: Numerical results for the action of a rectangle in $\mathbb{M}^2$.

yielding a predicted high-density expectation value of $\langle \mathbf{S}_{\mathcal{I}_c} \rangle \approx 0$. However we have not shown yet that formula Eq. (5.14) is applicable to the cylinder. The division of the causal interval in Fig. 5.5 has been chosen such that formula Eq. (5.5) for the faces and formulae Eq. (5.11) and (5.12) for the bilocal contributions of two intervals that share an edge or lie above and below a vertex can still be applied as the cylinder topology does not affect these cases. But the computation of contributions like (5,1),(6,1) and (8,1) differs from the Minkowski setup due to the nontrivial topology.

Recall

$$\langle \mathbf{S}_{\mathcal{I}_c} \rangle = \rho V - 2K \tag{5.19}$$

where

$$K = \rho^2 \int_{\mathcal{I}_c} d^2y \int_{\mathcal{I}_c \cap J^+(y)} d^2x \; p(\rho V_{xy}) \,. \tag{5.20}$$

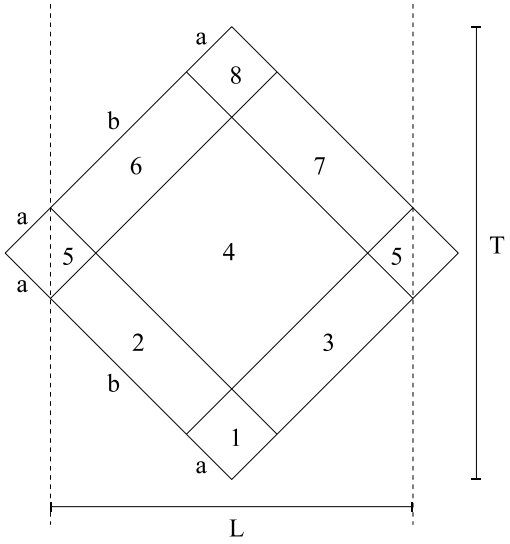

Figure 5.5: Tiling of the interval $\mathcal{I}_c$ with $L \leq T \leq 2L$. a and b are the u and v coordinate lengths of the sides of the subintervals shown.

In general, K can be split into a sum of terms, $K = \sum_{\alpha=1}^{\infty} K_\alpha$ depending on how many homotopy classes of causal curves there are from y to x:

$$K_\alpha := \rho^2 \int_{\mathcal{I}_c} d^2y \int_{\mathcal{I}_c \cap J_\alpha^+(y)} d^2x \; p(\rho V_{xy}) \tag{5.21}$$

where

$$J_\alpha^+(y) := \{x \in J^+(y) \,|\, \exists \text{ exactly } \alpha \text{ homotopy classes of causal curves from } y \text{ to } x\}\,. \tag{5.22}$$

This split is motivated by the fact that V_{xy} strongly depends on the number of homotopy classes of causal paths between x and y. For our interval, $K_\alpha = 0$ for $\alpha > 3$.

From Fig. 5.5 we see the relation between a, b, T and L is:

$$\begin{aligned} a &= (T - L)/\sqrt{2} \\ b &= (2L - T)/\sqrt{2} \end{aligned} \tag{5.23}$$

The causal volume V_{xy} for $x \in J_\alpha^+(y)$ for $\alpha \geq 3$ is at least $(a + b)^2$ so K_3 is suppressed by at least $\exp(-\rho(a + b)^2)$ and can thus be neglected as

$L = \sqrt{2}(a+b)$ is assumed to be large in discreteness units of $\rho^{-\frac{1}{2}}$.

The values for K_1 and K_2 are [37]

$$\begin{aligned} K_1 &= \frac{\rho V}{2} + \frac{1}{2}\exp(-\rho a^2) - (1+\rho ab)\exp(-\rho a(a+b)) + \text{corr.} \\ K_2 &= -\frac{2}{(a+b)^2\rho} + \exp(-\rho a(a+b))\,[1+\rho ab \\ &\quad + \frac{1}{(a+b)^4\rho^2}\left((6+2\rho(a+b)(2a+b) - \rho^2(a+b)^2b^2 + \rho^3(a+b)^3ab^2\right) \\ &\quad -2\exp(-\rho a(a+b))(3+4\rho a(a+b)+2\rho^2a^2(a+b)^2)\big)\big] + \text{corr.} \quad (5.24) \end{aligned}$$

where "+ corr." stands for neglected terms suppressed by $\exp(-\rho(a+b)^2)$. However we will keep terms with factors $\exp(-\rho\, a^2)$ and $\exp(-\rho\, a\,(a+b))$ since for T only slightly larger than L the value of a will be very small and these terms are then significant.

The overall action is

$$\begin{aligned} \langle \mathbf{S}_{\mathcal{I}_c} \rangle &= -\exp(-\rho a^2) + 2(1+\rho ab)\exp(-\rho a(a+b)) \\ &\quad + \frac{4}{(a+b)^2\rho} + \exp(-\rho a(a+b))\,[1+\rho ab \\ &\quad + \frac{1}{(a+b)^4\rho^2}\left((6+2\rho(a+b)(2a+b) - \rho^2(a+b)^2b^2 + \rho^3(a+b)^3ab^2\right) \\ &\quad -2\exp(-\rho a(a+b))(3+4\rho a(a+b)+2\rho^2a^2(a+b)^2)\big)\big] + \text{corr.} \quad (5.25) \end{aligned}$$

For $T > 2L$ consider a division of the interval into regions 1 and 2 as shown in Fig. 5.6. The expected DA is the sum of the expected actions for regions 1 and 2 and the bilocal contribution $\langle \mathbf{S}_{21} \rangle$.

It can be shown [37] that the expected action for region 1 and the bilocal contribution cancel (up to exponentially small terms) and the result is just given by the expected action of region 2 which can be obtained from Eq.(5.25) by setting $a = L/\sqrt{2}, b = 0$ (and now neglecting all exponentials as a is no longer close to 0):

$$\langle \mathbf{S}_{\mathcal{I}_c} \rangle = \frac{8}{L^2\rho} + \text{corr.}\,. \quad (5.26)$$

Fig. 5.7 shows a plot of the analytic expectation value for the cylinder action compared to simulation results. For $T \to L$ the action approaches the Minkowskian limit 1. For T only slightly greater than L the exponen-

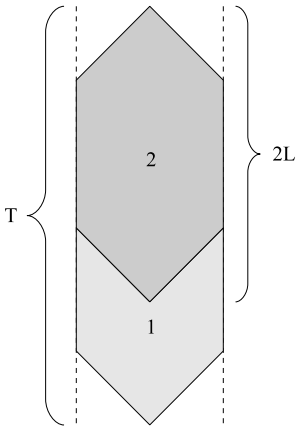

Figure 5.6: Division of interval when $T > 2L$.

tial terms dominate and cause a downwards spike. As $T \to 2L$ the non-exponential correction, $\frac{8}{\rho L^2}$ (which comes from K_2) dominates. However this also tends to zero in the limit $\rho \to \infty$ so $\langle \mathbf{S}_{\mathcal{I}_c} \rangle \approx 0$ as initially predicted. Indeed it can be shown explicitly that the bilocal contributions from pairs of intervals that do not share an edge or vertex tend to zero as $\rho \to \infty$ and so the formula $F - E + V$ can be applied to intervals of the cylinder. More generally, the previous argument regarding null tilings of causally convex regions of $\mathbb{M}^2$ can be given here, and we conclude that $\langle \mathbf{S} \rangle \approx 0$ for general topologically non-trivial causally convex regions of the cylinder.

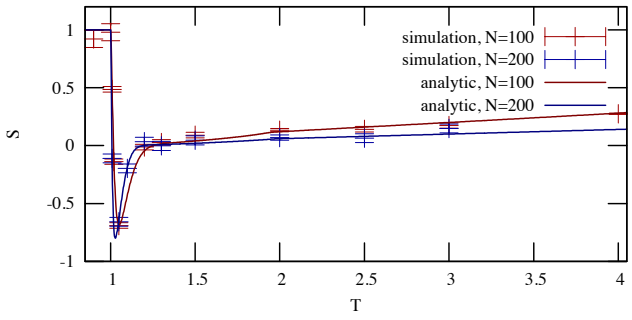

Figure 5.7: The expected action of a cylinder-interval for $L = 1, \langle N \rangle = 100$ and $\langle N \rangle = 200$ compared with simulation results.

5.4 The flat trousers

We investigate now a causally convex neighbourhood of the flat 1+1 trousers spacetime in which two S^1's join to form a single S^1. The trousers spacetime is a piece of $\mathbb{M}^2$ with cuts and identifications as shown in Fig. 5.8. Although the singularity, P, at which the topology changes is by some definitions not strictly in the spacetime since the metric degenerates there, nevertheless the causal order is well defined at the singularity: it is clear what the causal past and causal future of P are. Therefore we will consider P as a point of the manifold. Note that in any sprinkling into the trousers almost surely no element will be sprinkled at P.

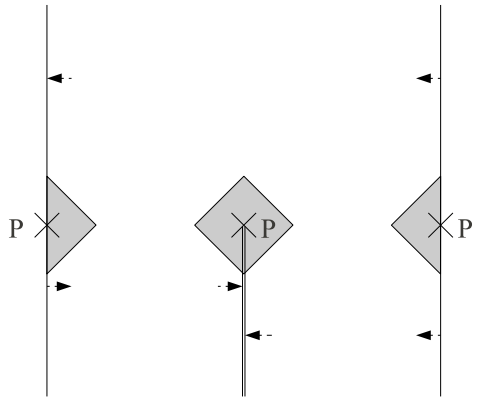

Figure 5.8: The trousers spacetime. P is the singularity – all three instances of P are identified – and the shaded region is a neighbourhood of P. There is a vertical cut down from the central copy of P with the two legs identified as shown.

Let $\mathcal{N}$ denote the neighbourhood of P shown as the shaded region in Fig. 5.8. It consists of two flat intervals each with P as their midpoint, identified across "branch cuts" from P to their past tips. $\mathcal{N}$ is topologically a disc if P is included the manifold and if the formula (5.14) holds then the expected DA of $\mathcal{N}$ would be equal to 1 in the limit of large density.

Let the volume (area) of each of the two intervals be $4a^2$ and consider the null tiling into 8 intervals, $\mathcal{I}_i$, $i = 1, \ldots, 8$, shown in Fig. 5.9. The interval $\mathcal{I}_1$ comprises the two triangles labelled $1'$ and $1''$ and the interval $\mathcal{I}_2$ comprises the triangles labelled $2'$ and $2''$. Adopting the same notation

for the bilocal discrete action of two intervals used in (5.10) we have

$$\langle \mathbf{S}_{\mathcal{N}} \rangle = \sum_{i=1}^{8} \langle \mathbf{S}_{\mathcal{I}_i} \rangle + \sum_{\substack{i,j=1 \\ j<i}}^{8} \langle \mathbf{S}_{ij} \rangle \,. \tag{5.27}$$

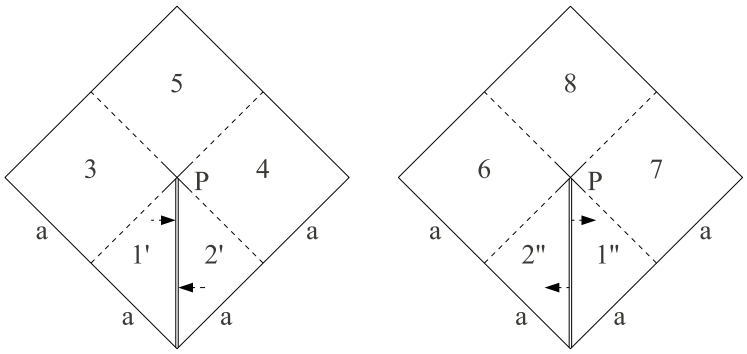

Figure 5.9: Null tiling of $\mathcal{N}$ into 8 intervals.

For each i, $\langle \mathbf{S}_{\mathcal{I}_i} \rangle \approx 1$. The bilocal terms are nonzero when the intervals $\mathcal{I}_i$ and $\mathcal{I}_j$ share an edge and in that case $\langle \mathbf{S}_{ij} \rangle \approx -1$. There are 8 edges so these contributions cancel the contributions of the 8 individual intervals. The only other nonzero bilocal terms are $\langle \mathbf{S}_{ij} \rangle$ where $i = 5, 8$ and $j = 1, 2$ and their sum is the contribution of the vertex at the singularity. These 4 terms are equal by symmetry so we have $\langle \mathbf{S}_{\mathcal{N}} \rangle = 4 \langle \mathbf{S}_{51} \rangle$.

The causal interval between $x \in \mathcal{I}_5$ and $y \in \mathcal{I}_1$ is shown in Fig. 5.10 and we deduce that

$$\langle \mathbf{S}_{51} \rangle = -2 \int_a^{2a} du_x \int_a^{2a} dv_x \int_0^a du_y \int_0^a dv_y \, \rho^2 \, p(\rho V_{xy}) \,. \tag{5.28}$$

where

$$V_{xy} = \Delta u \Delta v - (v_x - a)(a - u_y) \,. \tag{5.29}$$

This gives

$$\langle \mathbf{S}_{\mathcal{N}} \rangle = 4 \ln(\rho a^2) + 4(\gamma - 1) + \mathrm{O}\left(\frac{1}{\rho a^2}\right) \tag{5.30}$$

where γ is Euler's constant. We see that the expected DA of the neighbourhood of the singularity does not tend to 1 or any constant but grows

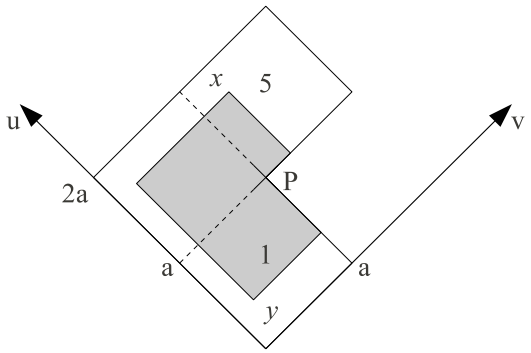

Figure 5.10: The causal interval between $x \in \mathcal{I}_5$ and $y \in \mathcal{I}_1$ is depicted in grey.

logarithmically with the density.

5.5 Discussion

We have shown that in the limit of infinite density, the mean of the Discrete Action will be 1 for any causally convex region of $\mathbb{M}^2$ including regions whose past and/or future boundaries contain spacelike segments. Since these spacelike segments may have nonzero geodesic curvature, the constancy of the mean of the DA suggests that it contains no contribution from the past or future boundaries.

Indeed a handwaving argument, consistent with the conjecture of the previous chapter, can be given as to why this should be so, even when $\mathcal{M}$ is curved. The boundary of a causally convex region $\mathcal{U} \subset \mathcal{M}$ consists of a future boundary and a past boundary intersecting in a co-dimension 2 spacelike surface. There is no timelike portion of the boundary. The mean of the DA is a double integral over $\mathcal{U}$ which can be done in either order. The integrand is a retarded 2-point function,

$$\rho\mathcal{L}(x,y) = \frac{\rho}{\sqrt{-g}}\delta^{(2)}(x,y) - 2\rho^2\, p(\rho V_{xy})C(x,y) \tag{5.31}$$

where $C(x,y) = 1$ if $y \in J^-(x)$ and 0 otherwise. Let us assume the density is high enough that a sprinkled causal set can capture the curvature of $\mathcal{M}$, *i.e.* at each point $y \in \mathcal{M}$ there is a local inertial frame in which the curvature components are small compared to the density. If we do the x integration

first, at fixed y, then the resulting function $\rho L(y)$ is approximately $\frac{1}{4}R(y)$ unless y is too close to the future boundary. If it is within length $\rho^{-\frac{1}{2}}$ of the boundary then the range of the x integration will not be large enough for the approximation to hold [8]. Then we do the integration over y to get approximately the usual Einstein-Hilbert bulk term together possibly with some contribution from the integral over the points y close to the future boundary, *i.e.* possibly some kind of future boundary term. But there is no contribution from the past boundary at all. Now reverse the order of integration: do y first and then x. Now there appears to be no contribution from the future boundary. This can only happen if neither boundary contributes. So the only points where some boundary contribution can come in, is from the points which are close to both past and future boundaries *i.e.* from the spacelike co-dimension 2 "corners" where the past and future boundaries intersect. The argument holds when the past and future boundaries are partly spacelike as well as when they are wholly null. There is no reason, from this argument, that timelike boundaries could not contribute however and we saw evidence that they do from the results for the rectangle.

This heuristic reasoning would have to be backed up with further evidence from simulations of the Discrete Action but it suggests that there is no Gauss-Bonnet formula for the $2d$ Discrete Action. The $2d$ Gauss-Bonnet Theorem can hold because, as the geometry of the bulk surface is varied, the extrinsic curvature of the boundary changes and the right combination of bulk and boundary terms can remain constant. In $2d$ the co-dimension 2 "corner" is an S^0, *i.e.* 2 points, and if the only boundary contributions are from these 2 points, these couldn't compensate for the changing bulk term. Another reason not to expect the DA to satisfy a Gauss-Bonnet formula is that it appears that the appropriate Lorentzian analogue of the Euclidean formula is of the form "bulk term + boundary term + corner terms" $= 2\pi i\chi$ rather than $2\pi\chi$ [33, 38] (see also [31, 32]). Both the bulk and boundary terms are real but the formula can hold because the corner contributions are Lorentzian angles which can be complex. However, the Discrete Action is real.

This putative lack of boundary terms could explain why the expected DA for any causally convex region of $\mathbb{M}^2$ is the same. The continuum bulk term is zero. If the mean of the DA is indeed close to the continuum bulk

term plus only a contribution from the S^0 corners then that should be the same for all causally convex regions. Presumably, the difference for the neighbourhood of the singularity of the trousers comes from a boundary effect of the non-standard causal structure around the singularity which has a double lobed past and future. These issues all remain to be investigated.

There are a large number of open questions. What does happen in $2d$ curved spacetimes? Will the results continue to bear out the conjecture that the expected DA is approximately the Einstein-Hilbert term plus a constant from the S^0 corner? What is the significance in quantum gravity of the results for the interval, trousers and rectangle? For example, the result for the rectangle suggests that the expected DA contains boundary contributions proportional to the length of any timelike boundary. Can we use the DA to give an argument against the appearance of "holes" and "edges" in spacetime? Or for or against topology changing processes such as the trousers?

Chapter 6

Counting The Entropy of Causal Horizons

6.1 Counting Entropy of Any Causal Horizon

There is a substantial body of evidence that the laws of thermodynamics apply to all causal horizons, where a causal horizon is the boundary of the causal past of a timelike curve of infinite proper length in the future direction [39]. This universality is powerfully argued for in [40]. Bringing together general relativity, quantum field theory, semiclassical gravity, black hole physics and thermodynamics, this body of work is a major achievement that speaks of the unity of physics. It is also a work in progress whose final significance for the nature of space, time and matter is unknown. There is however a growing consensus that the thermodynamics of causal horizons should arise from the statistical mechanics of some microscopic degrees of freedom and in this chapter we investigate the identity of these degrees of freedom starting with two observations.

First, in order for causal horizons to be modelled at all, spacetime – however it is described – must possess a causal ordering so that notions such as "causal curve" and "causal past" (or their analogues) are meaningful. Secondly, if spacetime is continuous then, prima facie, the entropy should be infinite: a quantum field contributes an infinite entanglement entropy to the total entropy of a black hole due to modes of unboundedly high frequency that straddle the horizon [41]. The Bekenstein-Hawking black hole entropy is, however, finite and equal to the area of the horizon in Planck units,

up to a factor of order unity. Therefore, in order to have the best chance of explaining horizon entropy, spacetime should be discrete or atomic at Planckian scales. The strategy, then, is to seek a universal microscopic explanation of the entropy of causal horizons based on a causal set.

As we saw in chapter 2, given a spacetime $(\mathcal{M}, g)$ such as 4-d Schwarzschild, say, a causal set, $(\mathcal{C}, \preceq)$, that could underly $\mathcal{M}$ can be generated by sprinkling. We will assume that such a causal set is the reality to which $(\mathcal{M}, g)$ is an approximation. This is a kinematical assumption: quantum considerations mean that reality should correspond to something more like a "superposition" of causal sets. Nevertheless, kinematics can be a useful starting point for statistical mechanics and quantum mechanics need make us no more squeamish about the statement, "Spacetime is a causal set", than about the statement, "A gas is a bunch of molecules."

Within $\mathcal{C}$ there are analogues of the entities relevant to the question of horizon entropy. The analogue of a timelike curve is a *chain*, a totally ordered subset of $\mathcal{C}$. A future infinite chain is the analogue of a future infinite timelike curve. The past $P(A)$ of any subset A of $\mathcal{C}$ is well-defined: $P(A) := \{y \in \mathcal{C} \,|\, \exists x \in A \text{ s.t. } y \preceq x\}$. A causal horizon is identified with a partition of the spacetime into two regions, the past of a future-infinite chain γ, $P(\gamma)$, and its complement, $\bar{P}(\gamma)$. One has to work harder to identify spacelike hypersurfaces but there is evidence that it can be done [42].

The defining characteristic of a causal horizon, $\mathcal{H}$, is that it partitions spacetime into two regions $\mathcal{M} = \mathcal{M}_{\text{aut}} \cup \bar{\mathcal{M}}$, where $\mathcal{M}_{\text{aut}}$ is the past of the timelike curve and evolves autonomously if relativistic causality is respected. It is natural to suppose that this dichotomy is the source of horizon entropy and indeed, the actions for causal sets [8] defined in chapter 4 lends itself to a proposal in this direction because, as we saw already, the actions are *bilocal*.

6.2 Spacetime Mutual Information

The bilocal nature of $S^{(d)}$, c.f. section 4.1.2, implies that the action of the spacetime region with a horizon $\mathcal{H}$ to the past of some non-timelike surface Σ, $\mathcal{C}_\Sigma = X \cup Y \subset \mathcal{C}$ where $X = J^+(\mathcal{H}) \cap J^-(\Sigma)$ and $Y = J^-(\mathcal{H}) \cap J^-(\Sigma)$,

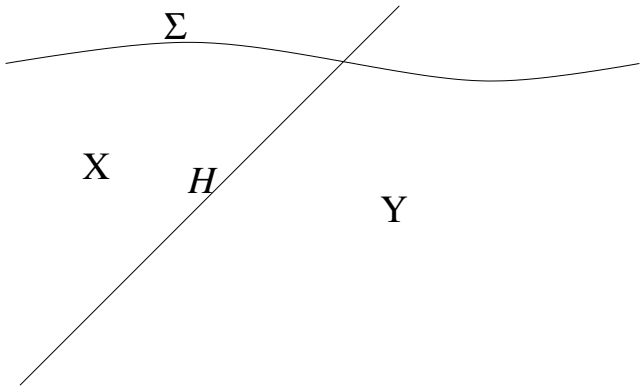

Figure 6.1: A schematic picture of a spacetime with a horizon $\mathcal{H}$ and a constant time hypersurface Σ, where $X = J^+(\mathcal{H}) \cap J^-(\Sigma)$ and $Y = J^-(\mathcal{H}) \cap J^-(\Sigma)$.

see figure 6.1, is

$$S^{(d)}[\mathcal{C}_\Sigma] = S^{(d)}[X, X] + S^{(d)}[Y, Y] + S^{(d)}[X, Y]. \tag{6.1}$$

In analogy with the mutual information of thermodynamic systems we define the *Spacetime Mutual Information* (SMI) to be

$$\mathcal{S}^{(d)}_\Sigma[X, Y] = \left(\frac{l_p}{l}\right)^{d-2} \left(S^{(d)}[X, X] + S^{(d)}[Y, Y] - S^{(d)}[\mathcal{C}_\Sigma]\right). \tag{6.2}$$

The SMI in d-dimensions can be easily found using the causet action (4.11). It is given by

$$\mathcal{S}^{(d)}_k[X, Y] = \beta_d \epsilon_d^{\frac{d+2}{d}} \sum_{x \in X} \sum_{\substack{y \in Y \\ y \prec x}} f_d(n(x, y), \epsilon_d), \tag{6.3}$$

where β_d is given in table 3.1, $\epsilon_d = (l/l_k)^d$, $n(x, y) := |I(x, y)| - 2$ and in $3d$

and $4d$

$$f_3(n,\epsilon_3) = (1-\epsilon_3)^n\left[1 - \frac{27\epsilon_3 n}{8(1-\epsilon_3)} + \frac{9\epsilon_3^2 n(n-1)}{8(1-\epsilon_3)^2}\right], \tag{6.4}$$

$$f_4(n,\epsilon_4) = (1-\epsilon_4)^n\left[1 - \frac{9\epsilon_4 n}{1-\epsilon_4} + \frac{8\epsilon_4^2 n!}{(n-2)!(1-\epsilon_4)^2} - \frac{4\epsilon_4^3 n!}{3(n-3)!(1-\epsilon_4)^3}\right]. \tag{6.5}$$

For $l_k = l$ these reduce to simpler expressions

$$\mathcal{S}^{(2)}[X,Y] = 2N_1[X,Y] - 4N_2[X,Y] + 2N_3[X,Y] \tag{6.6}$$

$$\mathcal{S}^{(4)}[X,Y] = \frac{4}{\sqrt{6}}(N_1[X,Y] - 9N_2[X,Y] + 16N_3[X,Y] - 8N_4[X,Y)). \tag{6.7}$$

Recall that if $Y \subset J^-(X)$ then $N_i[X,Y]$ counts the $(i+1)$-element inclusive order intervals such that the future most point is in X and the past most is in Y.

Consider a sprinkling $\mathcal{C}$ of a spacetime $(\mathcal{M}, g)$, with a causal horizon $\mathcal{H}$ which is identified with a partition of $\mathcal{C}$ into two regions $P(\gamma)$ and $\bar{P}(\gamma)$. Let Σ be the causet analogue of a non-timelike hypersurface intersecting $\mathcal{H}$ on some codimension 2 surface $\Omega = \mathcal{H} \cap \Sigma$, and define regions X and Y to be $\bar{P}(H) \cap P(\Sigma)$ and $P(\mathcal{H}) \cap P(\Sigma)$ respectively. Using the conjecture for the continuum limit of the causet action, (4.16), we see that the SMI is

$$\langle \mathcal{S}_k^{(d)}[X,Y] \rangle = b_d \frac{A^{(d)}(\Omega)}{l_p^{d-2}}, \tag{6.8}$$

where $l^d = V/N$, $A^{(d)}(\Omega)$ is the volume of Ω.

We conjecture that the SMI gives the continuum value for the horizon entropy. In order to give credibility to this proposal we must first confirm that equation (6.8) holds. But even then the SMI would only deserve the title of entropy if we were able to prove a GSL from it, in a dynamical quantum theory of causal sets.

6.3 Numerical Analysis

We test (6.8) by computing the SMI of spacetimes partitioned by a causal horizon. The setups used in the numerical simulations are defined below. If a setup is used in both $3d$ and $4d$ we only define the $4d$ one explicitly, the $3d$ one being the obvious dimensionally reduced version. Define $A_i := A^{(4)}(\mathcal{H} \cap \Sigma_i)$ and $L_i := A^{(3)}(\mathcal{H} \cap \Sigma_i)$, $i = 1, 2$. Each simulation calculates expected SMI for the relevant setup by averaging $\mathcal{S}_k^{(d)}$ over 10 sprinklings, where we set $l_k = 3l$ and $l_k = 2l$ in $3d$ and $4d$ respectively.

6.3.1 Rindler Horizon

We sprinkle points x_i, $i = 1, \ldots, N$ into a region of Minkowski defined by $t \in [-0.5, 0.5]$, $x, z \in [-1.5, 1.5]$ and $y \in [-6, 6]$ where $\{t, x, y, z\}$ are Cartesian coordinates (in 3d drop the z). The horizon $\mathcal{H}$ given by $t = x$, is that of an observer uniformly accelerated in the positive x-direction, and Σ_1 and Σ_2 are the surfaces $t = 0.5$ and $t = -0.5$ respectively, see figure (6.2). Hence $A_1 = A_2 = 36$ and $L_1 = L_2 = 12$. Define $X = \{x_i : t(x_i) > x(x_i),\ i = 1, \ldots, N\}$ and $Y = \{x_i : t(x_i) < x(x_i),\ i = 1, \ldots, N\}$.

6.3.2 deSitter Cosmic Horizon

We sprinkle points x_i, $i = 1, \ldots, N$ in a region of dS spacetime given by $\eta \in [-0.5, 0.5]$, $\chi, \theta \in [0, \pi]$ and $\phi \in [0, 2\pi]$ where $(\eta, \chi, \theta, \phi)$ are global conformal coordinates in which the metric takes the form $ds^2 = \sec^2(\eta)(-d\eta^2 + d\Omega_3^2)$, and $d\Omega_3^2$ is the metric of a 3-sphere. The horizon is that of a cosmic observer at the south pole $\chi = \pi$ and is given by the surface $\eta = \chi - \frac{\pi}{2}$, and Σ_1 and Σ_2 are given by $\eta = 0.5$ and $\eta = -0.5$ respectively, see figure (6.3). Hence $A_1 = A_2 = 4\pi$ and $L_1 = L_2 = 2\pi$. Define $X = \{x_i : \eta(x_i) > \chi(x_i) - \frac{\pi}{2},\ i = 1, \ldots, N\}$ and $Y = \{x_i : \eta(x_i) < \chi(x_i) - \frac{\pi}{2},\ i = 1, \ldots, N\}$.

6.3.3 Null Collapsing Shell Black Hole Horizon

We consider a spherical shell of collapsing null matter given by $t = -r +$ const, const $\gg 1$ and consider the portion of the horizon which lies inside the shell, i.e. before the shell passes its event horizon, where the spacetime is flat. We choose our coordinates so that the horizon is given by the hyper surface $t = r - 1$, and sprinkle points x_i, $i = 1, \ldots, N$ in a cylindrical region

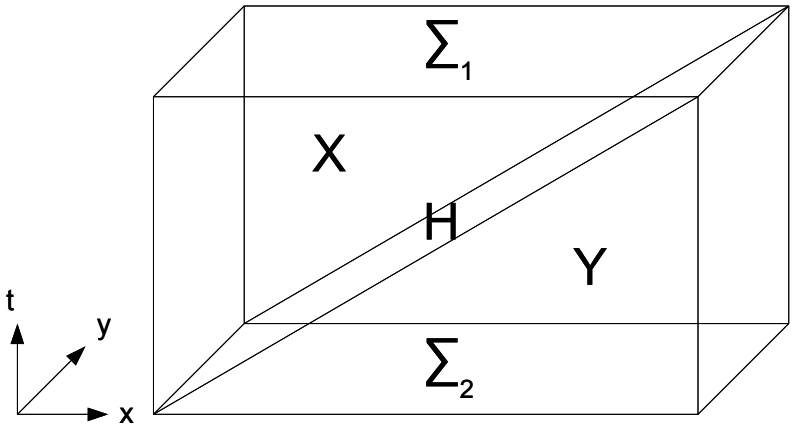

Figure 6.2: A (2+1)-dimensional diagram of the setup used in the Rindler simulations. The null surface H represents a portion of the infinite Rindler horizon of an observer uniformly accelerated in the positive x-direction. Σ_1 is a constant time slice at which we wish to evaluate the entropy of the horizon, whilst Σ_2 (also a constant time slice) has been introduced to render the sprinkling region finite.

of Minkowski space defined by $t \in [-0.7, 0]$, $r \in [0, 1.7]$, $\theta \in [0, \pi]$, $\varphi \in [0, 2\pi]$, where Σ_1 and Σ_2 are defined by $t = 0$ and $t = -0.7$ respectively, see figure (6.4). Hence $A_1 = 4\pi$ and $A_2 = 4\pi(0.3)^2$. Define $X = \{x_i : t(x_i) > r(x_i) - 1 \; i = 1, \ldots, N\}$ and $Y = \{x_i : t(x_i) < r(x_i) - 1, \; i = 1, \ldots, N\}$.

6.3.4 Results

To analyse the data we first note that rearranging (6.8) gives

$$\frac{V^{\frac{d-2}{d}}}{A_1^{(d)} + A_2^{(d)}} \langle \mathcal{S}_k^{(d)}(X, Y) \rangle = b_d N^{\frac{d-2}{d}}, \tag{6.9}$$

where $A_1^{(d)} := A^{(d)}(\mathcal{H} \cap \Sigma_1)$ and $A_2^{(d)} := A^{(d)}(\mathcal{H} \cap \Sigma_2)$, and $A_1^{(d)} = A_2^{(d)}$ for the Rindler and deSitter setups. We will call the left hand side of the above equation the renormalised SMI, or rSMI for short.

Figures 6.6 and 6.5 show a log-log plot of the rSMI as against N. A two-parameter power-law fit with the function $f(c_d, d, N) = c_d N^{k_d}$ gives in

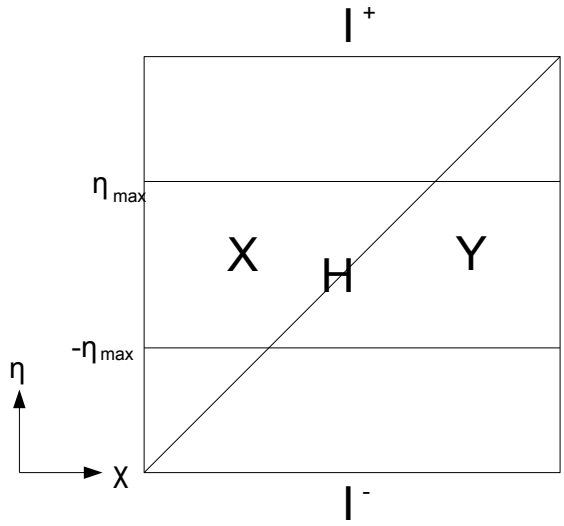

Figure 6.3: Penrose diagram of deSitter spacetime. The cosmic horizon of an observer sitting on the south pole of the constant η slices is shown, together with the region into which we sprinkle, bounded by $\pm\eta_{\max}$. The constant η-time surface $\eta_{\max}$ is the time at which we evaluate the entropy of the horizon H.

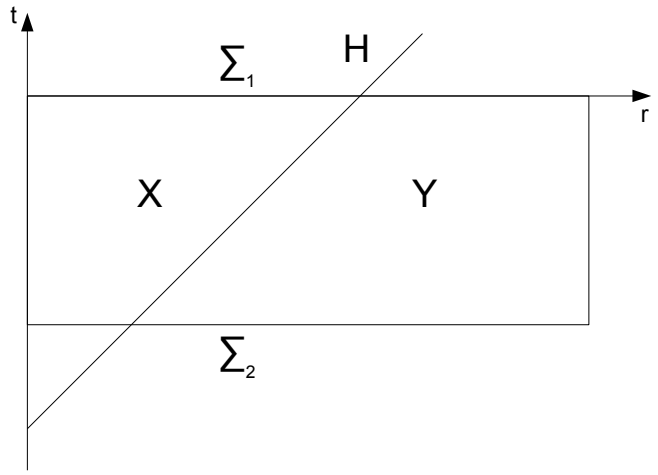

Figure 6.4: Collapsing shell black hole. The region depicted in the diagram is the inside of a null collapsing shell of matter (not shown in the picture), where the spacetime is flat, and H is the horizon. The boxed region is a cylinder of radius $r = 1.7$, and height $t = 0.7$, representing the portion of the spacetime which we sprinkle into.

$3d$

$$\text{Rindler:} \quad b_3 = 0.83 \pm 0.05, \quad k_3 = 0.33 \pm 0.01, \tag{6.10}$$

$$\text{dS:} \quad b_3 = 0.34 \pm 0.08, \quad k_3 = 0.39 \pm 0.02, \tag{6.11}$$

and in $4d$

$$\text{Rindler:} \quad b_4 = 1.29 \pm 0.41, \quad k_4 = 0.47 \pm 0.02, \tag{6.12}$$

$$\text{dS :} \quad b_4 = 1.17 \pm 0.35, \quad k_4 = 0.48 \pm 0.02, \tag{6.13}$$

$$\text{Collapsing shell:} \quad b_4 = 2.67 \pm 2.00, \quad k_4 = 0.42 \pm 0.06, \tag{6.14}$$

where we fitted data for $N \geq 2^{18}$ only.

Having established that the data is broadly consistent with $k_d = (d-2)/d$ we fix b_d more precisely by fixing k_d and refitting the data to $g(b_d, N) = b_d N^{(d-2)/d}$, $d = 3, 4$. We find

$$\text{Rindler:} \quad b_3 = 0.789 \pm 0.002, \tag{6.15}$$

$$\text{dS :} \quad b_3 = 0.73 \pm 0.01, \tag{6.16}$$

and

$$\text{Rindler:} \quad b_4 = 0.86 \pm 0.01, \tag{6.17}$$

$$\text{dS :} \quad b_4 = 0.88 \pm 0.01, \tag{6.18}$$

$$\text{Collapsing shell:} \quad b_4 = 0.95 \pm 0.03. \tag{6.19}$$

(It would be nice at this point to compare these values of b_d with those found in chapter 4, but since we don't believe the action of $3d$ and $4d$ flat intervals to have reached the asymptotic regime, it would not make much sense.)

6.4 Discussion

We have provided numerical evidence that in the limit of infinite density, for Rindler, deSitter and collapsing shell black hole horizons, the expected SMI is proportional to the area of the codimension 2 surface defined by the intersection of the horizon, $\mathcal{H}$, with a spacelike hypersurface Σ. Furthermore,

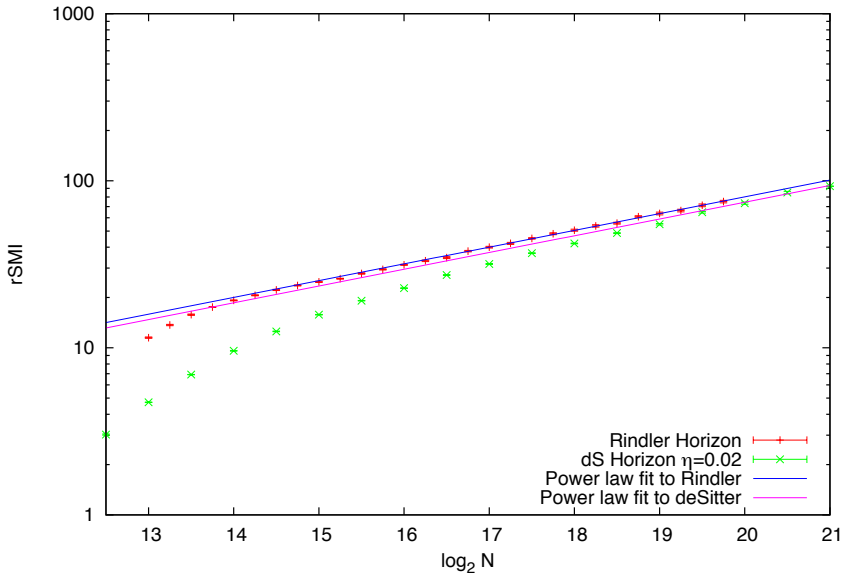

Figure 6.5: log-log plot of simulation data for the Rindler and deSitter setup in $3d$, varying density ρ with a power law fit of Rindler data only. Data averaged over 10 runs. Fit function $f(b_d, k_d, N) = b_d N^{k_d}$.

in $4d$, our data is consistent with the constant of proportionality, b_4, being universal, which is not surprising given that the SMI is defined via the causet action. In fact, this can be seen as evidence in favour of the conjecture for the continuum limit of the causet action, albeit only for the term proportional to the codimension 2 boundary of the spacetime region. In $3d$ the data is inconsistent with the universality of b_3, but a quick look at figure 6.5 suggests that the deSitter data has not quite reached the asymptotic regime yet.

It is worth appreciating the cancellations occurring in calculating the SMI. Figure 6.7 shows a plot of the the individual contributions to the SMI for the Rindler setup in $4d$. As we can see each contribution grows much faster than $O(\sqrt{N})$, [1] and only once all these contributions are added together with the specific pattern of coefficients used in the action, does the growth reduce to $O(\sqrt{N})$.

Taking the SMI to be defined by equation (6.3), it is surprising that it is

[1] We can also note that for low N each contribution scales differently, and only as $N \to \infty$ do they tend towards similar growth. This is because these simulations are of the non-local SMI, i.e. with $l_k > l$, so that each layer is not just the number of order intervals of some particular size, but includes order intervals of all sizes.

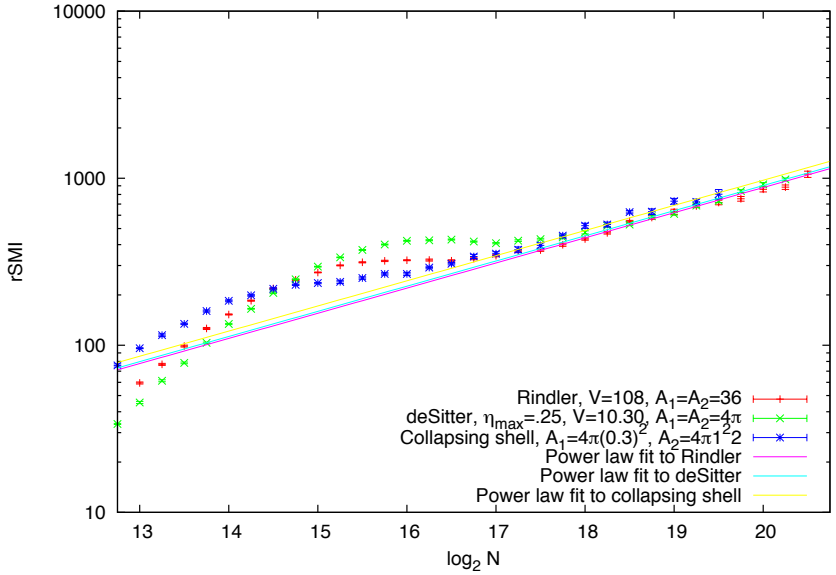

Figure 6.6: log-log plot of simulation data for the Rindler, deSitter and collapsing shell setup in $4d$, varying density ρ with a power law fit of all three data sets. Data averaged over 10 runs. Fit function $f(b_d, k_d, N) = b_d N^{k_d}$.

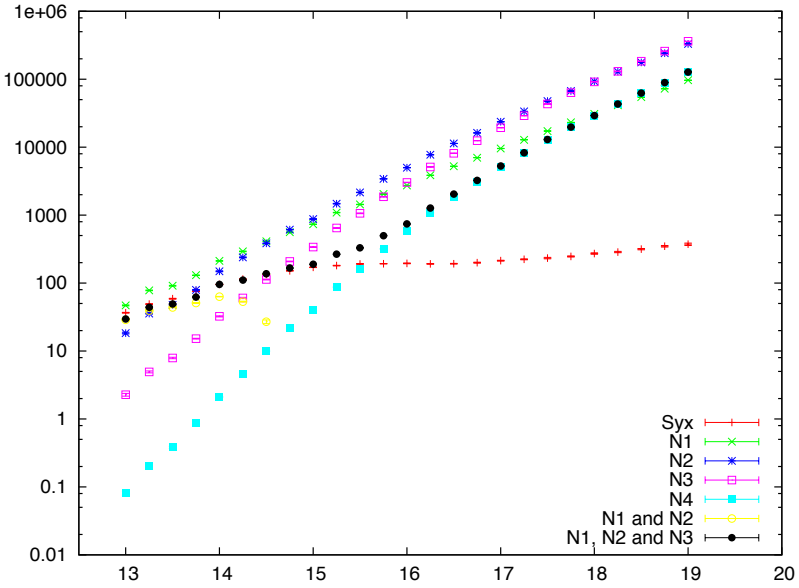

Figure 6.7: A log-log plot of the various contributions to the SMI (for the $4d$ Rindler setup) taken separately. It should be noted how each contribution grows much faster than $O(\sqrt{N})$, and only when taken together, in the precise combination given by the action (or SMI), does the SMI approach $O(\sqrt{N})$, in the asymptotic limit.

"working" at all, in the sense that (6.8) holds. It must be that $\langle \mathcal{S}_k^{(d)}(X,Y)\rangle$ is effectively localising at the horizon even though the definition is global. One possible explanation is that the SMI is effectively counting links local to the intersection of some constant time surface with the horizon, and the non-link counting terms in the SMI are there to provide a Lorentz invariant way of introducing cancellations without which the result would be infinite [43, 8, 26].

If the proposal "works" in the sense of giving the continuum value for the entropy in cases where it is defined, then we will be faced with the task of explaining why this quantity is, physically, an entropy. In other words, we will need to prove the Generalised Second Law from the fundamental dynamics of the discrete theory. It is encouraging that the spacetime mutual information relates to dynamics through being the information missing from the action. It is also encouraging that the proof scheme of Sorkin [44] – a generalisation of his proof of the GSL in semiclassical gravity [45] – is set up in causal terms. The challenge is to understand entropy and reformulate Sorkin's proof scheme in the fully spacetime setting of the sum-over-histories approach to quantum theory that causal sets seem to demand.

In [40] it is stated, "One of the key questions is whether the local notion of horizon entropy *density* is a valid concept, or whether something essentially global is involved." The proposal we have made is that horizon entropy is global in the sense of pertaining to a causally defined dichotomy of spacetime *and yet* it is effectively localized. The answer to Jacobson and Parentani's key question would then be, "Yes and yes."

Chapter 7

Conclusion

7.1 Summary

Following a brief introduction to causal sets in Chapters 1 and 2, we showed in Chapter 3 how it is possible to define a one-parameter family of wave operators, B_k, on causal sets well-approximated by 4 dimensional spacetimes, whose continuum limit (provided certain assumptions hold) gives both the continuum d'Alembertian and the scalar curvature of the approximating manifold, i.e.

$$\lim_{\rho\to\infty} \bar{B}_k\phi(x) = \Box\phi(x) - \frac{1}{2}R(x)\phi(x).$$

This result is proof of concept that the non-locality of causal sets, emerging from the interplay between Lorentz invariance and discreteness, can be tamed, and that (approximately) local dynamics can be defined.

In Chapter 4 we used this result to define the scalar curvature, $\mathcal{R}$, and the action, $S[\mathcal{C}]$, for causal sets and conjectured that for sprinklings of globally hyperbolic normal neighbourhoods, $\mathcal{N}$,

$$\lim_{l\to 0}\langle S[\mathcal{C}]\rangle = \frac{1}{2l_p^{d-2}}\int_{\mathcal{N}} d^dx\sqrt{-g(x)}R(x) + \frac{b_d}{l_p^{d-2}}A\left(N_f \cap N_p\right).$$

(If the region $\mathcal{N}$ contains timelike boundaries, Ξ, then we conjectured that the continuum limit was dominated by the divergent term $\frac{a_d}{l_p^{d-2}l}\int_\Xi d^{d-1}x\sqrt{-h(x)}$). We then studied the expected action of various spacetime regions which, together with the results of Chapters 5 and 6, provided evidence in favour of this conjecture.

Chapter 5 was devoted to a detailed study of the action of $2d$ causal sets,

for which we concluded that, although the action appears to be topological, it is most likely unrelated to the Lorentzian extension of the Gauss-Bonnet theorem.

Finally in chapter 6 we used the action to define the spacetime mutual information (SMI)

$$\mathcal{S}_{\Sigma}^{(d)}[X,Y] = \beta_d \epsilon_d^{\frac{d+2}{d}} \sum_{x\in X} \sum_{\substack{y\in Y \\ y\prec x}} f_d(n(x,y),\epsilon_d),$$

and conjectured that its mean is the continuum entropy of causal horizons, i.e.

$$\langle \mathcal{S}_k^{(d)}[X,Y] \rangle = b_d \frac{A^{(d)}(\Omega)}{l_p^{d-2}}.$$

We then provided numerical evidence in favour of this claim.

7.2 Outlook and Future Work

The work in this thesis has probably raised more questions than answers. In this final section we give a list of projects, inspired by the work described in this thesis, that we intend to explore in the future.

- Generalising the proof of chapter (3) to other dimensions.
- Proving a stronger version of (3.8) by weakening the assumptions. In particular we would like to prove the result in the presence of generic caustics.
- Establishing the phenomenological role played by the meso-scale l_k in the propagation of both classical and quantum fields on a fixed causal set background.
- Investigating the scalar quantum field theory built using the Lorentz invariant non-local continuum d'Alembertian $\bar{B}_k$.
- Providing more conclusive evidence for the conjecture about the continuum limit of the causet action (4.16), possibly analytically. In particular we would like strong evidence for the bulk Einstein-Hilbert term.

- Now that we have an action we can study quantum dynamics for causal sets. As we explained in the introduction, by QCSD we mean a PI (or SOH) dynamics, i.e.

$$Z = \sum_{\mathcal{C}} e^{iS[\mathcal{C}]/\hbar}. \tag{7.1}$$

  Some work in this direction has recently been done [46]. We wish to extend this further.

- Use the $2d$ causet action to study topology change for $2d$ causets. We already know the causet action for a trousers spacetime so the next step would be to calculate the action for the other $2d$ topology change, the creation of a circle from nothing. These result could prove useful in understanding whether certain types of topology change are suppressed in $2d$ QG, c.f. [38].

- Provide further evidence for the relation between the SMI and the entropy of causal horizons. Harder (but more rewarding!): try to establish whether there is a link between the novel proposal for calculating the entropy of a spacetime region [47], and the SMI.

Appendix A

Integrals

A.1

We prove that (3.74) - (3.76) are zero in the limit This follows if

$$\rho^{\frac{3}{2}}\hat{\mathcal{O}}I_{m,n} = \hat{\mathcal{O}}\int_0^a dv \int_0^v du\, u^m v^n \psi(u,v) e^{-\rho u^2 v^2}, \tag{A.1}$$

tends to zero in the limit $\rho \to \infty$ for all $m+n \geq 5$. We will need the following identities

$$\hat{\mathcal{O}}\left(\frac{\mathrm{erf}(\sqrt{\rho}uv)}{\sqrt{\rho}}\right) = \frac{2}{\sqrt{\pi}} uv\hat{\mathcal{P}} e^{-\rho u^2 v^2} \tag{A.2}$$

$$\hat{\mathcal{P}}\left(\frac{\mathrm{erf}(\sqrt{\rho}uv)}{\rho^{\frac{3}{2}}}\right) = -\frac{2}{3\sqrt{\pi}} u^3 v^3 e^{-\rho u^2 v^2}. \tag{A.3}$$

where $\hat{\mathcal{P}} = \frac{2}{3}(H+1)(H+\frac{3}{2})$ so it annihilates ρ^{-1} and $\rho^{-\frac{3}{2}}$.

We first integrate $I_{m,n}$ by parts in u, then act with $\hat{\mathcal{O}}$ and use (A.2) to get

$$\begin{aligned} &\hat{\mathcal{P}}\int_0^a dv\, v^{m+n+1}\psi(v,v)e^{-\rho v^4} \\ &\quad - \hat{\mathcal{P}}\int_0^a dv \int_0^v du\, (m u^m \psi(u,v) + u^{m+1}\psi_{,u}(u,v)) v^n e^{-\rho u^2 v^2} \end{aligned} \tag{A.4}$$

We can deal with the first integral by acting with $\hat{\mathcal{P}}$ on the integrand

$$\int_0^a dv\, \psi(v,v) v^{m+n+1}(1 - \frac{7}{3}\rho v^4 + \frac{2}{3}\rho^2 v^8) e^{-\rho v^4}. \tag{A.5}$$

and then bounding each of the resulting integrals, e.g.

$$\int_0^a dv\,\psi(v,v)v^{m+n+1}e^{-\rho v^4} \leq ||\psi(v,v)||_1 \int_0^a dv\,v^{m+n+1}e^{-\rho v^4}$$
$$= \frac{||\psi(v,v)||_1}{4\rho^{\frac{m+n+2}{4}}}\left[\Gamma\left(\frac{m+n+2}{4}\right) - \Gamma\left(\frac{m+n+2}{4}, \rho a^4\right)\right], \qquad \text{(A.6)}$$

which is at least of order $1/\rho^{\frac{7}{4}}$ and hence goes to zero in the limit for all $m+n \geq 5$.

Next we deal with the second term in (A.4). Integrating by parts in u again gives $I_{m,n} = A + B$ where

$$A = \hat{\mathcal{P}}\int_0^a dv\,(mv^{m+n-3}\psi(v,v) + v^{m+n-2}\psi_{,u}(v,v))\frac{e^{-\rho v^4}}{2\rho}$$
$$- \frac{v^{n-2}}{2\rho}\begin{cases} \psi(v,v) & \text{if } m=1 \\ \psi_{,u}(v,v) & \text{if } m=0 \end{cases} \qquad \text{(A.7)}$$

$$B = -\hat{\mathcal{P}}\int_0^a dv\int_0^v du\,(m(m-1)u^{m-2}\psi + 2mu^{m-1}\psi_{,u} + u^m\psi_{,uu})\frac{v^{n-2}}{2\rho}e^{-\rho v^4}. \qquad \text{(A.8)}$$

Both instances of the second term in A are annihilated by $\hat{\mathcal{P}}$ so we only need to deal with the first term. Integrating by parts in v gives

$$-\frac{1}{12}(ma^{m+n+2}\psi(a,a) + a^{m+n+3}\psi_{,u}(a,a))e^{-\rho a^4}$$
$$+\frac{1}{12}\int_0^a dv\,\big(m(m-2)v^{m+n+1}\psi(v,v) + mv^{m+n+2}\psi_{,v}(v,v)$$
$$+(m-1)v^{m+n+2}\psi_{,u}(v,v) + v^{m+n+3}\psi_{,uv}(v,v)\big)\,e^{-\rho v^4}. \qquad \text{(A.9)}$$

The first term is $O(e^{-\rho})$ and all integrals in the second term are zero in the limit for $m+n \geq 5$, see (A.6).

Now consider B, integrating by parts with respect to u again and then

acting with $\hat{\mathcal{P}}$ and making use of (A.3) gives

$$B = -\frac{1}{6}\int_0^a dv\ \left(m(m-1)v^{m+n+1}\psi(v,v) + 2mv^{m+n+2}\psi_{,u}(v,v) + v^{m+n+3}\psi_{,uu}(v,v)\right) e^{-\rho v^4} \quad \text{(A.10)}$$

$$+\frac{1}{6}\int_0^a dv\ \int_0^v du\,(m(m-1)(m-2)u^m v^n\psi + 3m(m-1)u^{m+1}v^n\psi_{,u} + 3mu^{m+2}v^n\psi_{,uu} + u^{m+3}v^n\psi_{,uuu})e^{-\rho u^2 v^2} \quad \text{(A.11)}$$

The integrals in (A.10) are again as in (A.6). Those in (A.11) we can bound:

$$\int_0^a dv\ \int_0^v du\, u^m v^n \psi(u,v) e^{-\rho u^2 v^2} \leq ||\psi(u,v)||_1 \int_0^a dv\ \int_0^v du\, u^m v^n e^{-\rho u^2 v^2}. \quad \text{(A.12)}$$

The integral on the right can be evaluate explicitly and for $n = m$ gives

$$\frac{1}{8\rho^{\frac{m+1}{2}}}\left[\log(\rho a^4)\Gamma\left(\frac{m+1}{2}\right) - \Gamma\left(\frac{m+1}{2}\right)\psi^{(0)}\left(\frac{m+1}{2}\right) + G^{3,0}_{2,3}\left(\rho a^4\Big|\begin{matrix}1,1\\0,\ 0,\frac{m+1}{2}\end{matrix}\right)\right], \quad \text{(A.13)}$$

While for $n \neq m$ one gets

$$\frac{1}{2(m-n)}\left[\frac{1}{\rho^{\frac{m+n+2}{4}}}\left(\Gamma\left(\frac{m+n+2}{4}\right) - \Gamma\left(\frac{m+n+2}{4}, \rho a^4\right)\right) - \frac{a^{n-m}}{\rho^{\frac{m+1}{2}}}\left(\Gamma\left(\frac{m+1}{2}\right) - \Gamma\left(\frac{m+1}{2}, \rho a^4\right)\right)\right] \quad \text{(A.14)}$$

where $\psi^{(0)}$ is the digamma function and $G^{3,0}_{2,3}$ is the Meijer G-function, which decays exponentially in the limit.

A.2

We prove that $\hat{\mathcal{O}} I_{21} = O(\rho^{-2})$. Since absorbing a factor of $\frac{\pi}{6}$ into ρ does not affect the homogeneity operator, H, or $\hat{\mathcal{O}}$ the result follows if

$$\hat{\mathcal{O}}\int_a^L dw \int d\Omega_2 \int_0^{\frac{a^2}{\sqrt{h}}} dz f_1(w,z,\theta,\varphi) e^{-\rho z^2 h(w,\theta,\varphi)} = O(\rho^{-2}) \quad \text{(A.15)}$$

as $\rho \to \infty$ for a smooth enough function $f_1(w, z, \theta, \varphi)$. Integrating by parts in u,

$$\begin{aligned}
&\int_a^L dw \int d\Omega_2 \int_0^{\frac{a^2}{\sqrt{h}}} dz\, f_1\, e^{-\rho z^2 h} \\
&= \int_a^L dw \int d\Omega_2 \left[\frac{\sqrt{\pi}\,\mathrm{erf}(a^2\sqrt{\rho})}{2\sqrt{\rho h}} f_1(w, \frac{a^2}{\sqrt{h}}, \theta, \varphi) - \int_0^{\frac{a^2}{\sqrt{h}}} dz \frac{\sqrt{\pi}\,\mathrm{erf}(z\sqrt{\rho h})}{2\sqrt{\rho h}} f_{1,z} \right] \\
&= \rho^{-\frac{1}{2}} \int_a^L dw \int d\Omega_2 \frac{\sqrt{\pi}}{2\sqrt{h}} f_1(w, \frac{a^2}{\sqrt{h}}, \theta, \varphi) \\
&- \rho^{-\frac{1}{2}} \int_a^L dw \int d\Omega_2 \frac{\sqrt{\pi}}{2\sqrt{h}}\, \mathrm{erfc}(a^2\sqrt{\rho}) f_1(w, \frac{a^2}{\sqrt{h}}, \theta, \varphi) \\
&- \rho^{-\frac{1}{2}} \int_a^L dw \int d\Omega_2 \int_0^{\frac{a^2}{\sqrt{h}}} dz \frac{\sqrt{\pi}}{2\sqrt{h}}\, \mathrm{erf}(z\sqrt{\rho h}) f_{1,z}(w, z, \theta, \varphi)
\end{aligned} \tag{A.16}$$

The first term of (A.16) vanishes on application of $\hat{\mathcal{O}}$. Since $w \geq a$, the second term tends to zero exponentially in the limit $\rho \to \infty$ as are all derivatives of the second term w.r.t. ρ. Thus $\hat{\mathcal{O}}$ acting on the second term gives something that tends to zero in the limit.

We're left with the third term. We use the following property of $\hat{\mathcal{O}}$:

$$\hat{\mathcal{O}} \left(\frac{\mathrm{erf}(\sqrt{\rho h} z)}{\sqrt{\rho}} \right) = \frac{2}{\sqrt{\pi}} z \sqrt{h} \hat{\mathcal{P}} e^{-\rho z^2 h} \tag{A.17}$$

where $\hat{\mathcal{P}} = \frac{2}{3}(H+1)(H+\frac{3}{2})$ so $\hat{\mathcal{P}}$ annihilates ρ^{-1} and $\rho^{-\frac{3}{2}}$

Acting on the third term with $\hat{\mathcal{O}}$ gives

$$-\hat{\mathcal{P}} \int_a^L dw \int d\Omega_2 \int_0^{\frac{a^2}{\sqrt{h}}} dz\, z\, f_{1,z}(w, z, \theta, \varphi) e^{-\rho z^2 h}\,. \tag{A.18}$$

We repeat the steps of integrating by parts and discarding terms that vanish in the limit. We have to do it twice more before we obtain an integral we

can bound. So,

$$\begin{aligned}
&\int_a^L dw \int d\Omega_2 \int_0^{\frac{a^2}{\sqrt{h}}} dz\, z\, f_{1,z}(w,z,\theta,\varphi) e^{-\rho z^2 h} \\
&= -\rho^{-1} \int_a^L dw \int d\Omega_2 \frac{1}{2h} f_{1,z}(w,0,\theta,\varphi) \\
&+ \rho^{-1} \int_a^L dw \int d\Omega_2 \frac{1}{2h} f_{1,z}(w,\frac{a^2}{\sqrt{h}},\theta,\varphi) e^{-\rho a^4} \\
&- \rho^{-1} \int_a^L dw \int d\Omega_2 \int_0^{\frac{a^2}{\sqrt{h}}} dz\, \frac{e^{-\rho z^2 h}}{2h} f_{1,zz}(w,z,\theta,\varphi)\,. \qquad \text{(A.19)}
\end{aligned}$$

The first term is killed by $\hat{\mathcal{P}}$ and the second term (and its ρ derivatives) tends to zero exponentially fast as $\rho \to \infty$. The final term of (A.19) gives, on integration by parts,

$$\begin{aligned}
&-\rho^{-\frac{3}{2}} \int_a^L dw \int d\Omega_2 \frac{\sqrt{\pi}}{4h^{3/2}} \left(f_{1,zz}(w,\frac{a^2}{\sqrt{f}},\theta,\varphi) - f_{1,zz}(w,0,\theta,\varphi) \right) \\
&\quad + \rho^{-\frac{3}{2}} \int_a^L dw \int d\Omega_2 \frac{\sqrt{\pi}}{4h^{3/2}} \operatorname{erfc}(a^2\sqrt{\rho}) f_{1,zz}(w,\frac{a^2}{\sqrt{h}},\theta,\varphi) \\
&+\rho^{-\frac{3}{2}} \int_a^L dw \int d\Omega_2 \int_0^{\frac{a^2}{\sqrt{h}}} dz \frac{\sqrt{\pi}}{4h^{3/2}} \operatorname{erf}(\sqrt{\rho h}\, z) f_{1,zzz}(w,z,\theta,\varphi) \qquad \text{(A.20)}
\end{aligned}$$

The first term is killed by $\hat{\mathcal{P}}$ and the second and its derivatives are exponentially small. The third and final term of (A.20), on application of $\hat{\mathcal{P}}$ is

$$\begin{aligned}
&\hat{\mathcal{P}} \rho^{-\frac{3}{2}} \int_a^L dw \int d\Omega_2 \int_0^{\frac{a^2}{\sqrt{h}}} dz \frac{\sqrt{\pi}}{4h^{3/2}} \operatorname{erf}(\sqrt{\rho h}\, z) f_{1,zzz}(w,z,\theta,\varphi) \\
&\qquad = -\frac{1}{6} \int_a^L dw \int d\Omega_2 \int_0^{\frac{a^2}{\sqrt{h}}} dz\, z^3 e^{-\rho z^2 h} f_{1,zzz}(w,z,\theta,\varphi) \qquad \text{(A.21)}
\end{aligned}$$

where we made use of (A.3), and we have

$$\begin{aligned}
&\left| \int_a^L dw \int d\Omega_2 \int_0^{\frac{a^2}{\sqrt{h}}} dz\, z^3 e^{-\rho z^2 h} f_{1,zzz}(w,z,\theta,\varphi) \right| \\
&\qquad \leq \|f_{1,zzz}\|_2 \int_a^L dw \int d\Omega_2 \int_0^{\frac{a^2}{\sqrt{h}}} dz\, z^3 e^{-\rho z^2 h} \qquad \text{(A.22)}
\end{aligned}$$

The remaining integral can be done

$$\int_0^{\frac{a^2}{\sqrt{h}}} dz\, z^3 e^{-\rho z^2 h} = \frac{1}{2h^2\rho^2} \tag{A.23}$$

up to exponentially decaying terms as $\rho \to \infty$.

Consider now $\hat{\mathcal{O}} I_{22}$. Absorbing a constant factor into ρ as before, and another constant factor into the function which we rename $g(u,v)$ we want to bound

$$\begin{aligned} X :=& -\hat{\mathcal{O}}\rho \int_a^L dw \int d\Omega_2 \int_0^{\frac{a^2}{\sqrt{h}}} dz\, z^3 f_2(w,z,\theta,\varphi) e^{-\rho z^2 h} \\ =& H\hat{\mathcal{O}} \int_a^L dw \int d\Omega_2 \int_0^{\frac{a^2}{\sqrt{h}}} dz\, \frac{f_2}{h}\, z\, e^{-\rho z^2 h} \end{aligned} \tag{A.24}$$

where we adopt the notation that # is a constant numerical factor (not involving any of the parameters). Almost this integral appears in the proof above as (A.18) with $\hat{\mathcal{P}}$ replaced by $H\hat{\mathcal{O}}$, and this leads to

$$X = \#\hat{\mathcal{O}}\rho^{\frac{3}{2}} \int_a^L dw \int d\Omega_2 \int_0^{\frac{a^2}{\sqrt{h}}} dz \frac{f_{2,zz}}{h^{\frac{5}{2}}} \operatorname{erf}(\sqrt{\rho h} z) \tag{A.25}$$

up to exponentially small terms. We use the identity for $\hat{\mathcal{O}}$ (A.3) to get

$$X = \#H\hat{\mathcal{Q}} \int_a^L dw \int d\Omega_2 \int_0^{\frac{a^2}{\sqrt{h}}} dz\, z^3 \frac{f_{2,zz}}{h} e^{-\rho z^2 h} \tag{A.26}$$

$$\leq \#\|f_{2,zz}\|_2 H\hat{\mathcal{Q}} \int_a^L dw \int d\Omega_2 \int_0^{\frac{a^2}{\sqrt{h}}} dz\, \frac{z^3}{h} e^{-\rho z^2 h} \tag{A.27}$$

$$= \#\|g_{,zz}\|_2 H\hat{\mathcal{Q}} \int_a^L dw \int d\Omega_2 \frac{1}{2h^3\rho^2} \tag{A.28}$$

up to exponentially decaying terms as $\rho \to \infty$.

Consider finally I_{23}. We want to bound

$$Y := \hat{\mathcal{O}} \frac{\rho^2}{2} \int_a^L dw \int d\Omega_2 \int_0^{\frac{a^2}{\sqrt{h}}} dz\, z^6 f_3(w,z,\theta,\varphi)^2 e^{-\rho z^2 h}\,. \tag{A.29}$$

Integrating by parts,

$$Y = \hat{\mathcal{O}}\frac{\rho^2}{2}\int_a^L dw \int d\Omega_2 \left[\frac{15\sqrt{\pi}}{16h^{\frac{7}{2}}\rho^{\frac{7}{2}}}(1-\mathrm{erfc}(\sqrt{\rho}a^2))f_3(w,\frac{a^2}{\sqrt{h}},\theta,\varphi)^2 \right. \quad \text{(A.30)}$$

$$\left. -\int_0^{\frac{a^2}{\sqrt{h}}} dz \left(\frac{15\sqrt{\pi}}{16h^{\frac{7}{2}}}\frac{\mathrm{erf}(\sqrt{\rho h}\,z)}{\rho^{\frac{7}{2}}} - \left(\frac{15z}{8h^3\rho}+\frac{5z^3}{4h^2}+\frac{\rho z^5}{2h}\right)e^{-\rho z^2 h}\right) 2f_3 f_{3,z}\right]. \quad \text{(A.31)}$$

Using the same techniques as before it is straightforward to show that $|Y| \sim O(\rho^{-2})$.

A.3

We want to bound HI_{24}. Again we absorb a factor of $\frac{\pi}{6}$ into ρ.

$$\left|\rho\frac{\partial}{\partial\rho}I_{24}\right| = \left|\int_a^L dw \int d\Omega_2 \int_0^{\frac{a^2}{\sqrt{h}}} dz j(y) \left[\rho^4 z^{11} g^3 e^{-\rho z^2 h}\sum_{k=0}^{\infty}\frac{(-\rho)^k}{(m+3)!}z^{3m}g^m \right.\right. \quad \text{(A.32)}$$

$$\left.\left. -\rho^3 z^9 g^3 e^{-\rho z^2 h}\sum_{k=0}^{\infty}\frac{(-\rho)^k}{(m+2)!}z^{3m}g^m\right]\right| \quad \text{(A.33)}$$

where $j(y) = \frac{1}{2}\sqrt{-g}\phi(y)(w-z)^2$. The absolute value of both the sums are bounded above by $\exp(\rho z^3\bar{g}) \leq \exp(\frac{1}{2}\rho z^2 h)$ for all $y \in W_2$.

$$\left|\rho\frac{\partial}{\partial\rho}I_{24}\right| = \#\int_a^L dw \int d\Omega_2 \int_0^{\frac{a^2}{\sqrt{h}}} dz\,|j(y)|\,g^3\,\rho^3\,z^9\,(\rho z^2-3)e^{-\frac{1}{2}\rho z^2 h} \quad \text{(A.34)}$$

$$\leq \#c\rho^3\int_a^L dw \int d\Omega_2 \int_0^{\frac{a^2}{\sqrt{h}}} dz(\rho z^2-3)e^{-\frac{1}{2}\rho z^2 h} \quad \text{(A.35)}$$

$$= \#c\int_a^L dw \int d\Omega_2 \left(\frac{1}{h^6\rho^2}-\frac{3}{10h^5\rho^2}\right) \quad \text{(A.36)}$$

up to exponentially small terms, where again $c = \bar{g}^3\left\|\int d\Omega_2|j(y)|\right\|_2$ and $\bar{g} := \|g(w,z,\theta,\varphi)\|_2$. A similar calculation shows that terms H_2I_{24} and H_3I_{24} are bounded by the same expression just with different numerical factors.

Appendix B

Volume of Long Skinny Intervals

We show that the volume of an interval contained in a normal neighbourhood of $J^-(x)$, in FNC is given by (3.43). Consider a point y with *global* FNC (w, z, θ, φ). We can use the geodesic $\gamma(\theta, \varphi)$ to define *null* FNC (x^+, x^-, x^1, x^2) where coordinate x^+ is the affine coordinate along γ such that $x^+ = w$. Coordinate x^- is affine distance along a null geodesic, λ, from the "base point" p on γ with null FNC $(w, 0, 0, 0)$, whose tangent vector, when parallely transported to the the origin of coordinates, points in an antipodal direction to the tangent of $\dot{\gamma}$; furthermore we can chose the affine parametrisation such that $x^- = z$. x^1 and x^2 are coordinates in the (spatial) transverse directions. In null FNC the metric to quadratic order is

$$\begin{aligned} ds^2 &= 2dx^+dx^- + \delta_{ab}dx^a dx^b \\ &\quad - \left[R_{+\bar{a}+\bar{b}}\; x^{\bar{a}}x^{\bar{b}}(dx^+)^2 + \frac{4}{3}R_{+\bar{b}\bar{a}\bar{c}}x^{\bar{b}}x^{\bar{c}}(dx^+dx^{\bar{a}}) + \frac{1}{3}R_{\bar{a}\bar{c}\bar{b}\bar{d}}x^{\bar{c}}x^{\bar{d}}(dx^{\bar{a}}dx^{\bar{b}})\right] \\ &\quad + \mathcal{O}(x^{\bar{a}}x^{\bar{b}}x^{\bar{c}}) \end{aligned} \tag{B.1}$$

where all the curvature components are evaluated on the null geodesic, the barred indices $\bar{a}$ *etc.* run over the three transverse directions $-, 1, 2$ and unbarred over the spatial transverse directions 1 and 2 only. Rescaling the coordinates $x^+ \to \bar{x}^+ = x^+/z$, $x^- \to \bar{x}^- = x^-/(-z)$ and $x^a \to \bar{x}^a = x^a/\sqrt{z}$

we find that in the limit $z \to 0$ the metric is

$$ds^2 = zw\left(-2d\bar{x}^+ d\bar{x}^- + \frac{1}{w}\delta_{ab}dx^a dx^b + vR_{+a+b}(\bar{x}^+)\bar{x}^a\bar{x}^b(d\bar{x}^+)^2 + O(z)\right), \tag{B.2}$$

so that $\sqrt{-g} = z^2 w + O(z^3)$.

Consider a family of points $y(Z)$ in the normal neighbourhood with FNC $y = (W, -Z, 0, 0)$ where V is fixed and consider the limit $Z \to 0$ (after the coordinate rescaling defined above we have $y = (1, 1, 0, 0)$). Assume that the spacetime volume $V(y)$ of the causal interval $I(O, y)$ between the origin of FNC and $y(Z)$ tends to zero as $Z \to 0$. Then

$$V(y) = Z^2 h(W) + Z^3 f(W) + O(Z^4) \tag{B.3}$$

for unknown functions h and f. In global FNC, for a general point y with coordinates (w, z, θ, φ), we get

$$V(y) = z^2 h(w, \theta, \varphi) + z^3 g(w, z, \theta, \varphi), \tag{B.4}$$

where we absorbed all higher order corrections in g.

Bibliography

[1] D. M. T. Benincasa and F. Dowker, "Discrete, Lorentz Invariant Scalar Wave Operators." In preparation.

[2] D. M. T. Benincasa, F. Dowker, and B. Schmitzer, "The Random Discrete Action for 2-Dimensional Spacetime," *Class.Quant.Grav.* **28** (2011) 105018, arXiv:1011.5191 [gr-qc].

[3] D. M. T. Benincasa, F. Dowker, and D. P. Rideout, "Discrete causal order and the entropy of causal horizons." In preparation.

[4] S. Hawking, "Breakdown of Predictability in Gravitational Collapse," *Phys.Rev.* **D14** (1976) 2460–2473.

[5] L. Susskind, L. Thorlacius, and J. Uglum, "The Stretched horizon and black hole complementarity," *Phys.Rev.* **D48** (1993) 3743–3761, arXiv:hep-th/9306069 [hep-th].

[6] L. Susskind and L. Thorlacius, "Gedanken experiments involving black holes," *Phys.Rev.* **D49** (1994) 966–974, arXiv:hep-th/9308100 [hep-th].

[7] A. Almheiri, D. Marolf, J. Polchinski, and J. Sully, "Black Holes: Complementarity or Firewalls?," *JHEP* **1302** (2013) 062, arXiv:1207.3123 [hep-th].

[8] D. M. T. Benincasa and F. Dowker, "The Scalar Curvature of a Causal Set," *Phys. Rev. Lett.* **104** (2010) 181301, arXiv:1001.2725 [Unknown].

[9] R. D. Sorkin, "Forks in the road, on the way to quantum gravity," *Int. J. Theor. Phys.* **36** (1997) 2759–2781, gr-qc/9706002.

[10] J. B. Hartle, "The space time approach to quantum mechanics," *Vistas Astron.* **37** (1993) 569, gr-qc/9210004.

[11] J. B. Hartle, "Space-time quantum mechanics and the quantum mechanics of space-time," in *Proceedings of the Les Houches Summer School on Gravitation and Quantizations, Les Houches, France, 6 Jul - 1 Aug 1992*, J. Zinn-Justin and B. Julia, eds. North-Holland, 1995. gr-qc/9304006.

[12] R. D. Sorkin, "Quantum mechanics as quantum measure theory," *Mod. Phys. Lett.* **A9** (1994) 3119–3128, gr-qc/9401003.

[13] R. D. Sorkin, "Quantum measure theory and its interpretation," in *Quantum Classical Correspondence: Proceedings of 4th Drexel Symposium on Quantum Nonintegrability, September 8-11 1994, Philadelphia, PA*, D. Feng and B.-L. Hu, eds., pp. 229–251. International Press, Cambridge, Mass., 1997. gr-qc/9507057.

[14] J. Myrheim, "Statistical geometry," 1978. CERN preprint TH-2538.

[15] G. 't Hooft, "Quantum gravity: a fundamental problem and some radical ideas," in *Recent Developments in Gravitation (Proceedings of the 1978 Cargese Summer Institute)*, M. Levy and S. Deser, eds. Plenum, 1979.

[16] L. Bombelli, J.-H. Lee, D. Meyer, and R. Sorkin, "Space-time as a causal set," *Phys. Rev. Lett* **59** (1987) 521.

[17] D. B. Malament, "The class of continuous timelike curves determines the topology of spacetime," *J. Math. Phys.* **18** (1977) 1399–1404.

[18] A. V. Levichev, "Prescribing the conformal geometry of a lorentz manifold by means of its causal structure," *Soviet Math. Dokl.* **35** (1987) 452–455.

[19] S. W. Hawking, A. R. King, and P. J. McCarthy, "A new topology for curved space-time which incorporates the causal, differential, and conformal structures," *J. Math. Phys.* **17** (1976) 174–181.

[20] B. Riemann, "Über die hypothesen, welche der geometrie zu grunde liegen," 1868. Riemann's Habiliationsschrift, Göttingen, 1954.

[21] J. Henson, "The causal set approach to quantum gravity," in *Approaches to Quantum Gravity: Towards a New Understanding of Space and Time*, D. Oriti, ed. Cambridge University Press, 2006. arXiv:gr-qc/0601121.

[22] F. Dowker, "Causal sets as discrete spacetime," *Contemp. Phys.* **47** (2006) 1–9.

[23] F. Dowker, "Causal sets and the deep structure of spacetime," in *100 Years of Relativity Space-time Structure: Einstein and Beyond*, A. Ashtekar, ed. World Scientific, 2005. gr-qc/0508109.

[24] R. D. Sorkin, "Causal sets: Discrete gravity (notes for the valdivia summer school)," in *Lectures on Quantum Gravity, Proceedings of the Valdivia Summer School, Valdivia, Chile, January 2002*, A. Gomberoff and D. Marolf, eds. Plenum, 2005. gr-qc/0309009.

[25] L. Bombelli, J. Henson, and R. D. Sorkin, "Discreteness without symmetry breaking: A theorem," *Mod. Phys. Lett.* **A24** (2009) 2579–2587, arXiv:gr-qc/0605006.

[26] R. D. Sorkin, "Does locality fail at intermediate length-scales?," in *Approaches to Quantum Gravity: Towards a New Understanding of Space and Time*, D. Oriti, ed. Cambridge University Press, 2006. arXiv:gr-qc/0703099.

[27] M. Blau, D. Frank, and S. Weiss, "Fermi coordinates and Penrose limits," *Class.Quant.Grav.* **23** (2006) 3993–4010, arXiv:hep-th/0603109 [hep-th].

[28] G. Gibbons and S. Solodukhin, "The Geometry of small causal diamonds," *Phys.Lett.* **B649** (2007) 317–324, arXiv:hep-th/0703098 [HEP-TH].

[29] I. Gradshteyn, I. Ryzhik, A. Jeffrey, and D. Zwillinger, *Table of Integrals, Series, And Products*. Academic Press, 2007. http://www.mathtable.com/gr/.

[30] L. Glaser and F. Dowker, "A discrete lorentz invariant d'alembertian in various dimensions." In preparation.

[31] G. S. Birman and K. Nomizu, "The Gauss-Bonnet theorem for 2-dimensional spacetimes," *Michigan Math. J.* **31** (1984) 77–81.

[32] D. J. Jee, "Gauss-bonnet formula for general lorentzian surfaces," *Geometriae Dedicata* **15** (1984) 215–231.

[33] P. R. Law, "Neutral geometry and the Gauss-Bonnet theorem for two-dimensional pseudo-Riemannian manifolds," *Rocky Mountain Journal of Mathematics* **22** (1992) 1365–1383.

[34] S. Chern, "Pseudo-riemannian geometry and gauss-bonnet formula," *An. Acad. Brasil* **35** (1963) 17–26.

[35] A. Avez, "Formule de gauss-bonnet-chern en métrique de signature quelconque," *Rev. Un. Mat. Argentina* **21** (1963) 191–197.

[36] G. Brightwell. Talk at 'causets at dias ii,' dublin institute for advanced study, dublin, ireland, 14-18 dec. 2009., 2009.

[37] B. Schmitzer, "Topology and curvature on causal sets." Msc dissertation, imperial college, london, uk, 2010.

[38] J. Louko and R. D. Sorkin, "Complex actions in two-dimensional topology change," *Class. Quant. Grav.* **14** (1997) 179–204, gr-qc/9511023.

[39] G. Gibbons and S. Hawking, "Cosmological Event Horizons, Thermodynamics, and Particle Creation," *Phys.Rev.* **D15** (1977) 2738–2751.

[40] T. Jacobson and R. Parentani, "Horizon entropy," *Found.Phys.* **33** 323–348.

[41] L. Bombelli, R. K. Koul, J. Lee, and R. D. Sorkin, "A Quantum Source of Entropy for Black Holes," *Phys.Rev.* **D34** (1986) 373–383.

[42] D. Rideout and P. Wallden, "Spacelike distance from discrete causal order," *Class. Quant. Grav.* **26** (2009) 155013, arXiv:0810.1768 [gr-qc].

[43] D. Dou and R. D. Sorkin, "Black hole entropy as causal links," *Found. Phys.* **33** (2003) 279–296, gr-qc/0302009.

[44] R. D. Sorkin, "The statistical mechanics of black hole thermodynamics," in *Black Holes and Relativistic Stars*, R. M. Wald, ed. University of Chicago Press, 1998. gr-qc/9705006. Proceedings of the Symposium dedicated to the memory of S. Chandrasekhar, Chicago, IL, USA, 14-15 Dec 1996.

[45] R. D. Sorkin, "Toward a proof of entropy increase in the presence of quantum black holes," *Phys.Rev.Lett.* **56** (1986) 1885–1888.

[46] S. Surya, "Evidence for a Phase Transition in 2D Causal Set Quantum Gravity," *Class.Quant.Grav.* **29** (2012) 132001, arXiv:1110.6244 [gr-qc].

[47] R. D. Sorkin, "Expressing entropy globally in terms of (4D) field-correlations," arXiv:1205.2953 [hep-th].